Demonstration of the Feasibility of an Acoustic Flow Meter Utilizing Edge Tone Phenomena

A Thesis
Presented in Partial Fulfillment of the Requirements for the
Degree of Master of Science
with a
Major in Mechanical Engineering
in the
College of Graduate Studies
University of Idaho
by
Jason Thomas Palmer

Major Professor: Richard N. Christensen, Ph.D.
Committee Members: Michael McKellar, Ph.D.; David Arcilesi, Ph.D.
Department Administrator: Gabriel P. Potirniche, Ph.D.

August 2021

Authorization to Submit Thesis

This thesis of Jason Thomas Palmer, submitted for the degree of Master of Science with a Major in Mechanical Engineering and titled "Demonstration of the Feasibility of an Acoustic Flow Meter Utilizing Edge Tone Phenomena," has been reviewed in final form. Permission, as indicated by the signatures and dates below, is now granted to submit final copies to the College of Graduate Studies for approval.

Major Professor:	Richard N. Christensen, Ph.D.	Date
Committee Members:	Michael McKellar, Ph.D.	Date
	David Arcilesi, Ph.D.	Date
Department Administrator:	Gabriel P. Potirniche, Ph.D.	Date

Abstract

The research described herein explores the development of an acoustically driven flow meter for use with liquids in extreme environments; with a specific interest of applicability for use in nuclear reactors such as Molten Salt, Molten Sodium, and High Temperature Gas Reactors. The environments in these reactors are extremely hostile, especially to the sensitive electronics that are typically required of sensory equipment.

The acoustic signal generation component of the flow meter is solid state, void of moving parts and electronics, and can be either machined or 3D printed from virtually any material, thereby offering suitability to practically any single phase fluid and environment. Acoustic signals are allowed to propagate through the pipes, fittings, and structural framework where they are measured using piezoelectric sensors some distance from the device, allowing the sensitive electronics to be safe from harmful conditions.

The flow meter utilizes edge tone phenomena which produce a tone in which frequency is dependant on the volumetric flow rate through the device. The device was tested on a test loop where temperature and actual flow rate (measured with a Coriolis flowmeter) were controlled allowing generated frequencies to be correlated with their respective flow rates. The flow meter was tested with both water (30 °C) and Therminol 66 (100 °C) to provide the necessary data for the non-dimensional analysis which relates the flow rate, fluid properties, and geometry of the device to the tone produced by the flow meter.

Acknowledgements

I would like to give a special thanks to Dr. Richard Christensen for his expertise and guidance during my research. I would also like to thank the University of Idaho for the use of their facilities in which my research occurred. Additionally, I want to acknowledge the contributions of Nickolas Williams, who worked side by side with me for much of the preliminary research performed.

Funding for this project came from the following sources:

- Advanced molten salt flow sensor: release 39 under blanket master contract 154756.
  - Oak Ridge National Lab, Joel Mc Duffee.
  - Idaho National Lab, Piyush Sabharwall.
- Advanced flow meter for extreme environments: release 63 under blanket master contract 154756.
  - Idaho National Lab, Piyush Sabharwall.

Dedication

Dedicated to my wife, Jenny, for putting up with all the long days and late nights.

Table of Contents

List of Tables

List of Figures

List of Acronyms

LWR Light Water Reactor

PWR Pressurized Water Reactor

VHTR Very High Temperature Reactor

AFM Acoustic Flow Meter

ASGC Acoustic Signal Generation Component

SPC Signal Processing Component

FFT Fast Fourier Transform

PLA Polylactic Acid

DCET Double Coupled Edge Tone

Chapter 1: Introduction

1.1 Background

Flow rate information is crucial for the proper operation of heat exchangers and other processes across all industries. The flow of the coolant internal to a nuclear reactor, for example, needs to be very carefully controlled to ensure the core of the reactor remains within operating temperatures. This is similarly true for many heat exchangers in operation today. Very specific amounts of heat are desired to be removed from systems and this is controlled via flow moderation based on the flow rate measurements. There are situations where current flow meters fail to meet the environmental demands required of them. In these situations, an alternative is needed.

One environment where current flow meter solutions commonly fail is deep inside nuclear reactors. The core of a nuclear reactor is one of the most unforgiving environments that a flow meter could be subjected to. Reactor core temperatures can range from around 300 °C in the classic Light Water Reactors (LWRs) to (theoretically) over 900 °C in Very High Temperature Reactors (VHTRs) [4]. These temperatures alone are extreme and eliminate most flow meters as options. Furthermore, the temperature of these reactors is not even the biggest problem; radiation from fission and the radioactive decay of fission products pose even greater problems to flow meters and other instrumentation alike.

Digital electronics, which play an integral role in nearly all modern instrumentation, are very sensitive to radiation. Electronics very quickly become damaged and cease to function while under constant bombardment from nuclear radiation. Neutrons can very easily cause transmutations or displacements of the elemental silicon or gallium, the semiconductor most commonly used in electronics [5]. Transistors, arguably the most important component of modern electronics, are particularly sensitive to radiation. The smallest of transistors can measure only a few nanometers across and have as little as 70 atoms make up the width of the transistor [6]. This incredible achievement of transistor size poses problems in radiological environments. Only a few transmutations or displaced silicon atoms can render a transistor useless. Other electronic components can be similarly damaged.

The downtime of a reactor to replace necessary instrumentation damaged by radiation effects can cost enormous sums in lost revenue and time. On June 17, 2005, the Callaway

Plant (Pressurized Water Reactor (PWR)) experienced an unintentional shut down for 107 minutes, totaling a power loss of 35.7 GW-hrs which resulted in about 1 million dollars of lost revenue [7]. An unplanned shutdown can be extremely costly to operations of a nuclear power plant. Typically, downtime is scheduled with the intent to perform as much critical maintenance on a reactor as possible to prevent revenue losses. The downtime schedule is dominantly driven by the anticipated failure of critical wear items in the reactor. Wear items can be instrumentation whose electronics are expected to be damaged by radiation. Eliminating points of failure such as this in a reactor could potentially increase the time between scheduled downtime for maintenance and decrease the probability of unscheduled shutdowns due to equipment failure, thereby potentially saving both time and money.

1.2 Scope of Work

There is a need in the harshest environments to separate instrumentation electronics from the location of detection. Therefore, the purpose of this thesis is to create an Acoustic Flow Meter (AFM) that uses the working fluid to generate an acoustic signal in the form of a vibration that can be transmitted through the piping and framework. Provided there is good direct metal to metal contact, an acoustic signal of sufficient amplitude could pass from the location of flow interest, which is also the point of vibration generation, to a remote, environmentally safe location for signal acquisition. At this location, all the sensitive electronics can be safely located to record and process the signal.

The AFM is designed to produce a tone whose frequency is proportional to the flow rate. As the flow rate increases the frequency also increases. As the flow rate decreases the frequency in turn decreases. The AFM is composed of two distinct parts, the Acoustic Signal Generation Component (ASGC) and the Signal Processing Component (SPC). The ASGC is to be installed at the point of desired flow measurement and the SPC in the environmentally safe location as shown in figure 1.1 and as described in the previous paragraph. The tones generated by the ASGC are to be recorded and analyzed by the SPC using a set of curves relating the frequency of the tones to the flow rate. The ASGC needs to be specifically built and tuned to the specific fluid, system noise, and typical operating conditions of the system the AFM is to be installed in. Special care needs to be taken to ensure the tones produced do not excite the natural frequencies of any system components.

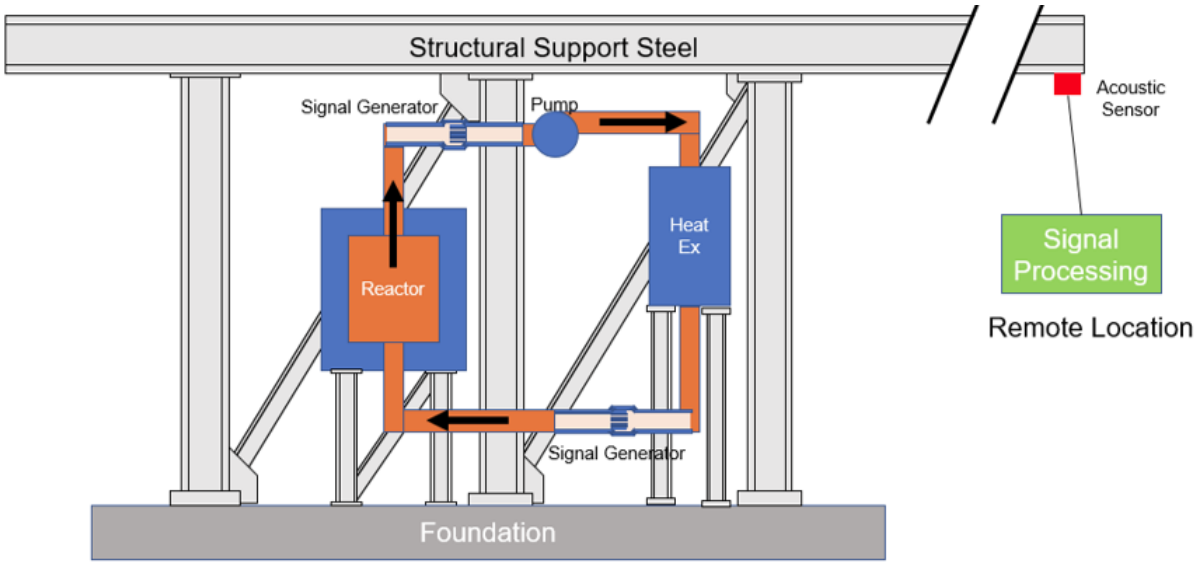

Figure 1.1: Simple diagram of the intended locations of the Acoustic Signal Generation Component (ASGC) and the Signal Processing Component (SPC) [1]

The idea to measure flow rate using an acoustic signal originated with Paul Marotta who is the CEO of MicroNuclear LLC, Brentwood, Tennessee. Due to the long standing relationship between MicroNuclear LLC and the University of Idaho in pursuing nuclear research, the proposals for an acoustic flow meter were written to be performed by the university of Idaho under the supervision of Dr. Richard Christensen (Director of the Nuclear Engineering Program). These proposals were approved and funded through the Idaho National Lab and Oak Ridge National Lab.

1.3 Thesis Outline

This work is separated into 6 chapters. Chapter 1 discusses the background for the project and why this research is of benefit, as well as the scope of the work to be performed. Chapter 2 goes over the relevant theory necessary for the project. The basic working theory of the free edge tone phenomena is explained. The dimensional analysis, as well as the Buckingham Pi theorem, are also discussed. Chapter 3 explains the two phases of the project, the exploratory phase, and the Therminol-66 phase. The design process of the prototypes as well as the loops built to test them are discussed in each respective phase. Chapter 4 analyzes and discusses the data obtained from the tests of the developed prototypes. Chapter 5 provides a summary of the project as well as the conclusions.

Chapter 6 discusses potential future work that can be performed.

Chapter 2: Theory

2.1 Edge Tones

Edge tones are common in musical instruments, most notably in the grand pipe organ. The typical pipe organ is composed of several key components such as those shown in figure 2.1. The languid serves as both the bottom of the air column and the ramp used to constrict and accelerate the fluid flow through the flue. The opening bounded by the languid and the tip of the labium is known as the mouth. As the air exits the flue it forms a type of jet with relatively high velocity. The jet impinges on the tip of the labium where it begins to oscillate from one side to the other. These oscillations are accompanied by noise making vortexes, which is how the pipe organ gains its voice. The principle of the jet oscillating from one side of the labium to the other is known as an edge tone. The edge tones found in pipe organs are known as coupled edge tones because one side of the labium is coupled to an air column which helps force the frequency of the oscillations to match the natural frequencies of the column [8].

Unlike those of the pipe organ, free edge tones are not coupled with an air column. Free edge tones operating in air are much better understood and researched than those of coupled edge tones or of those utilizing different fluids; although the fundamental physics between them are similar. The free edge tone in air consists of a flue, labium, and languid, like the coupled variety, although they typically go by different names as shown in figure 2.2, where the flue is better known as the jet orifice and the labium is better known as the knife edge. The term languid is only used when referring to pipe organs. Key dimensions of the edge tone (free and coupled alike) are the mouth height (h), the orifice diameter (d), and the mean exit velocity of the jet (v).

The free edge tone produces frequencies due to the flipping of the fluid jet across the knife edge. At low Reynolds numbers, it is generally accepted that this flipping action is caused by jet instability resulting from a feedback mechanism generated at the tip of the knife edge [9] [10]. The unstable jet tends to one side of the knife edge over the other. Whichever side the majority of the jet favors will see an increase in pressure. This increase in pressure produces a force on the jet causing it to flip to the other side. The other side's pressure builds until the jet flips back. This process continues indefinitely [11].

In order for the edge tone phenomena to occur, the knife edge must interact with the

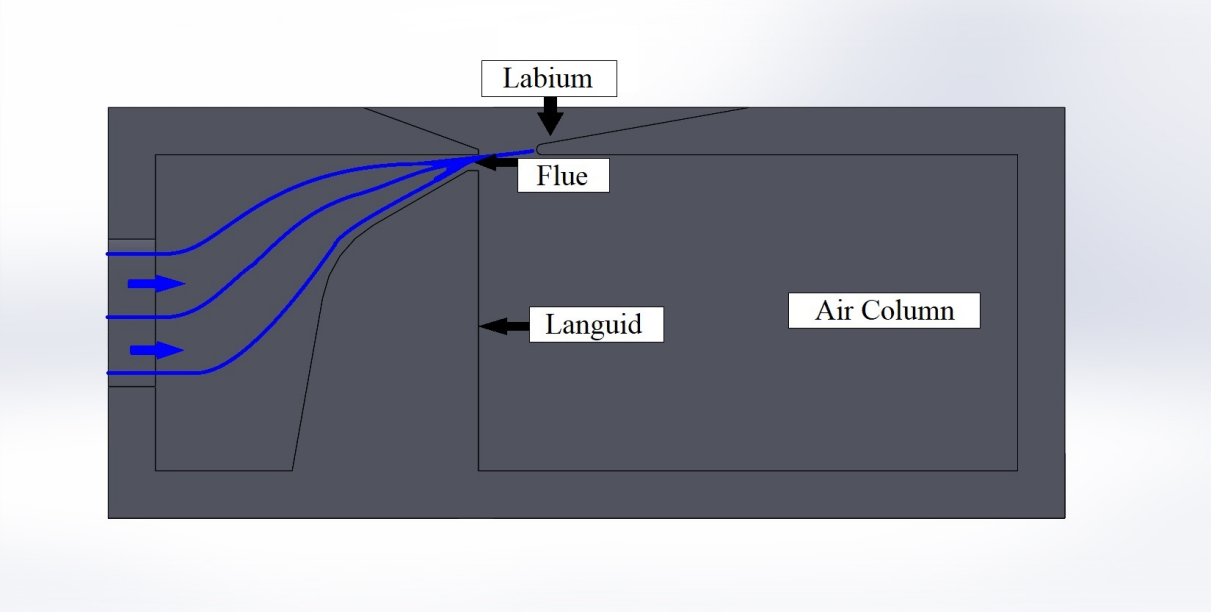

Figure 2.1: Simple diagram of a typical pipe organ with labels of key structural features. The blue lines indicate air entering the bottom of the pipe organ, proceeding through the flue before making contact with the tip of the labium where oscillations take place.

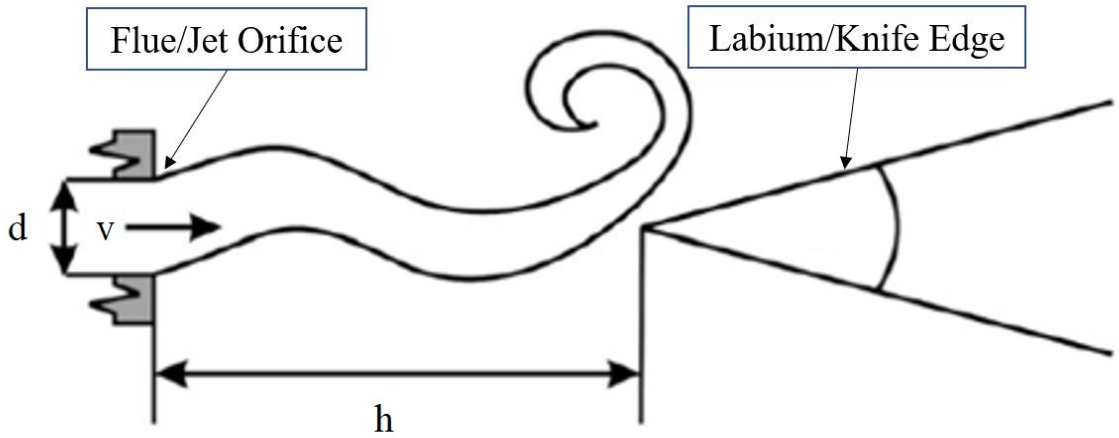

Figure 2.2: Simple diagram of a typical edge tone with labels of key structural features and dimensions.

jet while the jet is sufficiently unstable. The jet's instability increases as the distance from the orifice increases. If the knife edge is too close to the orifice, the jet will not have attained suitable instability and the phenomena will not occur. Similarly, if the knife edge is too far away, the jet will have become too unstable to oscillate across the knife edge. This creates a zone of functional instability in the jet where the knife edge must reside to produce the effect. The functional zone of the jet can be altered by adjusting the jet velocity, the orifice diameter, and fluid properties. If any of these are changed, the knife edge location must be adjusted accordingly to keep it within the functional zone.

Edge tone phenomena produce very distinct signals with various stages appearing at higher jet velocities. These stages can possess some degree of hysteresis and increase in slope as the stage number increases. Each stage is a separate frequency or peak from the output of a Fast Fourier Transform (FFT) of the signal produced by an edge tone. A typical example of the stages produced by an edge tone can be seen in figure 2.3 where f is the frequency and u is the mean velocity of the jet at the orifice. There is much debate about what exactly causes the different stages to appear as well as when the frequency will jump from one stage to another. It is possible for multiple stages to exist simultaneously, further complicating the already debated problem of the edge tone [11].

2.2 Dimensional analysis

Dimensional analysis is a tool commonly used in applied mathematics and engineering to make inferences about phenomena using the base quantities of the physical properties related to the phenomena. Using this tool, dimensionless numbers can be attained such as the well known Reynolds and Strouhal numbers. Dimensionless numbers can be used to find similarity between large objects and small models, as well as describe similar phenomena across many different applications.

The method of repeating variables and the Buckingham Π Theorem is a method by which dimensionless parameters can be obtained. First popularized by Edgar Buckingham, the theorem is among the simplest and most popular methods used to develop dimensionless parameters to describe phenomena today. The theorem produces dimensionless Π groups by multiplying and dividing the key parameters. There are six steps to working through the theorem and they are explained below [12].

Step one: List the parameters involved in the problem. Parameters must be independent from one another and must include the dependant variable. The number of valid

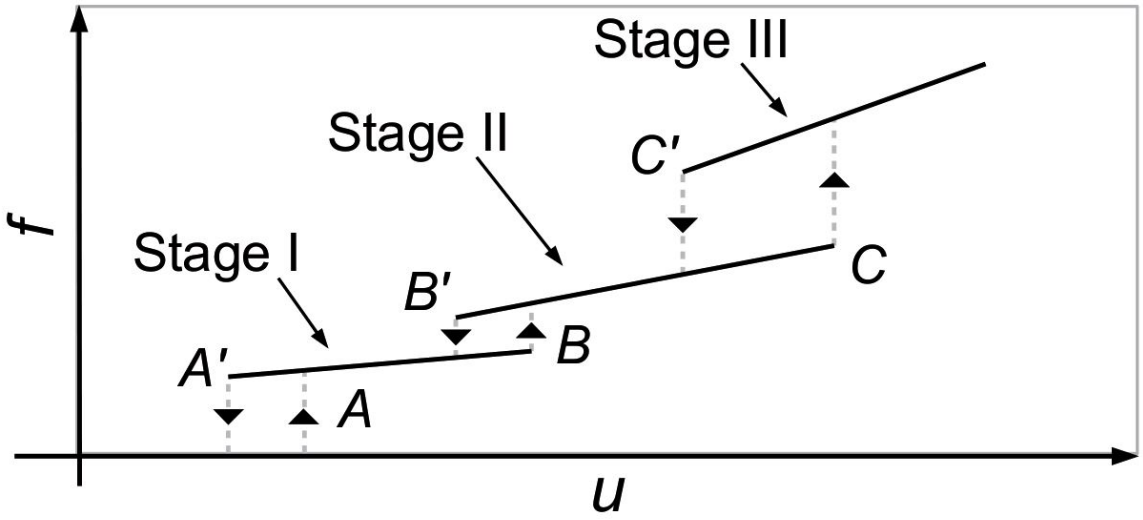

Figure 2.3: Typical shape and layout of edge tone produced stages. Hysteresis of the stages is illustrated by points A, B and C along with their respective primes. Primes indicate where on the stage the frequency jumps down to the lower stages during a decrease in jet velocity and A, B and C indicate the location where the frequency jumps up during a velocity increase. [2]

parameters identified is labeled as n [12].

Step two: Break down each of the parameters into their elementary dimensions. There are only seven elementary dimensions and they are length (L), mass (m), temperature (T), time (t), electric current (I), amount of light (C), and amount of mass (N). For example, a Newton, the si unit of force, is defined as having the base units $kg \cdot m \cdot s^{-2}$ using standard conventions. The Newton would be rewritten in the elementary units of mass, length, and time and would take the form $m \cdot L \cdot t^{-2}$ [12].

Step three: After breaking down all parameters into their elementary dimensions, count the number of dimensions present with a maximum of seven. The number of dimensions counted is given the variable j. The Theorem states that the number of Π groups (k) will be $k = n - j$. If at any point the analysis does not work out, first ensure enough parameters in step one were chosen, if that is not the problem, subtract 1 from j and restart on this step [12].

Step four: Choose the repeating parameters. These will be the parameters that can appear in all of the Π groups and they need to be chosen with care. The dependent variable should never be a repeating parameter. The repeating parameters must not be

able to form a dimensionless number by themselves. All of the elementary dimensions must be represented in the repeating parameters. Whenever possible it is recommended to pick the simplest parameters to be repeating [12].

In step 5: Form the Π groups by combining each parameter that was not chosen as repeating with the combinations of repeating parameters until the dimensionless groups are found. Repeating parameters can be raised to any exponent and multiplied by any pure constant to achieve dimensionless Π groups. The first Π group (Π_1) typically contains the dependant variable [12].

Step 6: Check that all Π groups are indeed dimensionless, and place the Π groups into the form $\Pi_1 = f(\Pi_2, \Pi_3 ... \Pi_k)$ [12]. The theorem is now complete and dimensionless numbers have been generated.

2.3 Dimensionless Numbers in Fluid Mechanics

Dimensionless numbers are used heavily in fluid mechanics to explain a wide variety of phenomena. The most common of which, rarely neglected in any fluids related paper, is the Reynolds number and is often used to determine whether a flow is turbulent or laminar. Many other numbers are used such as the Strouhal number, which characterizes vortex shedding due to bluff bodies; the Rayleigh number, associated with buoyancy driven flows; and many others [12].

The Reynolds number is of great interest to most fluid related problems; it is defined as the ratio of the inertial forces to the viscous forces. Theoretically, two fluids with the same Reynolds number will have the same flow characteristics. Similarly, the flows around two like objects of different sizes will behave in the same manner, providing the Reynolds numbers also match. This is very important in scaling efforts, such as testing jumbo jets for optimal wing aerodynamics. In place of a full sized wing, which would not fit in even the world's biggest wind tunnel, a smaller model can be made and used to simulate the conditions experienced on the full sized wing. The Reynolds number is also very commonly used to identify turbulent flows ie. $Re > 2300$ for pipes and $Re > 1400$ for parallel plates [12]. The Reynolds number is expressed as

$$Re = \frac{\rho v L}{\mu} \tag{2.1}$$

Where ρ is the density of the fluid, v is the velocity, L is the characteristic length and μ is the dynamic viscosity [12].

Figure 2.4: Typical vortex shedding caused by flow interference with a cylindrical bluff body. [3]

The Strouhal number is also a very commonly used dimensionless number in fluid mechanics, although less than the famous Reynolds. The Strouhal number is used to determine the frequency of vortices shed from a fluid flowing around a bluff body. The Strouhal number is expressed as

$$St = \frac{fL}{v} \tag{2.2}$$

where f is the frequency of the shed vortices, v is the mean velocity far upstream of the bluff body, and L is the characteristic length. The most heavily studied bluff body is the circular cylinder. Figure 2.4 shows a simple bluff body flow for reference. The Strouhal number is very commonly referenced in almost all fluid problems involving sound generation from a vortex.

2.4 Fourier Transform

In 1822, Joseph Fourier proved that a repeating function can be expressed as an infinite summation of cosine and sine wave functions called a Fourier series. Fourier series are very useful in mathematics and engineering and are commonly used as they can provide solutions to ordinary differential equations subjected to forced oscillations as well as partial differential equation approximations.

In signal processing applications the Fast Fourier Transform (FFT) is extremely useful as it allows a complex signal to be broken down into a Fourier series. This is the method employed to monitor equipment vibrations, compress audio, and to analyze just about every auditory experiment. A complex waveform is passed through a FFT which produces a Fourier series that sums to the original waveform. The amplitude and frequency of each

Fourier series term can be plotted producing an amplitude vs frequency graph. This plot can be used to identify the dominant frequencies that make up the waveform.

Chapter 3: Design and Methodology

This chapter discusses the design process and test methodology of an acoustic flow meter utilizing edge tone phenomena along with the design of the flow loop on which the flow meter was tested. At the beginning of the project, there was no functional theory as to how the acoustic flow meter would operate. Part of the project's requirements were to develop a design that would produce a tone that was proportional to the fluid flow. There were no restrictions as to how this was to be achieved, as long as the tone originated from the fluid without the use of electronics.

The project was split into two phases. The first phase was exploratory involving rapidly prototyping technologies to quickly test prototypes on a simple water based loop. The second phase began once a suitable prototype had been demonstrated on the simple water loop. This phase required a new, much more elaborate loop to be constructed. The new loop was to utilize a molten salt substitute, as the acoustic flow meter was originally intended to operate in nuclear conditions with molten salt (FLiBe). Temperature, reactivity, and health hazards associated with molten salts such as FLiBe pose many difficulties in the lab. FLiBe has a high operational temperature and contains Fluorine, lithium, and beryllium which are all very reactive and considered health hazards [13] [14] [15]. Constructing a suitable loop and prototype to withstand FLiBe would have been prohibitively expensive, hence the need for a substitute. Therminol-66, a popular heat transfer fluid, was the chosen substitute and the second loop was built accordingly.

3.1 Operating Conditions

Phase one operating conditions were not tightly controlled to promote the rapid testing of many different prototypes. Typically, water was straight from the tap and was allowed to freely heat up and/or cool down as laboratory conditions allowed.

Phase two required the Therminol-66 to be heated to 95°C where it achieved similarity of physical properties with that of FLiBe at typical molten salt reactor operational temperatures of around 600°C [16]. The Therminol-66 needed to be maintained around this temperature to ensure continued similarity.

3.2 Exploratory Phase

The purpose of the exploratory phase was to invent a method to measure the flow rate of a system through acoustic signals generated by the system's fluid. This, to the best of the author's knowledge, had never been performed before. It was decided by those invested and the researchers that the best course of action to develop such a device was to take an approach similar to how Thomas Edison invented the light bulb, namely, to make educated guesses and test them quickly.

3.2.1 Test Loop

The first loop was designed to operate with room temperature water, for the purpose of exploratory design and rapid testing of flow meter prototypes inspired from musical instruments. The loop consisted of an off the shelf submersible pump that resided in a sink filled with water. The water was pumped from the sink through a garden hose where it entered 4 feet of galvanized 3/4 inch pipe before passing through the prototype and continuing through another 8.5 feet of the same pipe where it was returned to the sink. Figure 3.1 shows a picture of this loop with a prototype installed. The loop was held up with 3D printed legs and featured a pressure relief valve for safety concerns.

Since the purpose of phase one was exploratory, the exact range of Reynolds numbers provided by the pump were of little concern. The submersible pump was chosen because it was inexpensive and relatively simple to set up and begin testing. The effective flow rate through the prototype was moderated using two valves. One valve was located at the start of the first 4 foot section of pipe and acted as a bypass to return a portion of the fluid straight back to the sink. Opening this valve reduced the flow through the prototype. Once that valve was fully open, the flow could be further reduced through the prototype by closing another valve down stream of the flow meter. This forced more fluid through the bypass. This method of flow moderation was chosen for its simplicity and to prevent putting unnecessary strain on the pump.

3.2.2 Instrumentation

The flow through the prototype was determined via a non contact ultrasonic flow meter (NCM B/E Series). The ultrasonic flow meter had a clamp on transducer that was located a sufficient distance after the prototype such that the flow became fully developed before the transducer. The ultrasonic flow meter output a 4-20 mA signal that was linearly

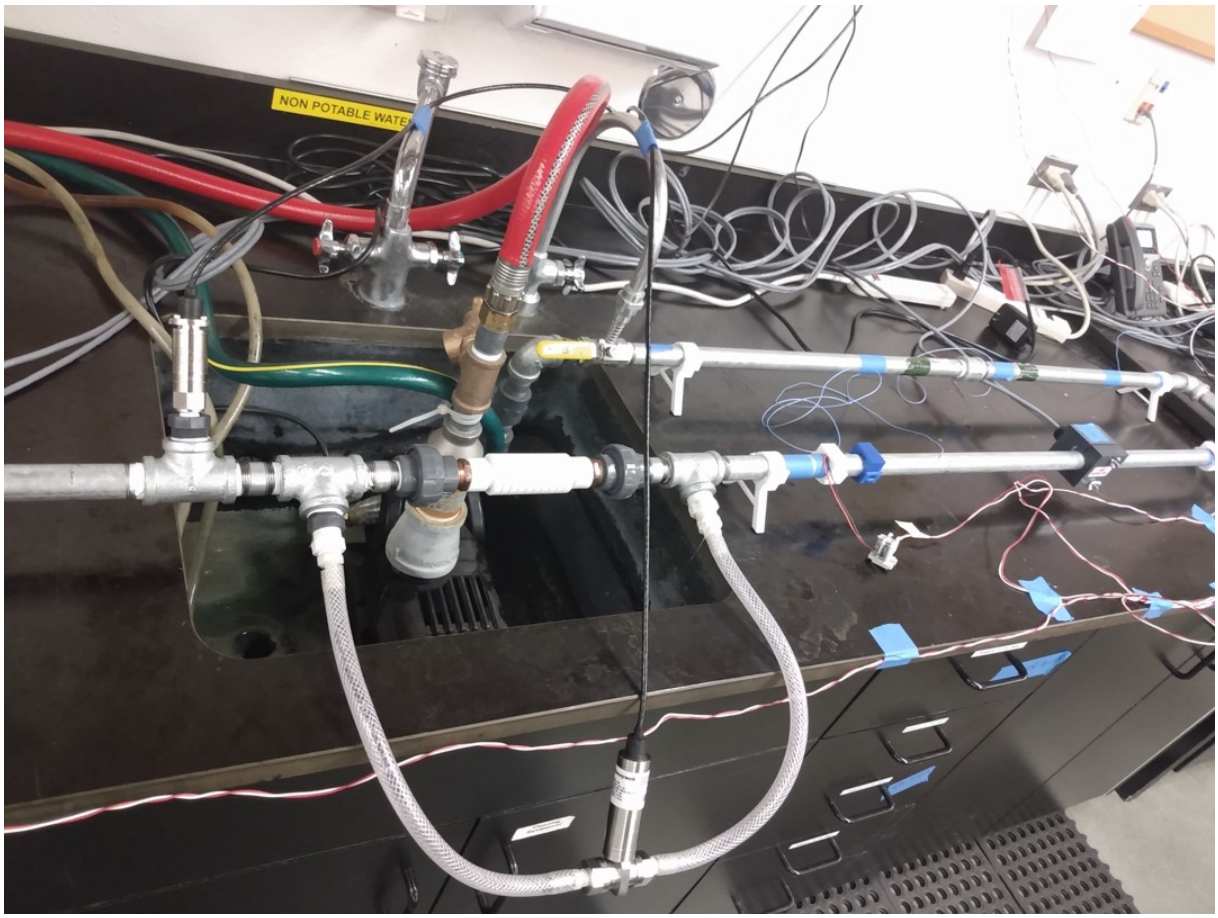

Figure 3.1: First experimental loop for rapid prototype testing.

Figure 3.2: Piezoelectric sensors.

proportional to the range of flow (0-60 GPM).

Pressure was measured in the loop using two Honeywell FP5000 pressure transducers with a range of 0-150 psi also with an output of 4-20 mA that was linearly proportional to the pressure. The first pressure transducer was located several inches upstream of the prototype and the second pressure transducer was a differential type. One leg of the differential transducer was located immediately before the prototype and the other was immediately after so that the pressure drop across the prototype could be best measured.

Vibrations produced from the prototypes (if any) were recorded using piezoelectric sensors like those shown in figure 3.2. The piezos produce a voltage that is proportional to the strain experienced by the ceramic disc. The sign of the voltage is dependant on whether it is compressive or tensile strain. Accelerometers are basically piezoelectric sensors with a mass on top of them. The mass is used to calibrate the magnitude of the voltage to a known force unit. To test the piezos, an accelerometer was purchased and the signals between them compared. There was no detectable difference between the piezos and the accelerometers measured signal frequencies. The amplitudes, however, did have some differences suggesting that the piezos were suitable for accurate frequency measurements only. Amplitudes measured from the piezos should only be used to observe trends.

Table 3.1: List of Equipment and instrumentation used on the Therminol-66 Loop

Equipment Name	Manufacterer	Part Number
Pressure Transducer	Honeywell	FP-5000
Differential Pressure Transducer	Honeywell	FDW
Thermocouple	Omega	KMQSS-125G-6
Coriolis Flow meter	Emerson	MMI-20022762
Gear Pump	Orberdorfer	N990
Accelerometer	PCB	352A24
Signal Conditioner	PCB	482A21
Piezioelectric sensor	Generic	N/A
Heater	McMaster-Carr	4668T1
PWM Controller	TempCo	TPC10063
Current Module	National Intruments	9203
Current Module	National Intruments	9203
Voltage Module	National Intruments	9223
Thermocouple Module	National Intruments	9213

Data acquisition was performed using a National Instruments CompactDaq chassis and several National Instruments modules alongside LabVIEW. Modules used include a NI-9223 which has 4 differential voltage inputs and can sample up to 1Ms/s/ch, and two NI-9203 modules that each have 8 current inputs and can sample up to 200ks/s. The ultrasonic flow meter and pressure transducers each require a separate NI-9203 module to function. The LabVIEW program recorded 20,000 samples at a rate of 20,000 Hz. The vibration data from the piezos was run through a FFT; the results of which were averaged with the last 10 seconds of data. Pressure, temperature, and flow rate data were similarly averaged.

The names, manufacturers, and models of all equipment and instrumentation used on the Therminol loop are listed in table 3.1. Because the first loop was only exploratory to find a suitable design, the equipment used on it is not included in this table.

3.2.3 Prototypes

In an effort to build and test prototypes as quickly and cheaply as possible, two Flash Forge Creator Pro 3D printers were purchased. The printers each had dual nozzles which allowed for dual material printing. The vast majority of prototypes were printed exclusively out of Polylactic Acid (PLA). There were a few designs that required the use of dissolvable supports to print properly. The material used for this was Polyvinyl

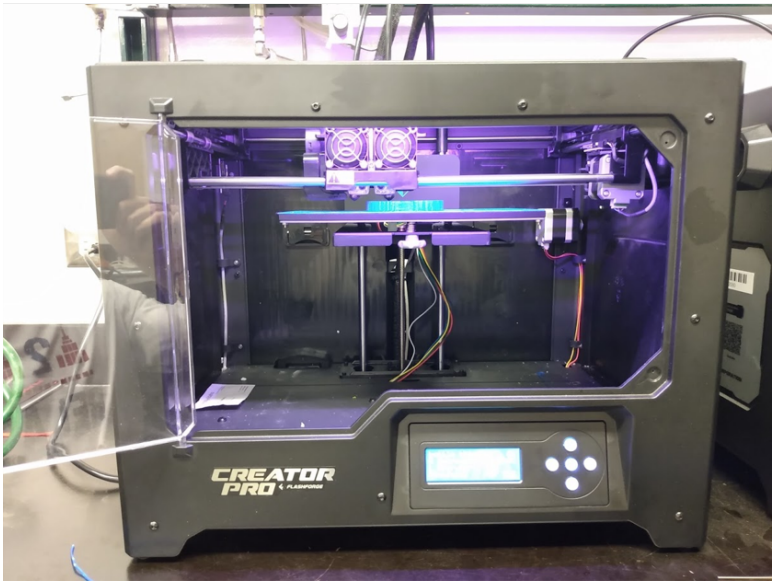

Figure 3.3: Flash Forge Creator Pro 3D printer

Alcohol because it is water soluble. A picture of the printer can be seen in figure 3.3.

PLA was the preferred plastic because of its printability, cost, resistance to warping, and dimensional accuracy. While easy to print, there are some significant draw backs to PLA. For one, it has a very low glass transition temperature of 60°C making it unsuitable for any tests of elevated temperature [17]. PLA also has poor layer to layer adhesion making the prototypes unsuitable for high pressures as well.

The subject of largest inspiration for prototype design was musical instruments. A musical instrument was researched and the method by which it produces sound was replicated in CAD with modifications so it could be 3D printed and connected to the loop, if practical, to test the idea. The printed design, if possible to be connected to the loop, was. If not, it was tested in the sink to see if any vibrations could be detected with the human ear or touch. Only the most notable designs are presented below.

3.2.3.1 Ball Percussion Prototype

One of the earliest designs of note was inspired by percussion instruments. This design can be seen in figure 3.5. As the flow enters the device, it enters several spiraling channels which all lead to a hollow doughnut shape in the center. The flow enters the doughnut where it pushes a ball around and around. The ball makes contact with the outer wall of the doughnut, thereby producing a measurable vibration.

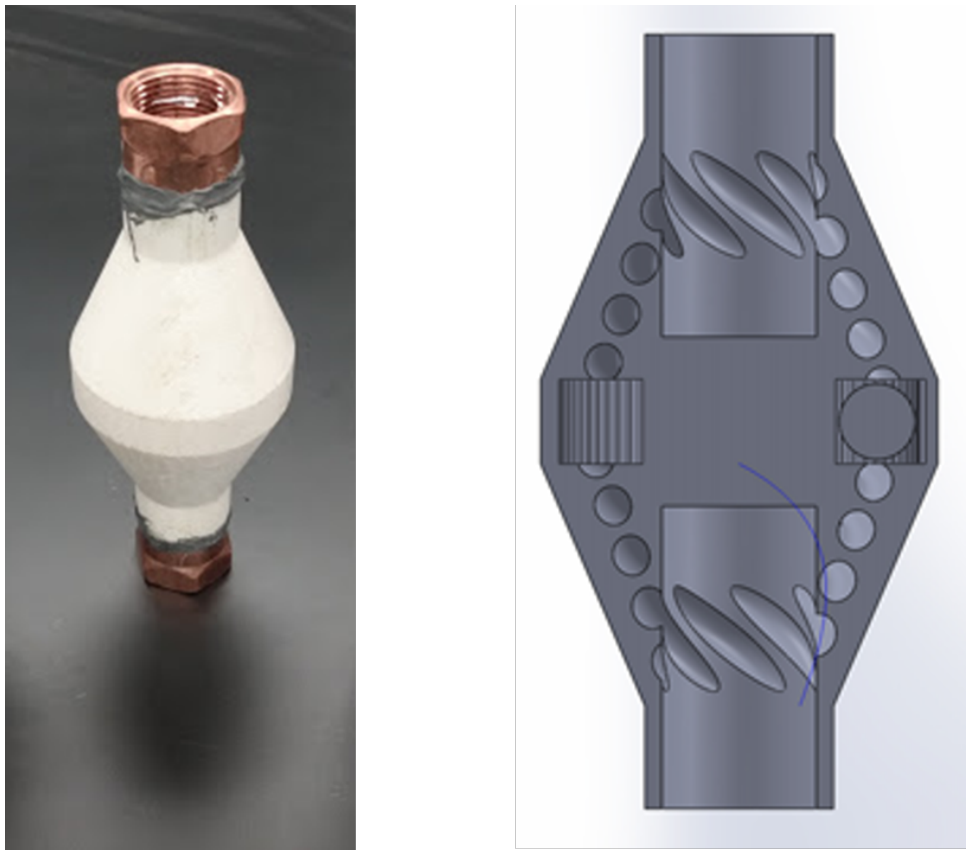

Figure 3.4: Percussion prototype as built (left) and CAD cross section (right)

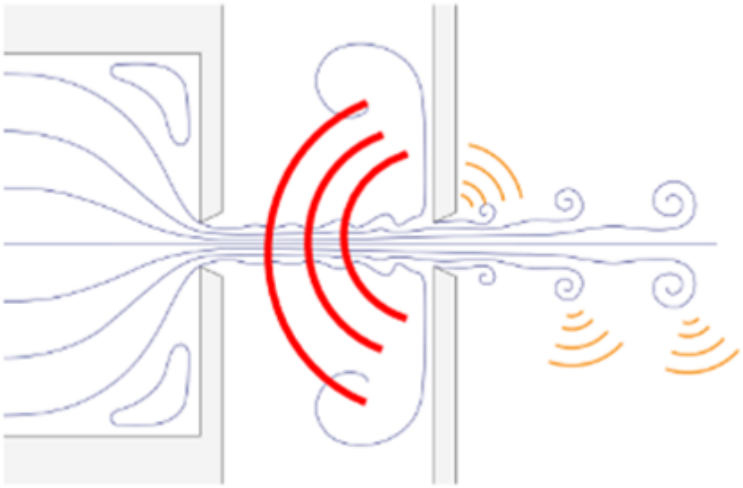

Figure 3.5: Drawing to illustrate the hole tone phenomena.

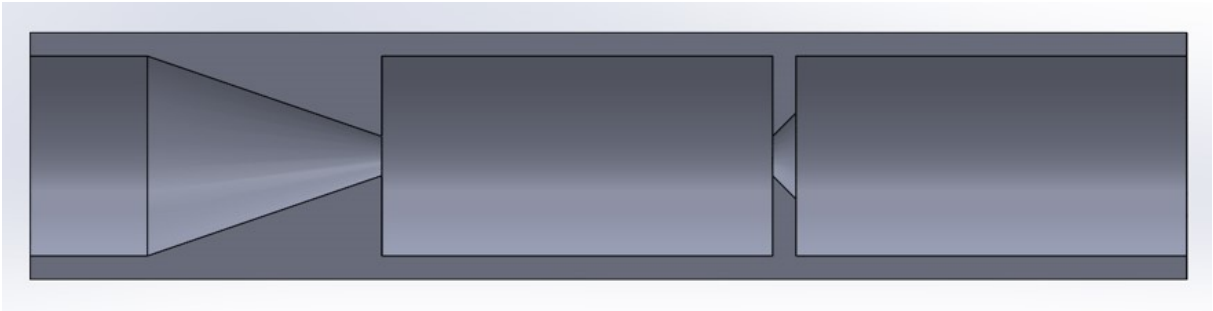

Figure 3.6: Cross section of the hole tone prototype.

3.2.3.2 Hole Tone Prototype

The hole tone phenomena is the same as that, which causes the whistle in tea kettles and bird calls. The hole tone functions via a jet that impinges on a plate with an orifice. As the jet passes through the orifice in the plate, vortices are shed producing the tone. This is illustrated in figure 3.6. This same idea was modeled and 3D printed to be tested and is shown in figure 3.6.

3.2.3.3 Harmonica Reed Prototype

Harmonicas function via a reed that vibrates as the fluid flows past it. The reed is a flexible piece of material that somewhat blocks the flow. As the fluid pressure builds up behind the reed, it eventually flexes allowing a portion of the fluid to pass, which lowers

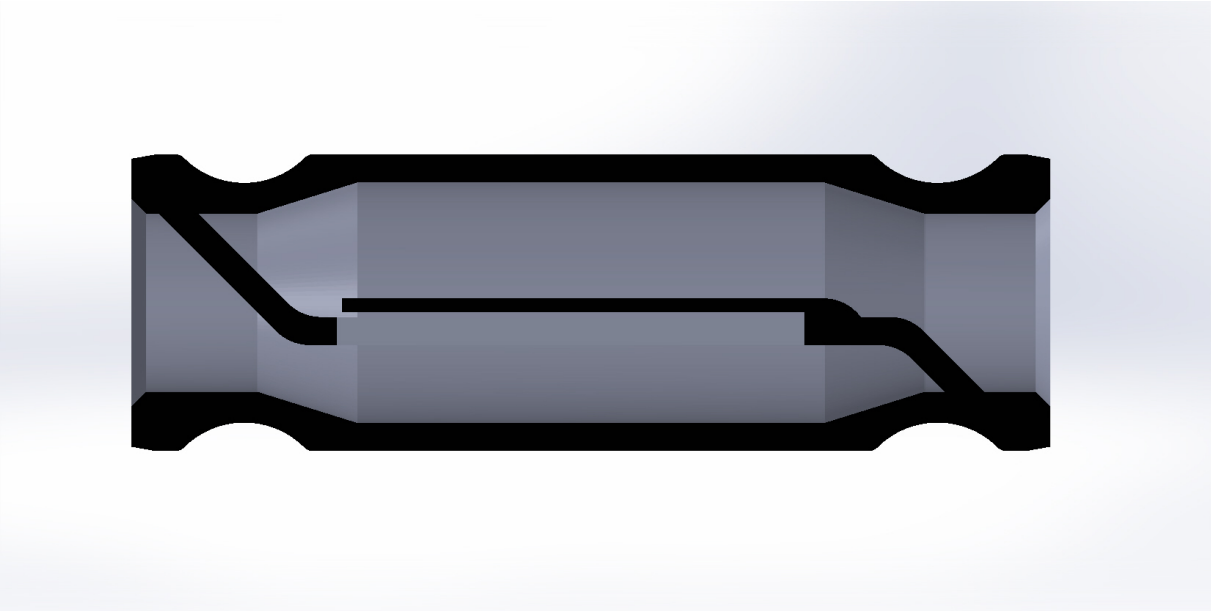

Figure 3.7: Harmonica style prototype cross section where flow enters from the left and then goes up past the horizontal reed in the middle before exiting through the right.

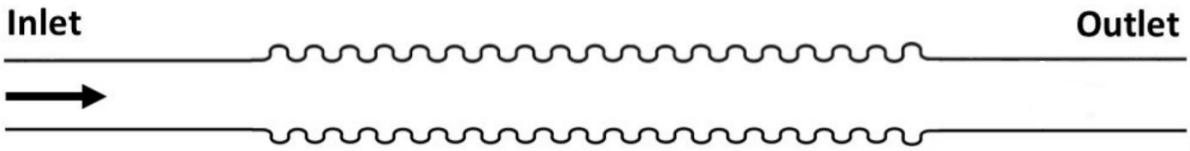

Figure 3.8: Corrugated pipe schematic.

the pressure and the reed returns to its original position. The pressure begins to rise again and this process repeats producing an undulating flow. Figure 3.7 shows the harmonica style prototype that was printed and tested.

3.2.3.4 Bellows Prototypes

The bellows style prototypes showed great promise. The bellows is a tube with a corrugated wall shape as shown in figure 3.8. The bellows shape produces sound by generating vortices in the troughs of the corrugations. This shape is commonly found in reusable straws, such as the one shown in figure 3.9, and can easily demonstrate the whistling phenomena by simply blowing into one side. This design was attempted several times and the different iterations can be seen in figures 3.10 through 3.13.

Figure 3.9: Corrugated straw.

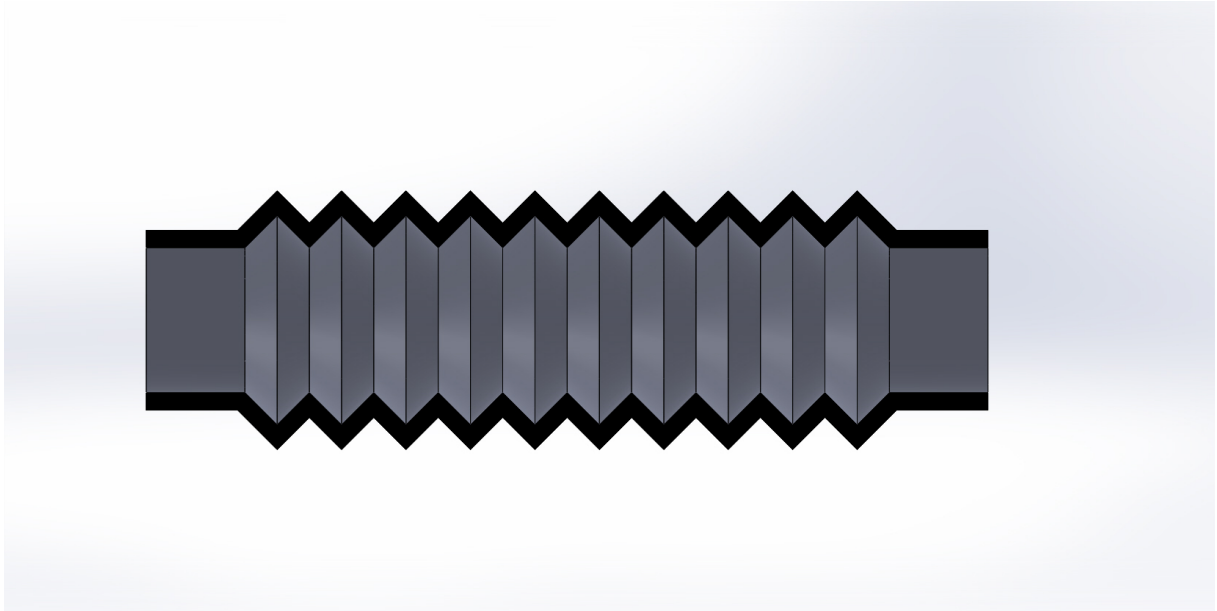

Figure 3.10: Bellows prototype cross section with 90 degree corrugations.

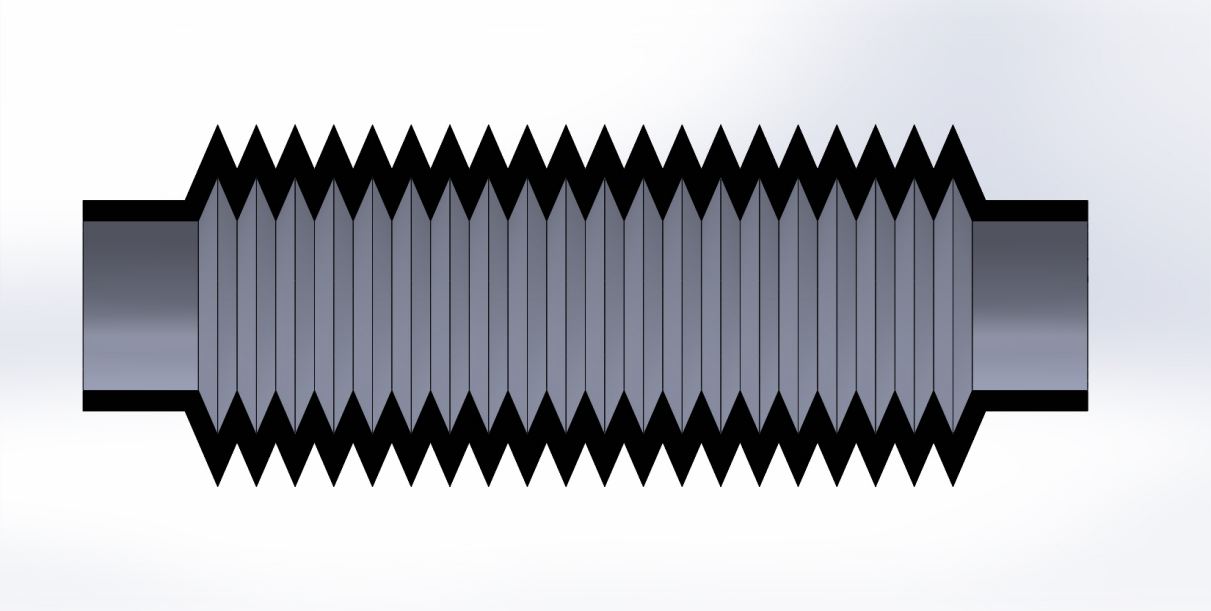

Figure 3.11: Bellows prototype cross section with 45 degree corrugations.

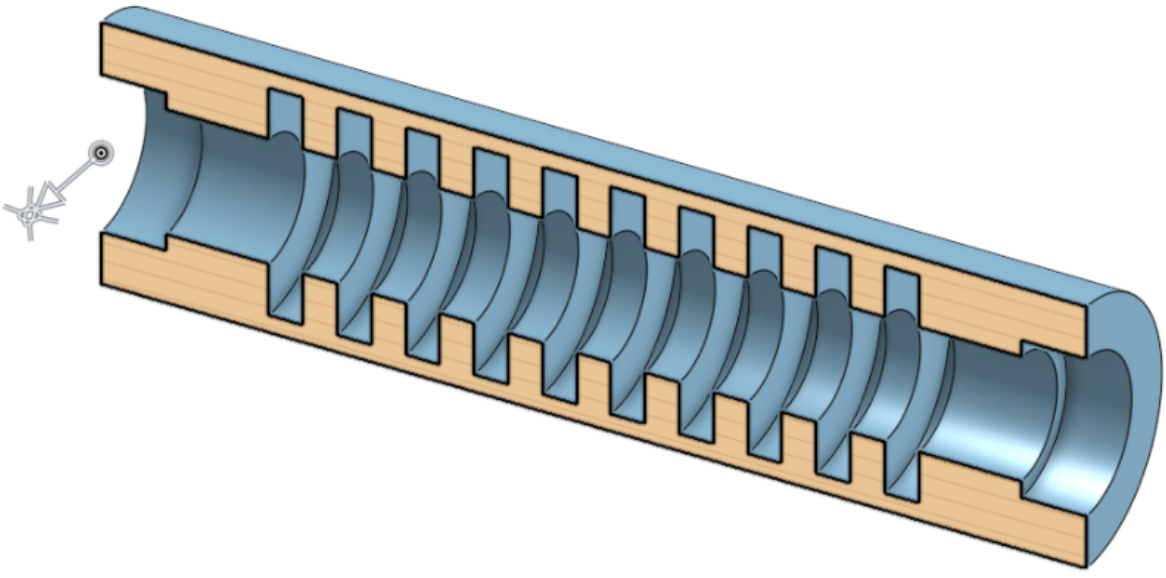

Figure 3.12: Bellows prototype cross section with square corrugations.

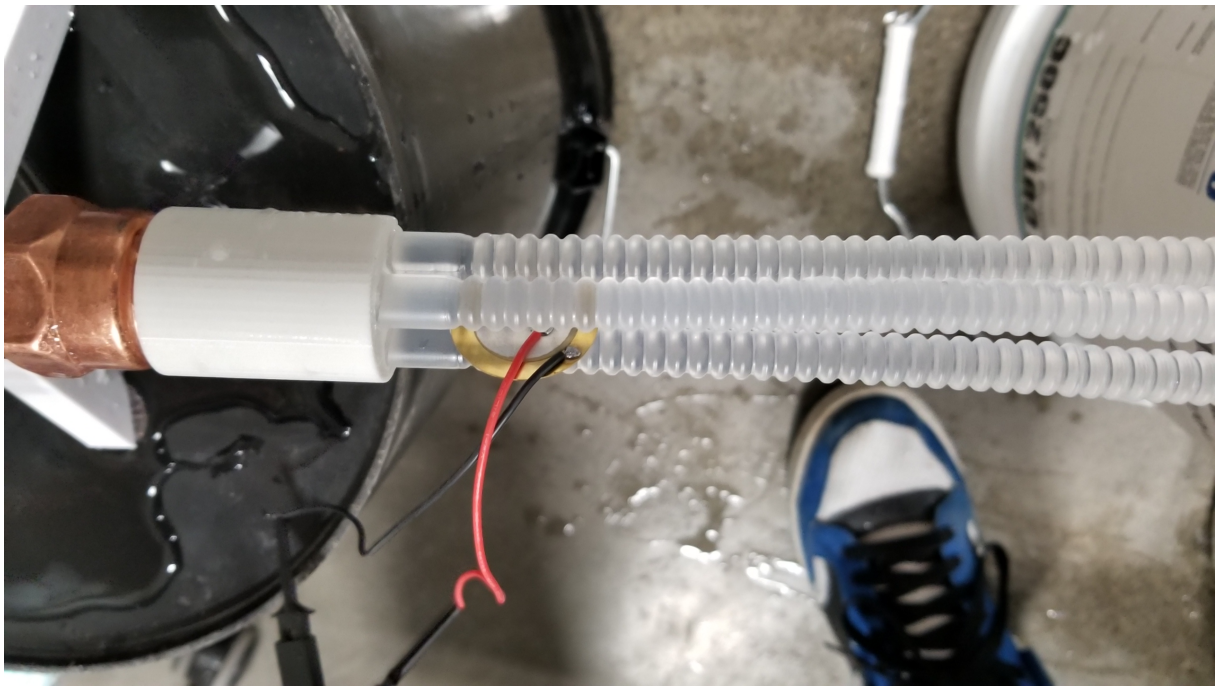

Figure 3.13: Bellows prototype with whistling corrugated straws.

3.2.3.5 Cavitation Prototype

Cavition causes massive shock waves in the liquid. The idea behind this prototype was to utilize the sound from cavitation to determine the flow rate via a cavitating venturi. A venturi is a gradual reduction of the pipe diameter, followed by a straight section before the pipe gradually expands back to the original diameter. To maintain the mass flow rate through a venturi, the velocity of the fluid must increase through the constricted section. This is accompanied by a reduction in the static pressure of the liquid. Cavitation occurs if the static pressure decreases below the vapor pressure of the liquid. Cavitation is when a liquid is vaporized due to a sudden local decrease in pressure. Bubbles of vapour quickly implode on themselves producing large shock waves in the liquid. The cavitation prototypes can be seen in figures 3.14 and 3.16.

3.2.3.6 Bluff Body Prototype

The bluff body prototype uses the same phenomena that common vortex flow meters use but in a different way. Vortex flow meters function by introducing a bluff body into the flow path of the fluid. The bluff body causes the creation of vortices behind it; these

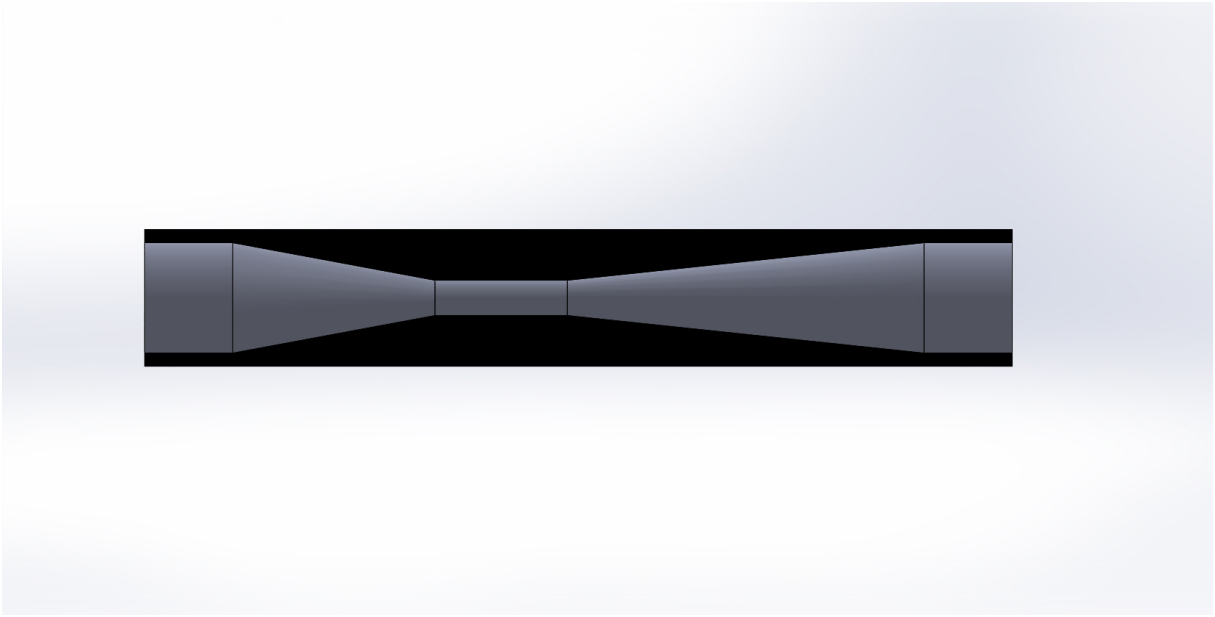

Figure 3.14: Cavitation prototype cross section with constriction down to 8 mm.

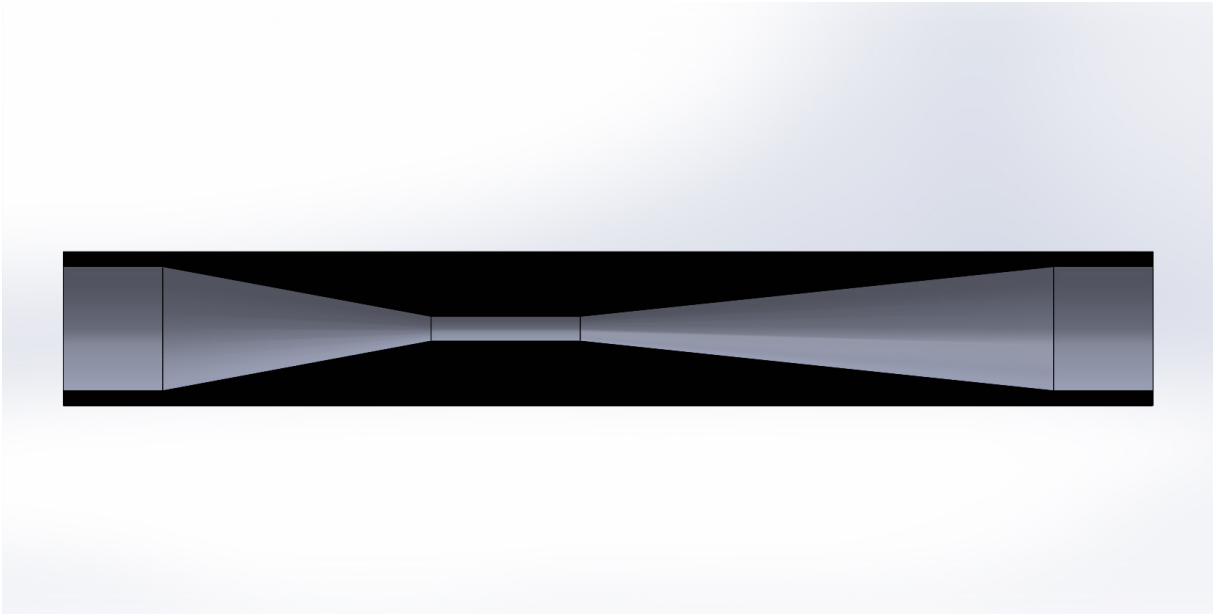

Figure 3.15: Cavitation prototype cross section with constriction down to 5 mm.

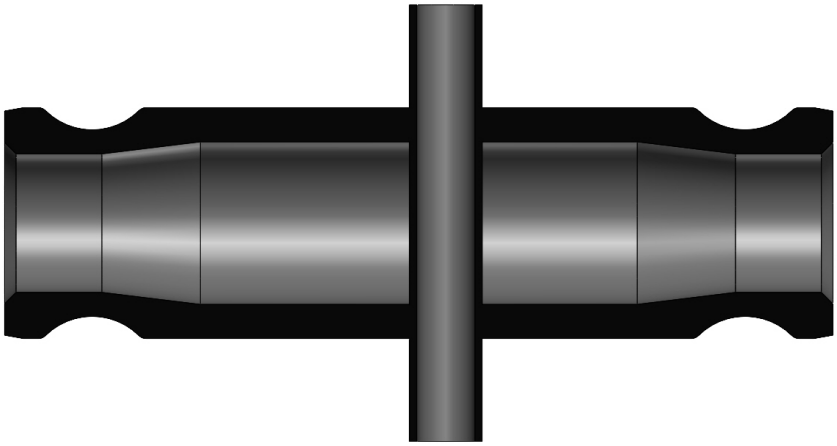

Figure 3.16: Bluff body prototype cross section.

vortices apply a small force on the bluff body causing it to vibrate. The vortex flow meter measures the displacement of the bluff body to determine the flow rate. Using this same principle, the bluff body prototype, as seen in figure 3.14, aimed to excite the natural frequency of an air column by using the air column itself as the bluff body. The tiny vibrations cause the middle of the air column to vibrate and if those vibrations match the wavelength of the air column, a tone should be produced.

3.2.3.7 Edge Tone Prototypes

The edge tone prototypes were originally inspired from pipe organs. A regular pipe organ was 3D printed to determine if it would function in air. After discovering it did indeed work in air, the pipe organ was fitted with a tube and placed in the sink on a whim. The pipe organ produced an audible tone and large physical vibrations when the flow was high and the device was fully submerged in water. The pipe organ tested can be seen in figure 3.17. Pipe organs do not make any effort to capture the air that is pushed through them. This makes for a problem when trying to use one as a flow meter as most flow applications desire to keep all the fluid within the system.

To fix the fluid loss problem and to allow the device to be placed on the loop, the pipe was reprinted with a section to capture the fluid and redirect it back into the piping.

Figure 3.17: 3D printed pipe organ cross section.

This modified pipe organ can be seen in figure 3.18. Initial concern with this was that the walls used to direct the flow back into the pipe would interfere with the operation of the edge tone and it would cease to function. To the best of the author's knowledge, this had never been attempted before. In addition, all previously tested edge tones in literature had at least one side of the mouth open to the environment thereby allowing the pressure to drop to atmospheric. In the modified pipe organ this is no longer the case and there needs to be enough pressure after the edge tone to allow the fluid to return through the loop to the sink. It was unknown if the pressure drop would be sufficient to continue producing a tone.

The act of capturing the fluid after it passes through the mouth and forcing it to continue through the rest of the loop did not cause the edge tone to cease functioning. It did, however, decrease the ability of the device to purge air bubbles trapped in the pipe organ portion. The modified pipe organ did not vibrate to its full potential until all bubbles had been purged. To fix this, a small slit was introduced as shown in figure 3.19 that allowed the bubbles to escape and purge from the system.

The success of the pipe organ design encouraged research into its operational mechanism which is the edge tone. Edge tones in literature have similar but ultimately different

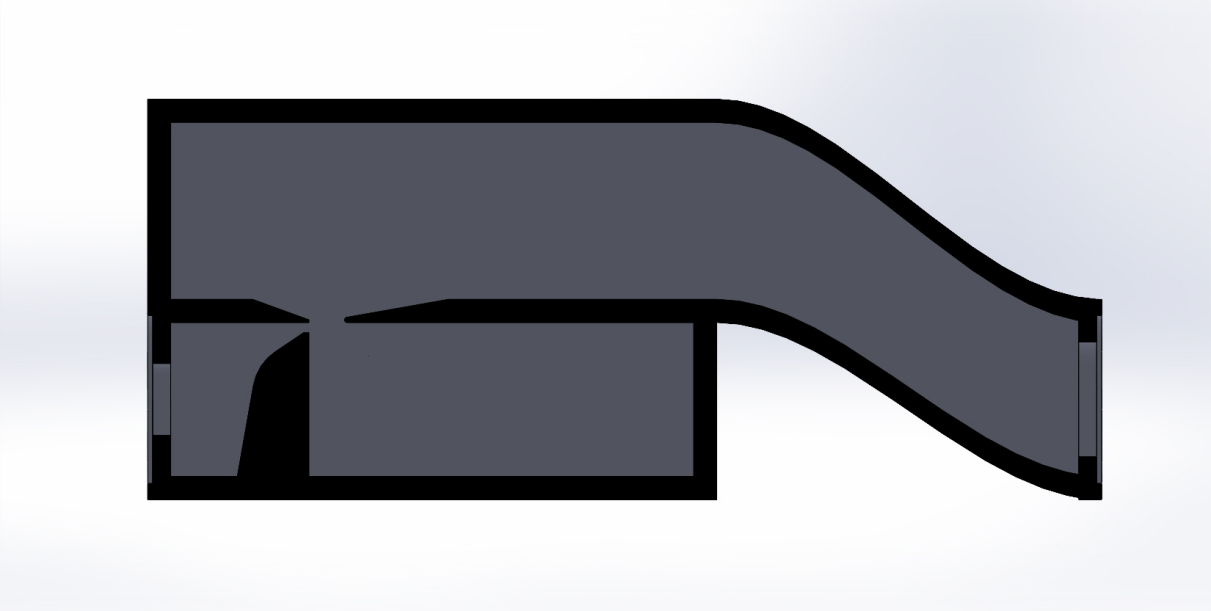

Figure 3.18: Modified 3D printed pipe organ cross section.

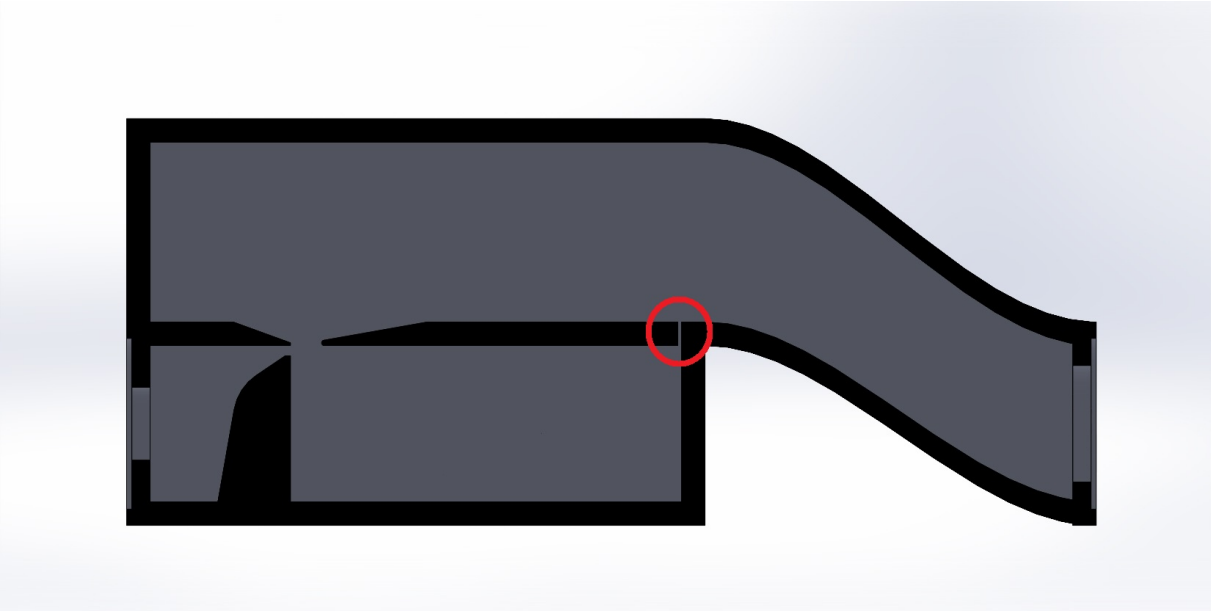

Figure 3.19: Modified 3D printed pipe organ cross section with slit as indicated by the red circle.

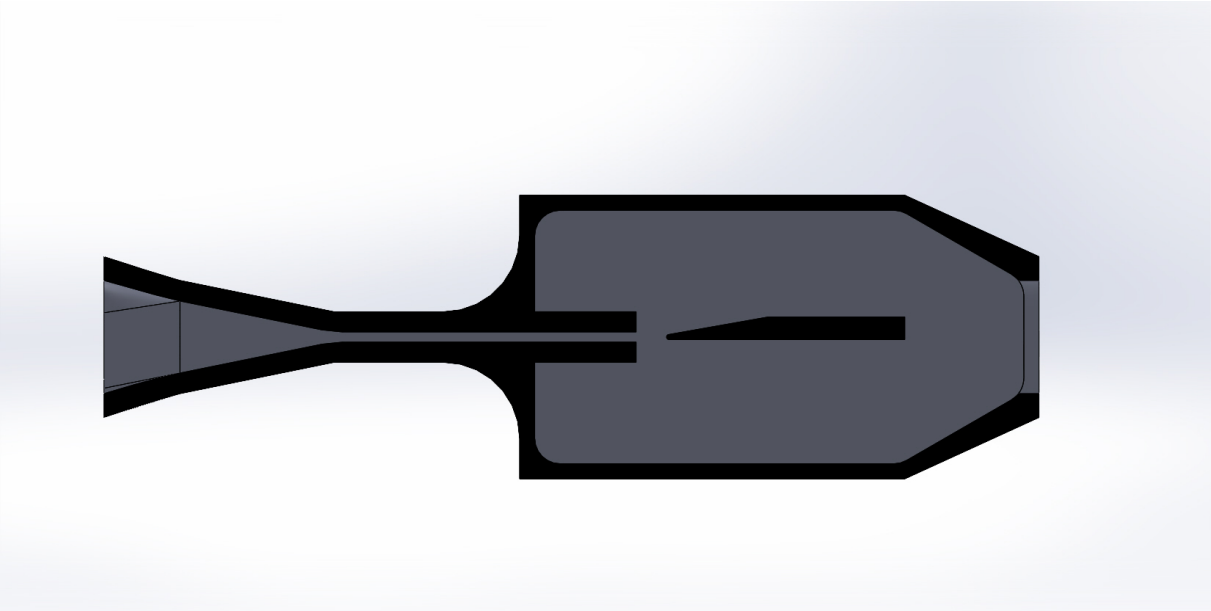

Figure 3.20: Edge Tone Prototype

form factors to that found in a pipe organ. Typically edge tones had the labium equivalent, the knife edge, positioned in the middle of a straight jet rather than have the jet shoot out at an angle to strike the tip of the labium like how it is in a pipe organ. Given that many pipe organs have open tops and allow fluid to escape on both sides of the labium, and edge tones in literature do just that. A major redesign was implemented to decrease losses in the device and decrease its form factor while also simplifying it. The results of this design change can be seen in figure 3.20.

Because of the success of the edge tone prototype, other designs were abandoned in favor of focusing on the the edge tone development. Many configurations of this design were printed and tested, each configuration changing one or multiple of the key dimensions: mouth height, orifice diameter, and width. This design proved to be extremely effective. While it was not perfect and certainly contained room for improved pressure drop, it provided a proof of concept for a functional acoustic flow meter with water as the working fluid, thus successfully concluding the exploratory phase of the project.

3.3 Therminol Phase

The second phase of the project called for the testing of an acoustic flow meter in a molten salt substitute. To do this, a second more sophisticated loop needed to be built.

Table 3.2: Table of the density viscosity ratios of FLiBe and Therminol-66.

	Temperature (K)	Density (kg/m^3)	Viscosity ($Pa \cdot s$)	Density Viscosity Ratio	Percent Difference (%)
FLiBe	880	1983.56	8.272E-3	239891.1	7.26E-7
Therminol-66	368.8	957.9	3.995E-3	239890.9	

Therminol-66 was chosen as the substitute. At 100°C it shares a density viscosity ratio to that of FLiBe at operating temperatures, this is shown in table 3.2. Because of the temperature requirement, the new loop needed a tank and heater with a controller to store and heat the Therminol-66 to the desired temperature. Additionally, the piping needed to be upgraded as the galvanized steel had begun to rust in places. A new larger pump was deemed necessary to increase the flow range and to pump the more viscous Therminol-66. The ultrasonic flow meter, while good for initial testing, had a high value of flow uncertainty and was hence also upgraded.

3.3.1 Therminol Test Loop

The new loop utilized 3/4 inch 304 stainless steel tubing with Swagelok fittings. Stainless steel ensured that there were no rusting problems, such as those experienced with the first loop, as well as ensuring material compatibility with the Therminol-66. The new loop utilized a similar flow moderation technique as the previous loop where a valve was placed before the device and after. The upstream valve acted as a bypass to remove a portion of the flow from the main loop. It was opened by varying amounts, thereby adjusting the flow through the prototype. Once the upstream valve was fully opened, the downstream valve was slowly closed to achieve even lower flow rates.

A picture of the prototype location on the loop can be seen in figure 3.21. There are valves immediately before and after the device, which when closed allow the prototype to be removed without draining the entire loop.

The upgraded pump is a 5 horsepower 3 phase 480V Oberdorfer N990 gear pump. This pump, as shown in figure 3.22, was chosen because it features dry graphite infused PTFE bearings. Gear pumps typically rely on the working fluid for both lubrication and cooling. The PTFE bearings allow for water, which is a very poor lubricant, to be pumped in the loop as well. Water was desired to be pumped before Therminol-66 as a safety control to ensure the loop and prototype could handle the expected increased pressures and flow

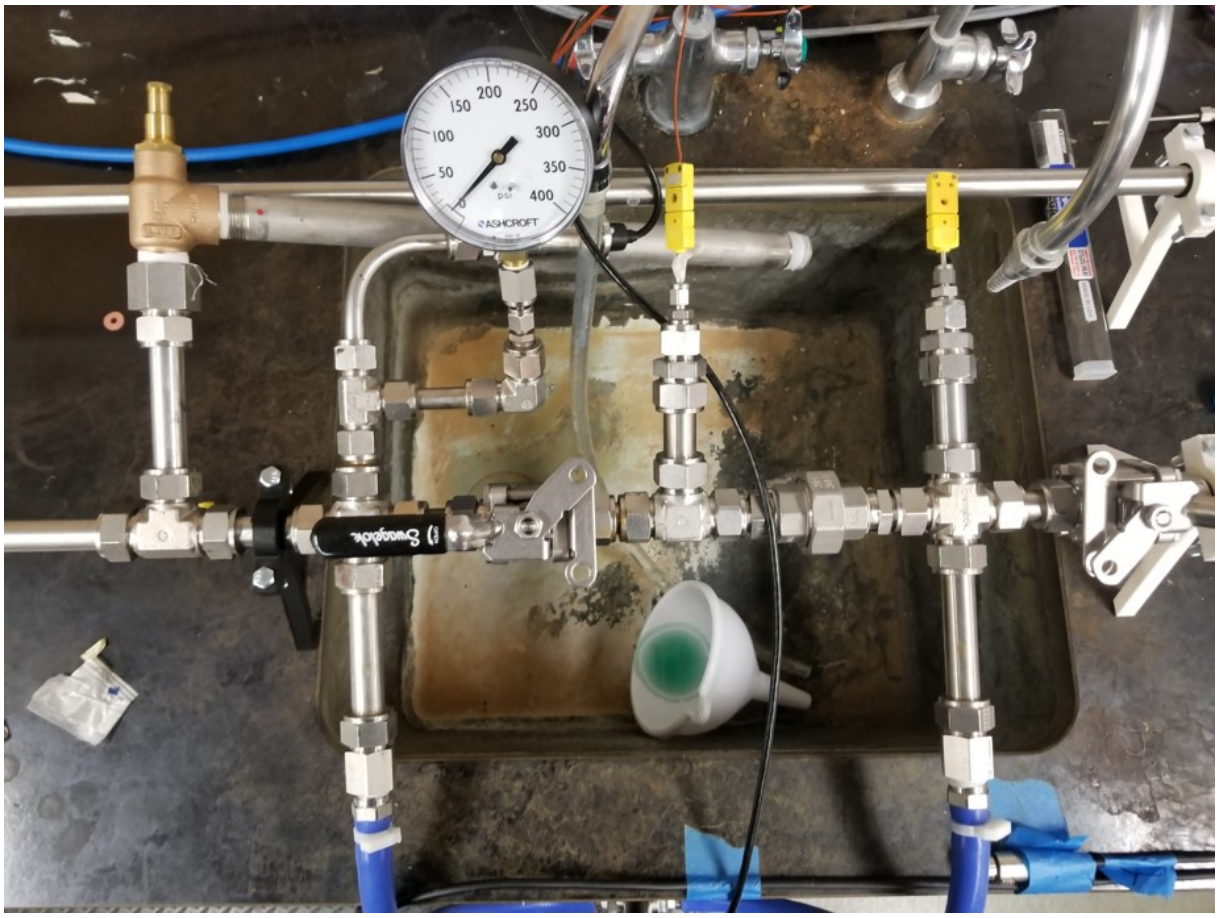

Figure 3.21: Therminol loop at the location where the sensors are located as well as where the prototype would be installed. The union would be separated and the prototype installed.

Figure 3.22: Oberdorfer gear pump

rates. A gear pump was chosen because of its naturally low flow rate fluctuations. This new pump was able to achieve flow rates of 53 GPM, a significant improvement over the previous pump. The new pump also resulted in large increases in pressure (70 psi at the highest) requiring the hoses to be upgraded for higher pressures at elevated temperatures.

The tank has an 800 Watt immersion heater and a type K thermocouple in the bottom of the tank. Fluid was originally returned through the top of the tank. The return hoses at the top were found to introduce air bubbles into the fluid, which were then sucked into the loop from via the pump. The air bubbles acted like pressure dampers in the prototype and prevented the proper pressure build up needed to produce edge tone oscillations. This problem was fixed by reattaching the hoses to the side of the tank below the fluid level.

3.3.2 Instrumentation

The new loop also had two temperature measurement locations furnished with Type K thermocouples before and after the prototype installation location. The pressure transducers from the previous loop were reused in a similar fashion. The same piezoelectric sensors as the previous loop were used to measure the vibrations; although instead of

using clamps, they were super glued to the pipe for better signal transmission. The piezo-electric sensors were assigned the colors blue, yellow, and white. The blue sensor was located directly on the prototype near the knife edge. The yellow sensor was located about 6 inches upstream of the prototype. The white sensor was located about 2 feet downstream of the prototype. The LabVIEW program was rewritten to make it more efficient and to process temperature data as well.

Ultrasonic flow meters, like the one on the old loop, generally have high uncertainty. For this reason, a Coriolis flow meter was acquired to replace them. The Non-Contact ultrasonic flow meter had an uncertainty of 5% across the flow range of the meter. The new Emerson Coriolis flow meter has an uncertainty of 0.5% and can be seen in figure 3.23 along with the tank.

3.3.3 Therminol Edge Tone Prototype

A new edge tone prototype was needed for the new loop as the previously used 3D printed prototypes were not able to withstand the increased temperatures and pressures. The new prototype, as shown in figure 3.24, was machined out of a solid block of aluminum. It shares a high degree of similarity with the previous edge tone prototypes. Machining multiple aluminum prototypes would have been prohibitively expensive. For this reason, this prototype was designed with the ability to adjust some of the key parameters explored in the previous phase. There are four visible M3 bolts located on the left side of the device. These bolts can be loosened and the orifice location slid forward and back to adjust the mouth height. There are two bolts perpendicular to each slide that are used to hold plates that govern the orifice diameter. These plates can be removed and replaced with ones of different thicknesses to adjust the orifice diameter. Two M3 bolts are used to hold the knife edge in place. This was done so that, if desired, the knife edge could be replaced with ones of different geometries. An aluminum top plate with a gasket was placed over the top after the mouth height and orifice diameter had been set to the desired dimensions. The top plate was bolted down with 24 M3 bolts along the perimeter of the prototype.

Figure 3.23: Emerson Coriolis flow meter and the tank in the back

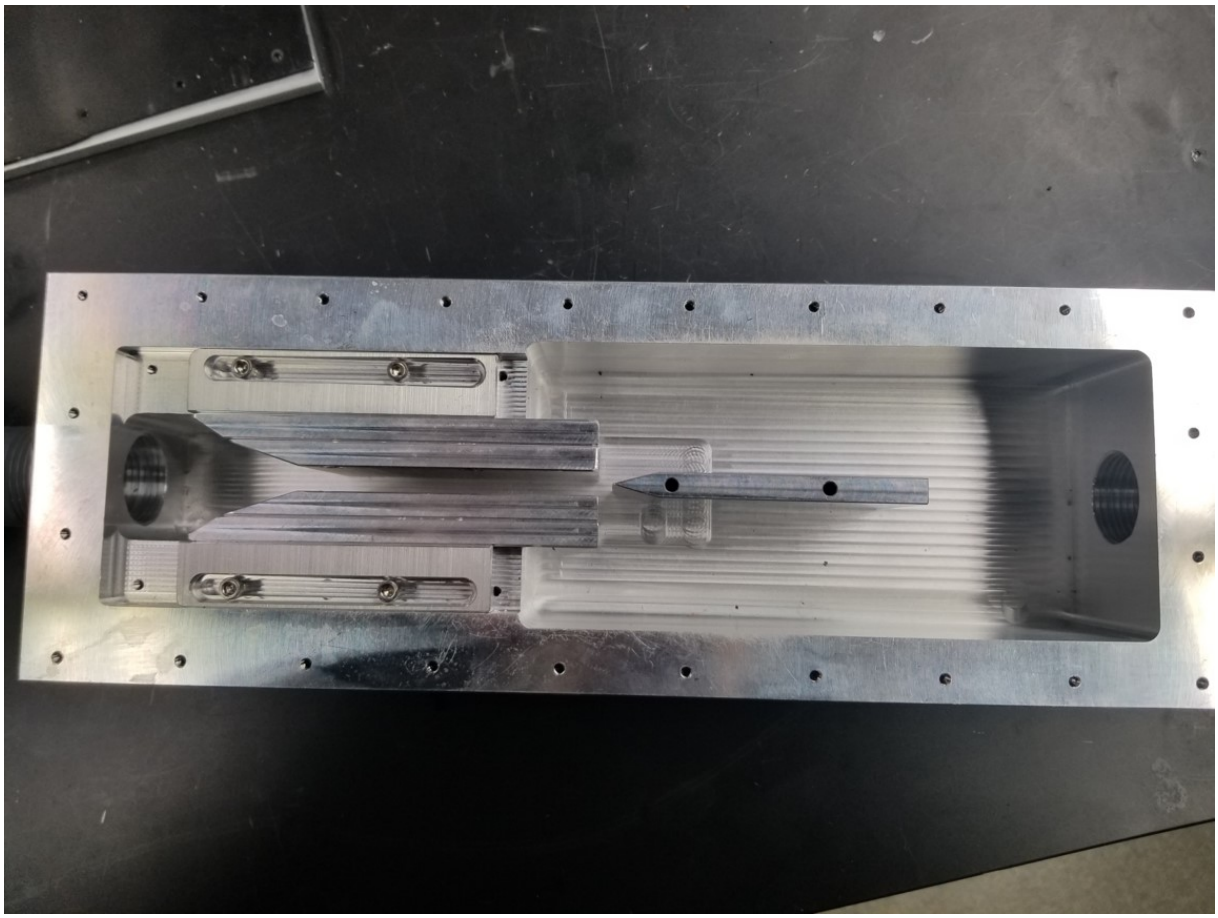

Figure 3.24: Aluminum edge tone prototype.

3.4 Data Processing

LabVIEW was used to acquire and organize the experimental data in such a way as to make it easy for a secondary Python code to read and analyze the data. A brief synopsis of each respective code as well as a process flow diagram for each will be presented in the following sections.

3.4.1 LabVIEW

The raw data acquired needed to be properly acquired and organized so that it could be properly analyzed. To do this a LabVIEW program was created to acquire the raw data, pass the vibration data through a FFT, and organize the other parameters such as the flow rate as measured by the Coriolis flow meter as well as the pressure and temperature data. The program would average the flow rate, pressure, and temperature data over the recording interval and save them as well as the FFT output into a single text file to later be opened and analyzed by a Python program. The program would be rerun for each flow rate tested thereby producing a separate file with temperature, pressure, flow, and vibration data for each flow rate. The process flow chart for this process can be seen in figure 3.25.

3.4.2 Python

The Python code was used to process the large number of data points and respective files acquired from the LabVIEW program. The Python code was designed to first open each file and organize the data for later processing. The organized vibration data could be smoothed using a hanning window if desired. Then the data (smoothed or unsmoothed) was analyzed with a peak detection function belonging to the ScyPi library.

Using the temperature data the fluid properties were calculated at each flow rate tested. The fluid properties where then used to calculate the dimensionless numbers of interest. The fluids were assumed to be in-compressible and hence unaffected by pressure changes.

The code would then begin plotting data as the user saw fit. The process flow diagram of the Python code can be seen in figure 3.26.

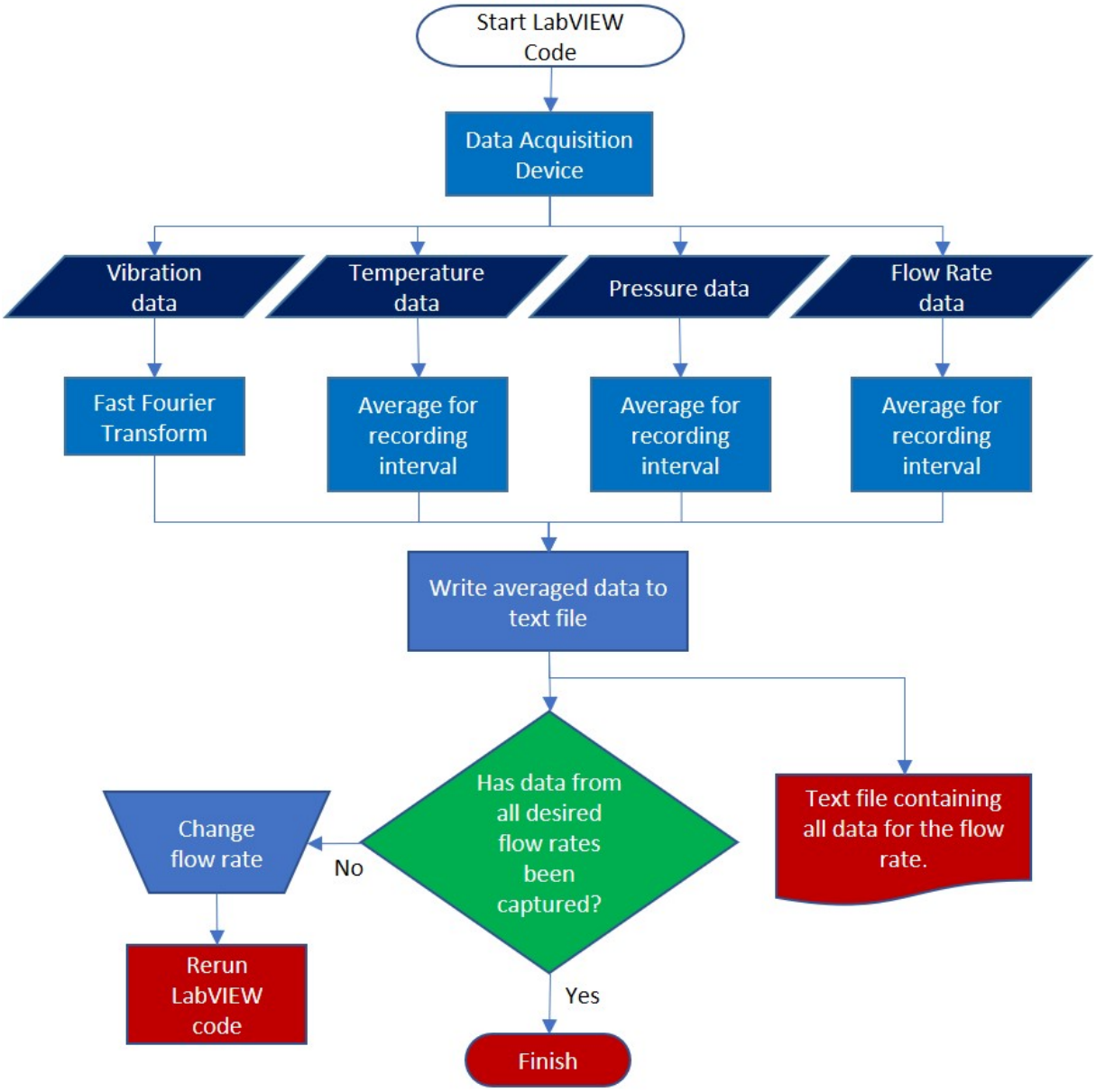

Figure 3.25: Process flow diagram for the LabVIEW program

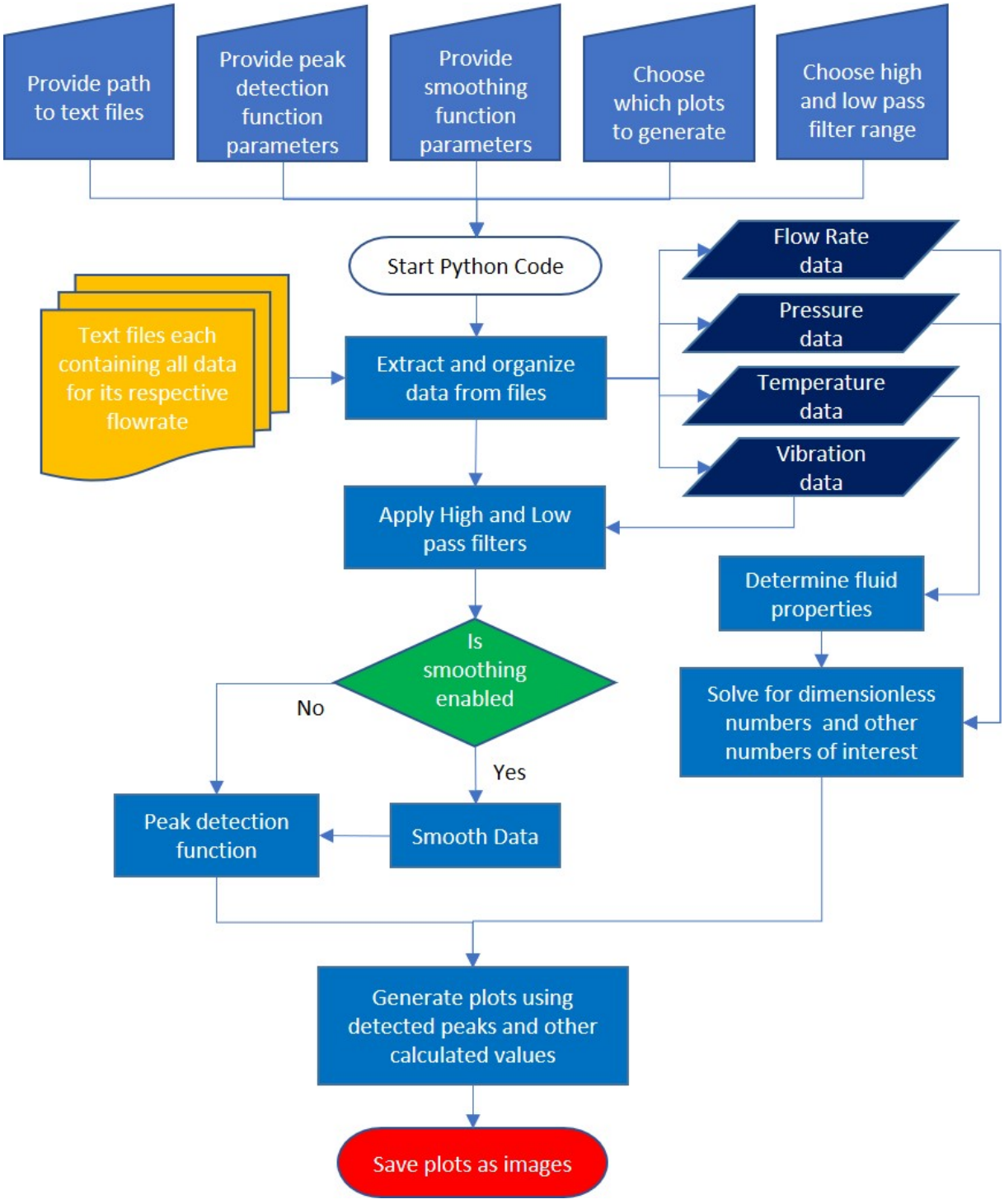

Figure 3.26: Process flow diagram for the Python code

Chapter 4: Results and Discussion

Because the nature of this project took place in two distinct phases, the results of these phases will be separately presented and discussed in the following sections.

4.1 Exploratory Phase Results

The exploratory phase produced many prototypes and lots of respective data. Each of the mentioned prototype's results will be discussed in the following sections.

4.1.1 Ball Percussion Prototype

The ball percussion prototype was one of the earliest "noise" making prototypes. While the ball did indeed roll around as intended, the tone produced had a high degree of randomness and did not cleanly relate to the flow rate through it. Additionally, the ball in the device was considered a wear item. The ball as it makes contact with the wall would slowly erode causing particulates to enter the system as well as require periodic replacement. For these reasons, the design was not explored further.

4.1.2 Hole Tone Prototype

The hole tone prototype did produce a measurable tone. However, its amplitude was incredibly low and the pressure drop across the device was devastatingly high. This design requires a very large degree of constriction and recirculation giving it an innately high pressure drop. For this reason, the design was abandoned for other more flow friendly alternatives.

4.1.3 Harmonica Reed Prototype

The harmonica reed prototype never actually produced a measurable tone. It was abandoned because, like the ball type, the reed is considered a wear item which is not optimal. It is hypothesised that the reed prototype could have functioned with more time put into it. The suspected reason for its failure was that the reed was too thin and did not possess the material stiffness required to snap back down after being pushed up by the water.

4.1.4 Bellows Prototypes

The bellows design took a relatively considerable amount of exploring before the discovery of the edge tone and its resulting abandonment. The bellows design held great appeal as it does not have any major obstructions to resist flow and is not an awkward shape making it an easy retrofit to nearly any system. There are multiple examples of corrugated tubes being used as whistling toys and the straws which whistle with little effort. These examples give merit to the idea. Unfortunately, none of the prototypes were able to generate measurable vibrations in water.

The first bellows prototype tested, shown in figure 3.12, had square grooves and proved ineffective. The prototype in figure 3.10 had 90°angle grooves and similarly produced no sound. The next design opted to use sharper angles, as seen in figure 3.11. This also made no vibrations. None of the previous 3 designs whistled in air either. It was thought that if the straws, which do whistle in air, were to have water pushed through them they might whistle. This led to the design in figure 3.13. The straws themselves did not vibrate when water passed through them. One possible reason for their non-function was the length required for water was beyond our manufacturing capabilities. It was discovered by cutting the straws to shorter lengths that it became more and more difficult to produce a whistle the shorter the straws were cut. It is hypothesised that the bellows design is unsuitable for liquids and requires properties that gases alone possess. The bellows may be a worthwhile endeavor to revisit for future flow meter research.

4.1.5 Cavitation Prototype

Cavitation, despite its potential benefits of extremely potent and efficient vibrations, was abandoned because cavitation can be very damaging to nearby components. Cavitation is a major cause of damage to fluid systems. The intense shock waves can literally erode the material away that is in contact. This could cause more problems than it solves in a fluid system. Neither of the cavitation meters actually resulted in cavitation, although there was very high confidence that it was achievable.

4.1.6 Bluff Body Prototype

The bluff body prototype also did not produce any measurable sound. This could have been because the frequency of the air column did not perfectly match the bluff body vortex shedding frequency. This idea did have merit although its amplitude of sound

would have likely been very low and would not function well for a variety of flow rates. In order for the air column to be excited, the vortex shedding frequency would have to match the frequency of the air column. The vortex shedding frequency is determined by the Strouhal number and is dependant on the velocity. This means that the air column would only vibrate at specific flow rates where the vortex shedding frequency was equal to harmonics of the air column's natural frequency.

4.1.7 Edge Tone Prototypes

The edge tone prototypes proved to be the most forgiving in accepted design parameters. Of the many edge tone prototypes tested, nearly every configuration produced at least some sound. These devices, their key dimensions, and resulting frequency ranges can be seen in table 4.1. Many of the prototypes listed were tested multiple times on multiple days to check consistency. The water temperature was typically between 20°C and 40°C. The same LabVIEW program was used to gather the raw data where it was output to a text file. The text files were imported into a Python program for additional processing and peak detection algorithms.

Table 4.1: Table of 3D printed edge tone results

Device ID	Mouth Height (mm)	Orifice Diameter (mm)	Width (mm)	Min Signal Flow (GPM)	Max Flow (GPM)	Low Frequency (Hz)	High Flow Frequency (Hz)	Pressure Drop At Max Flow (%)
ET0008L	5.5	2.0	30	3.98	8.3	304	531	—
ET0009LN	5.5	2.0	45	4.63	10.6	543	499	67.6
ET0009LB	5.5	2.0	45	4.46	10.5	517	491	66.2
ET0010L	5.5	2.0	23	2.97	7.3	230	654	84.8
ET0011L	6.0	2.0	30	3.80	9.0	240	1015	76.8
ET0012L	6.5	2.0	30	4.37	9.0	250	990	76.8
ET0013L	7.5	2.0	30	4.22	8.1	900	1018	84.1
ET0014L	4.5	2.0	30	4.10	7.7	225	775	81.3
ET0015L	3.5	2.0	30	2.72	8.8	218	892	77.7
ET0017L	5.5	3.0	30	8.20	11.5	380	933	57.2
ET0020L	2.0	2.0	30	—	—	—	—	—
ET0021L	5.5	2.5	45	5.5	12.0	450	410	51.2
ET0022L	5.5	2.5	45	5.42	11.7	510	480	—
ET0023L	5.5	3.0	45	6.71	12.5	482	398	42.5
ET0024L	5.5	2.5	45	5.61	11.7	222	406	—
ET0025L	4.0	3.0	45	7.28	12.6	282	447	40.6
ET0027L	10.0	3.0	45	7.75	12.4	530	528	42.4
ET0028L	5.5	4.0	45	10.30	13.3	453	510	—

Devices ET0009LB and ET0009LN are duplicates of each other and were both tested multiple times. It can be seen that there are minor differences in how these two prototypes performed. This could be due to small dimensional differences between the two prototypes, differences in water temperature, differences between the brands of plastic used, or uncertainty in the flow measurement.

The prototype labeled ET0012L was one of the most tested devices as it produced some of the cleanest looking plots, was amongst the loudest, and showed a very clear stage jump. A plot of the data can be seen in figure 4.1. The plot shows the recorded tone as a function of jet velocity. The plot was of the same device tested seven times on individual days. Some tests were performed while increasing the flow through the device and others while decreasing the flow.

The plot shows a distinct shift to another stage around 7 m/s. This is very typical of edge tones studied in literature and closely resembles figure 2.3 which provides confidence that the tones observed are the result of edge tone phenomena. It is interesting to note that in these tests there was no observed hysteresis effects as described in literature. Moreover, it is of note that the lower stages did not disappear with the presence of new ones; this had been observed before in literature and granted greater confidence of the edge tone. Figure 4.2 shows another of the plastic edge tone prototypes. The rest of the plastic edge tone prototypes showed similar results.

4.2 Therminol Phase Results

To begin the Therminol-66 testing, the loop needed to first be tested with cold water to ensure that the aluminum prototype could endure the increased pressures, that there were no leaks, and to clean out any debris that may have entered the loop during assembly. All valves on the loop were closed and the tank was filled with water via a bucket and funnel. Once filled, the aluminum prototype was installed on the loop. All valves were then opened and the loop was inspected for leaks. After verifying there were no leaks, the valve before the prototype was closed and the bypass valve was fully opened. This forced 100% of the flow through the bypass and none through the prototype. The pump was turned on and the loop was reinspected for leaks. Slowly, the valve before the prototype was opened to allow gradual amounts of water through the prototype and the rest of the

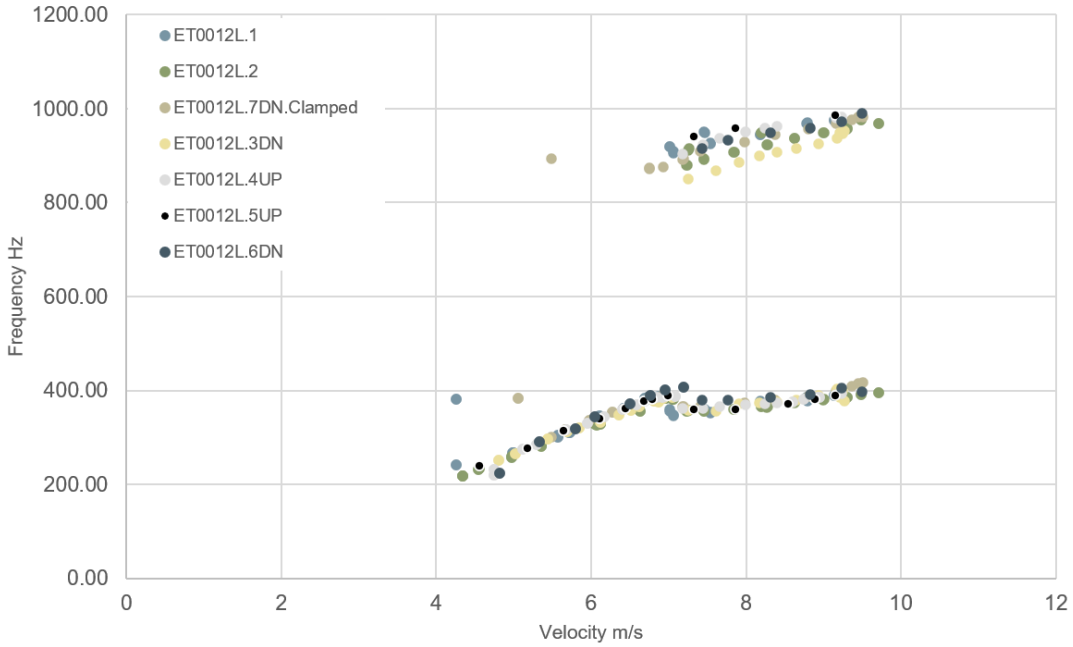

Figure 4.1: Frequency vs jet velocity of edge tone prototype ET0012L.

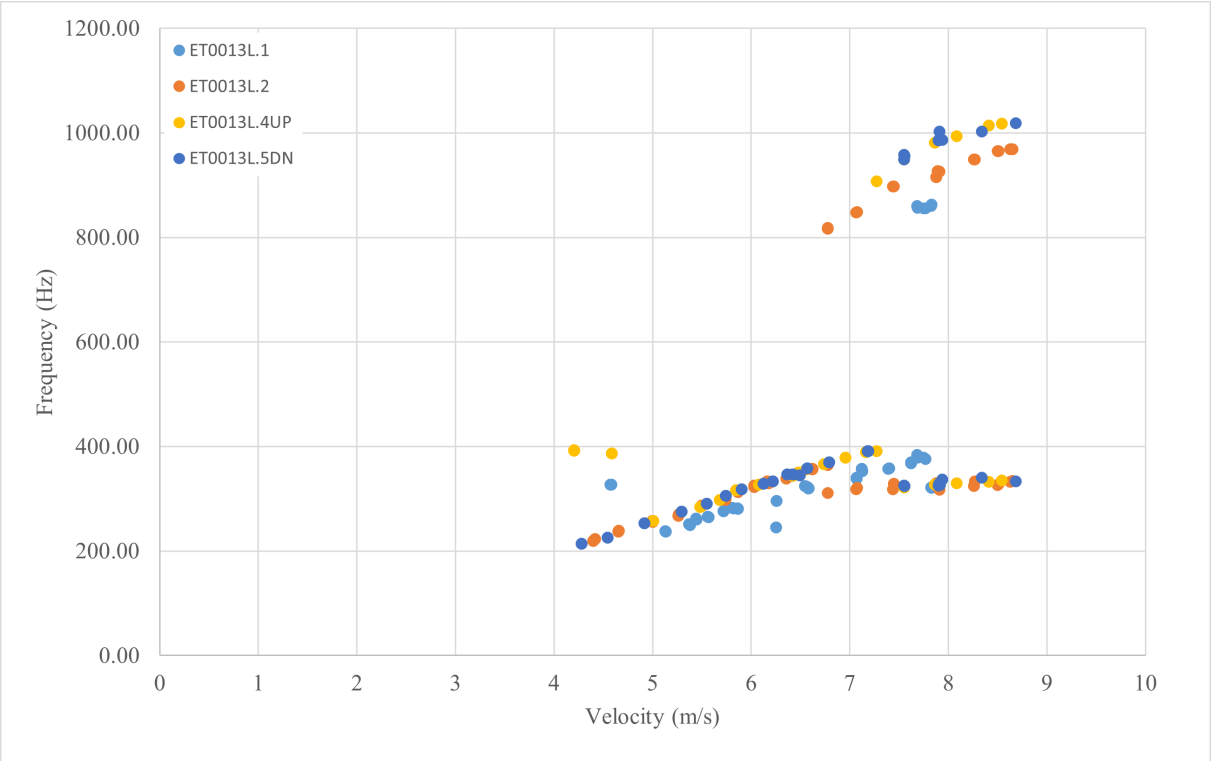

Figure 4.2: Frequency vs jet velocity of edge tone prototype ET0013L.

loop. Once all valves were open, the bypass valve was slowly closed to increase the flow through the prototype and the rest of the loop. When the bypass was fully closed and all flow was forced through the prototype, the pump was shut off and the loop prepared for Therminol-66. The loop was continuously inspected for leaks and the pressure gauge was monitored throughout this process.

To prepare for Therminol-66 the loop first needed to be fully dried out. The water was pumped out of the tank. Then the hoses were all removed from the tubing. As much water as possible was dumped from the tubing before an air compressor was attached to the loop to forcibly blow air through the loop. Air was blown through the loop sections until they were all dry. The loop was then left for a few days to ensure dryness. The hoses were then reattached to the loop and the tank filled with Therminol-66 following the same steps as those laid out for water. The Therminol was allowed to heat up to 100°C before turning on the pump.

The aluminum prototype was configured with a mouth height of 9 mm and a jet orifice of 3 mm. A longer mouth height was needed with the aluminum prototype than was needed with the plastic ones because of the difference in surface finish. The rougher

surface finish on the 3D printed parts caused the jet to reach greater levels of instability quicker than in the smoothly machined aluminum prototype. At full flow (53 GPM) through the prototype and 100°C the Therminol-66 in this configuration produced an audible tone similar to those heard in the plastic devices.

Three piezoelectric sensors were located on the loop for comparison. One sensor was located directly on the prototype near the tip of the knife edge, another was located on the flat of the cross about 6 inches upstream of the prototype, and the third was located about 3 feet downstream of the prototype. All three sensors were super glued to their respective locations.

The LabVIEW program continually showed the previous second of data so that the average flow rate, as measured by the Coriolis flow meter, could be used to manually meter the flow through the device. Data was recorded roughly every 0.5 GPM. To capture data, the LabVIEW program outputs an average of the previous ten, one second recordings including all three piezoelectric sensors, both pressure transducers, the flow meter, and the temperature before and after the device as measured with the thermocouples. The LabVIEW program then wrote all this data into a text file. Each flow rate tested was placed into its own separate file for later analysis.

The raw vibration data as measured from the piezos was a complex wave form. Before writing data to the text file the LabVIEW program performed a FFT on the signal with a resolution of one hertz and a range up to ten thousand hertz. The FFT for each sensor and each flow rate was the form of the vibration data exported to the previously mentioned text files. Due to the relatively large bin size of 1 hertz of the FFT as well as the size of the markers uncertainty is not included as it is expected to be negligible compared to the bin size and marker size.

A Python program was written that automatically imported the data from the text files into appropriately organized lists. Each set of FFT data was subjected to a peak detection algorithm developed by Scipy Libraries, which is a free open source Python library. The peak detection function finds local maxima, compares them to other local maxima, and either accepts or rejects the point based on user parameters. These parameters are distance, prominence, height, and relative height.

Distance indicates the minimum horizontal distance that can span between two accepted peaks. If more than one peak is found in this span, the best of those found based on the other parameters is selected.

Prominence compares each peak to the peaks around it. If the peak is too similar in size and shape to others around it, it is discarded. The value assigned to prominence indicates the required level of uniqueness the peaks must have to be accepted.

Height sets a minimum amplitude that all points must exceed otherwise they are rejected.

Relative height compares the width of the peak to the amplitude. The point is rejected if the ratio of the height to width is less than the value assigned.

The data from the FFT is very rough and noisy, making it difficult for the peak detection function to identify only the most interesting peaks. To assist with peak detection, a Hanning window was applied to smooth out some of the noise. A typical FFT is shown in figure 4.3. It shows the raw data in red, the smoothed data in black, and the peaks identified of both the raw and smoothed data as blue and yellow crosses respectively. It can be seen that the smoothed signal significantly improves the ability of the peak detection to find only the most relevant peaks. The smoothing operation does not perfectly preserve the frequency of the peaks and so peaks detected in the smoothed data cannot be used for detailed analysis. The peaks detected in the smoothed data are only used to find areas of interest to be zoomed in on and then true values are analyzed.

The detected smoothed peaks up to 10,000 Hz across the flow range from 53 GPM to 5 GPM are shown in figure 4.4. From this figure, it can be seen that there are many stages present. In previous literature, the highest number of stages to be recorded (to the best of the author's knowledge) was only 4 [18]. This plot shows that between about 25 GPM and 40 GPM forty simultaneous stages can be counted. This is significantly more stages than has ever been observed before. Stages are assigned numbers from one to the max number of stages, with one being the lowest stage.

There is a high degree of confidence that the data presented in this plot is correct, due to the similarities it shows to the data gathered in the exploratory phase as well as literature. Note that the slope of the stages increases as the stage number increases, just as expected from an edge tone. Also, note that higher stages seem to become increasingly unstable. This is similar to what is seen in figures 4.1 and 4.2 where the higher stage is not as smooth as the lower. Higher stages generally appear at higher flow rates. From observation, the next stage up seems to appear sooner at the higher stages than the lower and appears to reach an asymptote where many stages appear almost simultaneously.

It is important to note some key differences between the edge tones typically seen in

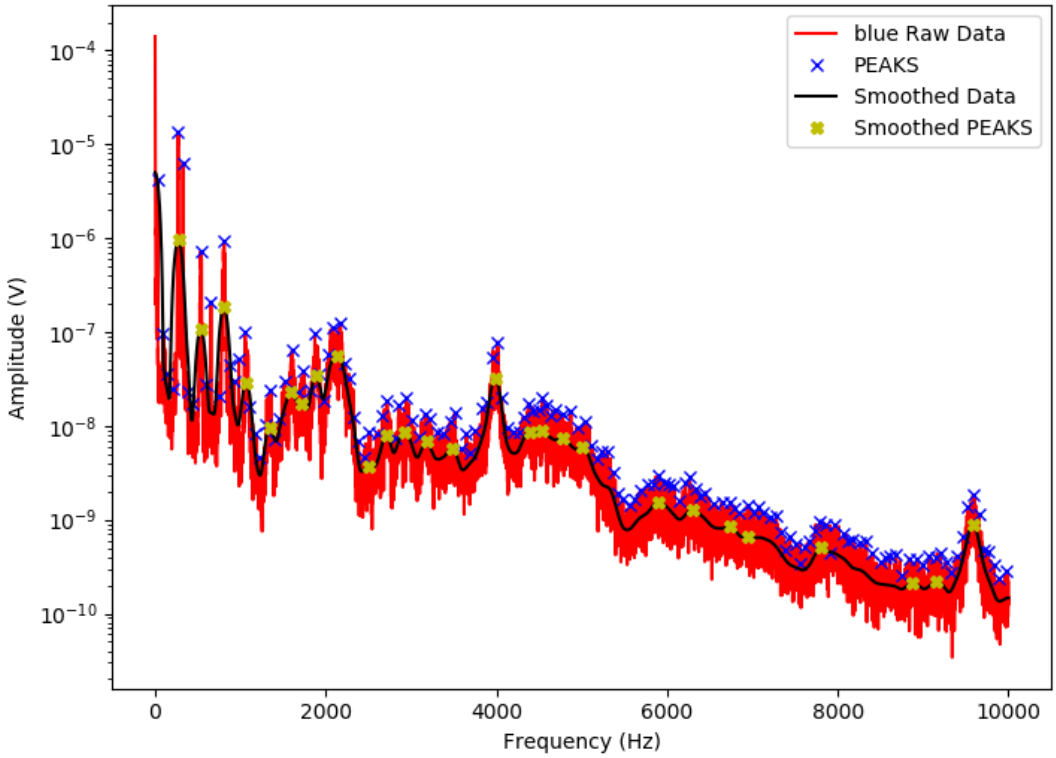

Figure 4.3: FFT of the edge tone signal at 51 GPM. With smoothing function and identified peaks before and after smoothing super imposed.

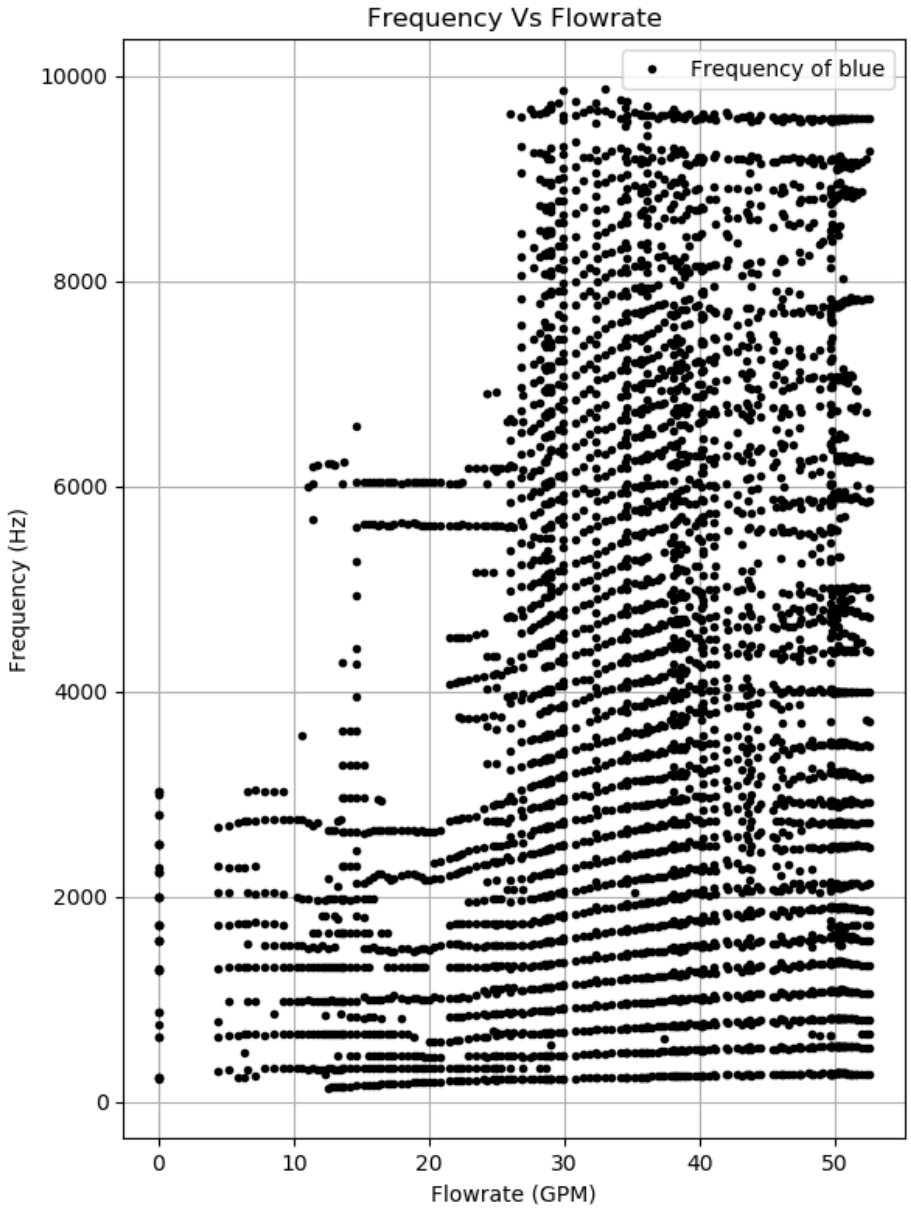

Figure 4.4: Frequency vs flow rate of all detected peaks from 0 to 10,000 Hz across the entire flow range.

literature and the one tested here. The edge tones in literature are almost exclusively free edge tones in air at relatively low Reynolds numbers (Re<5000). Only a single paper on edge tones in water was found, and it was both a free edge tone and was operating with relatively low Reynolds numbers [19]. The coupled edge tone phenomena is not very well explored and is the closest to that presented in this project. However, the edge tone presented in this project is neither a coupled nor a free edge tone. It is in a classification of its own and will be referred to as a Double Coupled Edge Tone (DCET) to differentiate it from free and coupled edge tones. Additionally, the Reynolds numbers of these experiments range from 4000 to 65,000 which is much higher than has ever been explored before.

For the development of a flow meter, only the biggest and clearest stages will be of interest. It can be seen in figure 4.4 that the lowest stages are the biggest and, if they follow the trend of higher stages being increasingly unstable, then it stands to reason that the lower stages would be more stable. Figure 4.5 shows only those stages below 1000 Hz. In this figure, stages 1,2,3 and part of 4 can be clearly seen. There appears to be a small amount of curvature to stage 1 in the lower flow regime where at about 25 GPM there is a small disturbance before becoming linear. A FFT for this same section is shown in figure 4.6 where the peaks of the smoothed function are those plotted in figure 4.5. It can be seen that stage 1 is clearly the largest and most stable stage and will hence forth be the stage analyzed with the most scrutiny.

Figure 4.5 shows some interesting data that was not visible on the larger plot when tracking peaks up to 10,000Hz. It can be seen that there are four full stages present and two sub stages located between stages 0-1 and 2-3. Stages and sub-stages are marked in figure 4.7. The sub-stages are a phenomenon that has not been seen in current literature. From this data it is hypothesized that the sub-stages appear between every other stage. Amplitudes are too small at higher frequencies to identify any sub stages higher than sub stage two.

It can be seen that all stages tend to gradually increase in slope from stage to stage. The slope of the full stages are considerably steeper than those belonging to the sub stages. Both the full and sub stage's slope increase at higher stages. The slopes are estimated in figure 4.8 and table 4.2. The slope of the full stages increases at a greater rate than the slope of sub-stages based on this data.

As previously mentioned, the lowest stage is of the greatest interest for flow meter

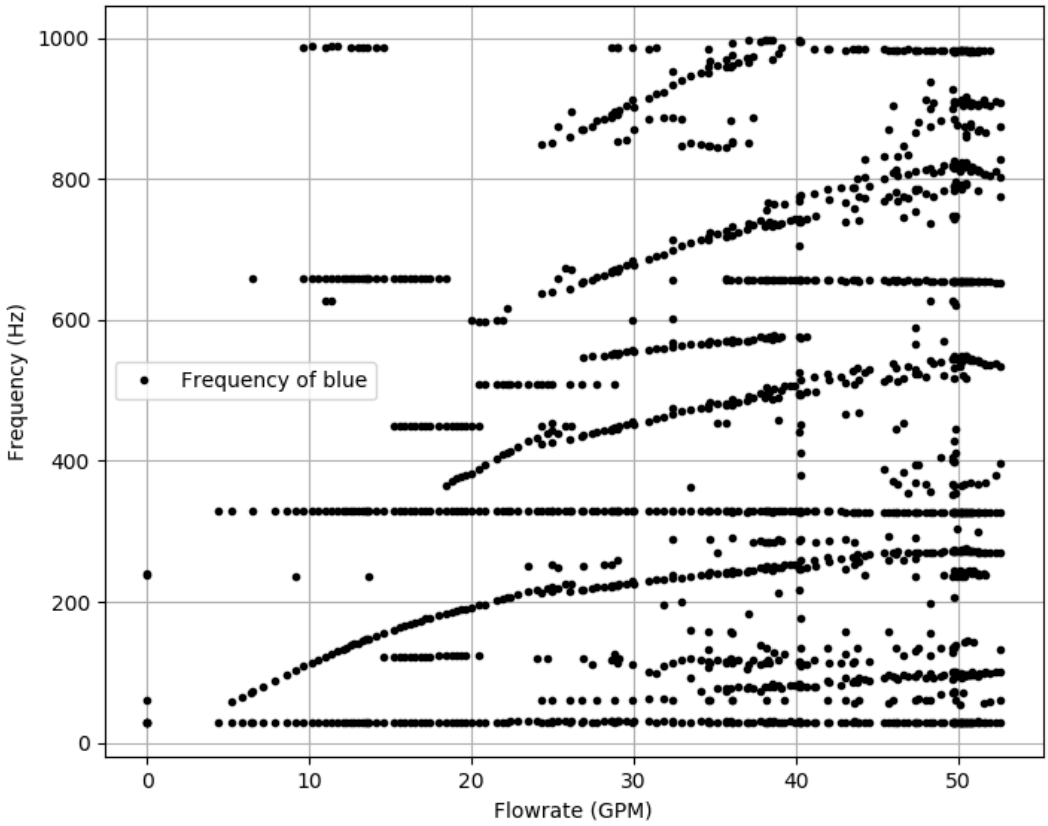

Figure 4.5: Frequency vs flow rate of all detected peaks from 0 to 1000 Hz across the entire flow range.

Table 4.2: List of slopes for stages 1 - 4 and sub stages 1 - 2.

Stage	Slope
1	2.6
2	4.5
3	7.0
4	10.3
Sub Stage	
1	1.45
2	2.17

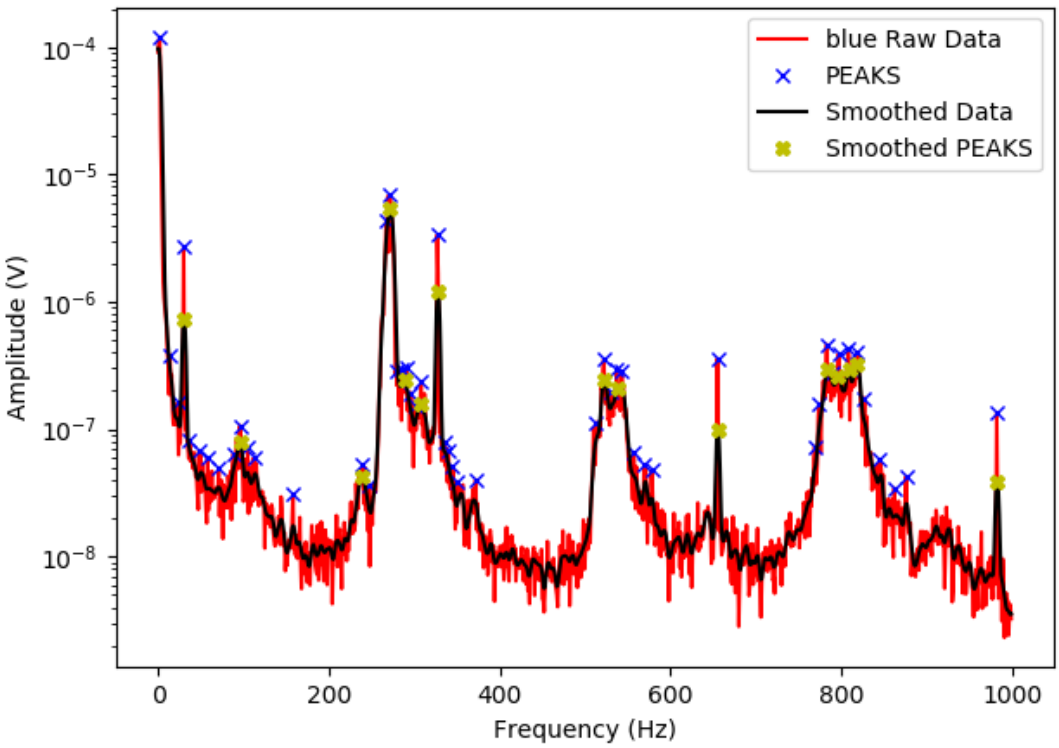

Figure 4.6: FFT of the edge tone signal at 49 GPM. With smoothing function and identified peaks before and after smoothing super imposed.

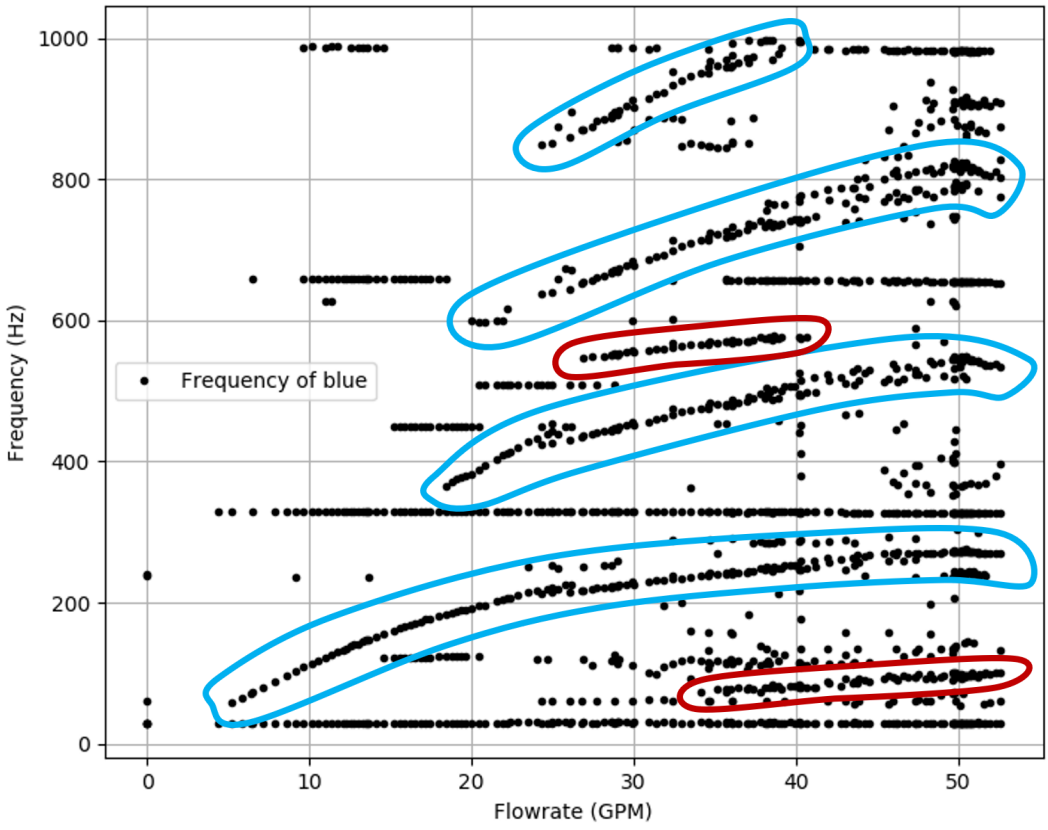

Figure 4.7: Frequency vs flow rate of all detected peaks from 0 to 1000 Hz across the entire flow range. Full stages are circled in blue and sub-stages in red.

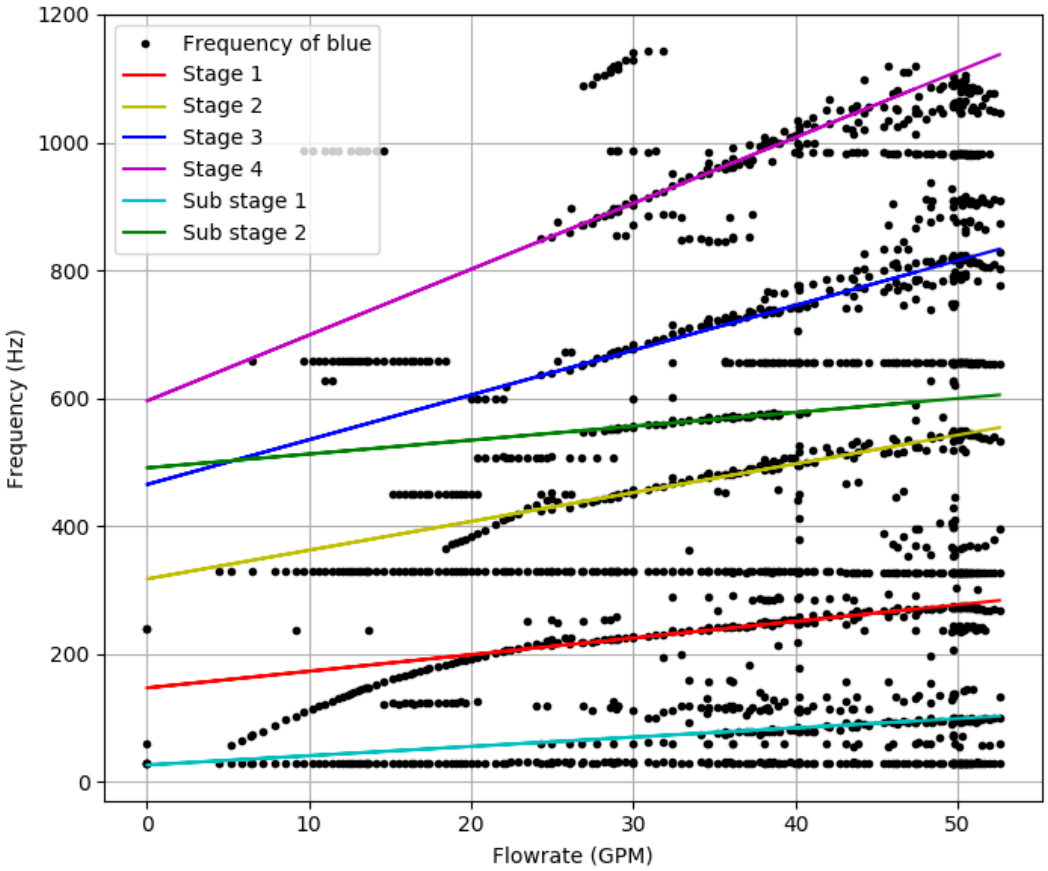

Figure 4.8: Frequency vs flow rate of all detected peaks from 0 to 1150 Hz across the entire flow range. Estimated slopes of both full and sub stages are superimposed on data.

development because it is the longest, smoothest, and has the lowest frequency. Low frequency waves tend to lose energy slower than high frequency waves. This is beneficial for transmitting signals long distances. Stage one's smoothness is important because it provides less uncertainty that the flow rate corresponding to the flow is correct. The length of stage one allows for a larger operational flow range of the flow meter. Stage one will need to be isolated for further study.

Due to the complex nature of the data, as well as the shear number of points, isolating just one stage can be a daunting task. The simplest method to do this would be to cherry pick data one point at a time. This method would work but would make future data analysis long and tedious. To automate the stage isolating, a very rough logarithmic curve fit was placed over stage one and can be seen in figure 4.9. The curve was used to determine approximately where the points of stage one were located so that all data outside a range of plus or minus 30 Hz from the curve could be rejected leaving only stage one. To ensure the data captured from this process is actually stage one, figures 4.10 and 4.11 show a FFT and the isolated unsmoothed curve respectively. It is obvious in the FFT plot that there is a small difference in the frequency of detected peaks between the smoothed and unsmoothed data. All data from this point on will be the raw numbers measured.

Previous figures have shown a small disturbance in the data at around 25 GPM. This is also the location where the curve appears to switch to become linear. Figure 4.13 shows the amplitude of each point on the curve. It is clear from this that at a Reynolds number of about 25,000 there is a very prominent increase in the amplitude of the signal. This is the same location as the disturbance where the curve becomes linear. Looking at the the amplitude around Re = 40,000, it looks like the signal is bifurcating. This is supported by the spreading of the frequency data at this location. It is hypothesised that at a Reynolds number of about 25,000 the peak begins to separate into two. Why this occurs is not yet known, so for this reason the edge tone flow meter will need to operate before the bifurcation. This is unfortunate as it limits the applicable flow range of the device, at least until the bifurcation is better understood.

A key parameter of any flow meter is the pressure drop across the device. Figure 4.13 shows the pressure of the system just before the prototype and the differential pressure measured across it. At the highest flow of about 53 GPM the system pressure was at about 44 psi and the differential was about 21 psi. At around 13 GPM the pressure begins

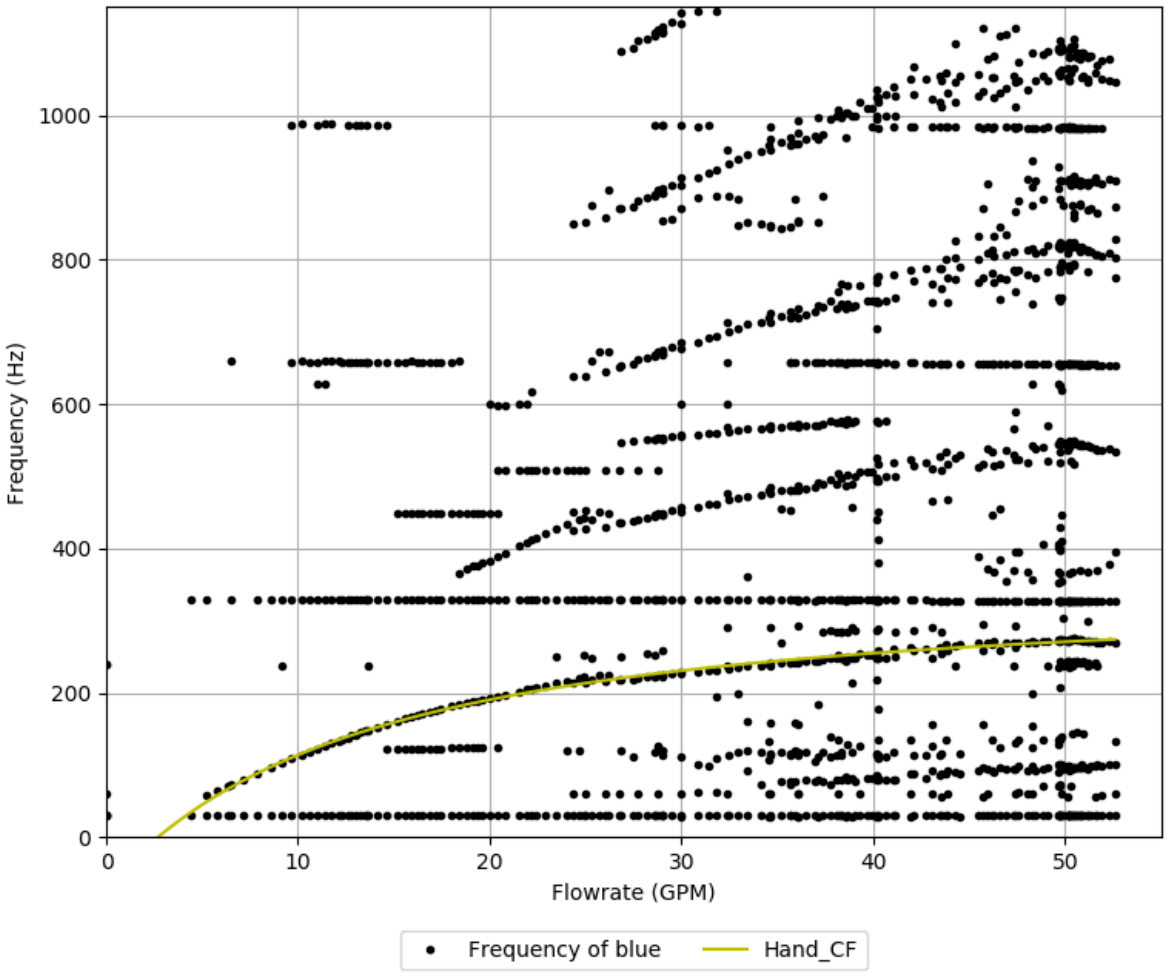

Figure 4.9: Frequency vs flow rate of all detected peaks from 0 to 1150 Hz across the entire flow range with rough curve fit super imposed.

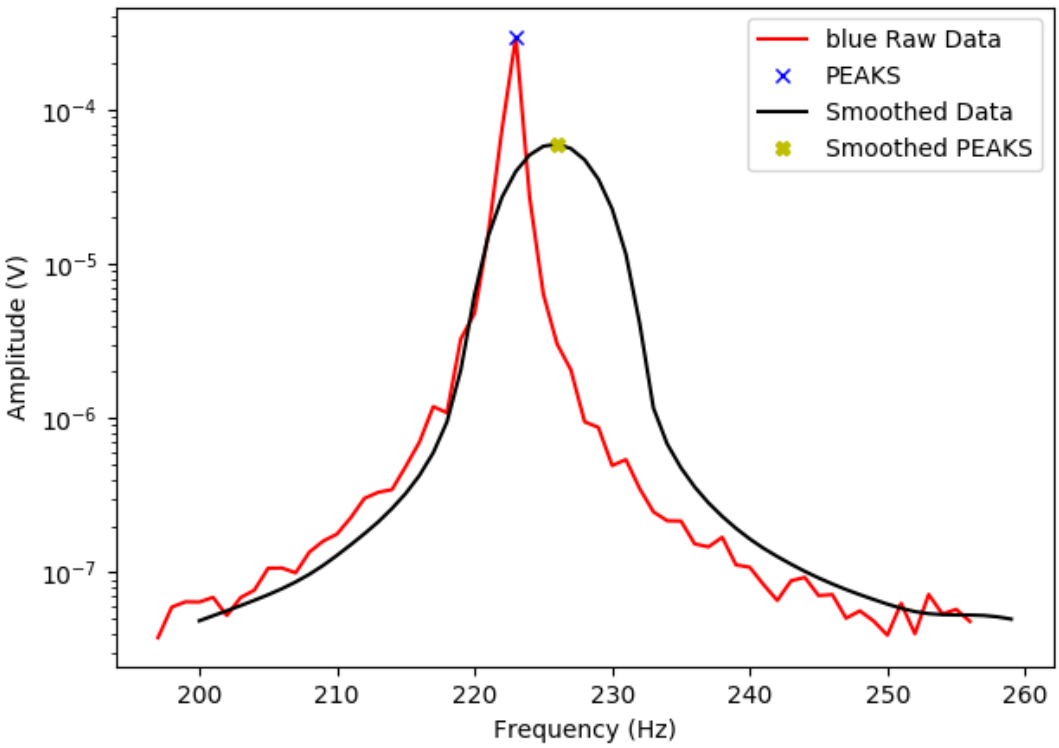

Figure 4.10: FFT at 29 GPM with all data 30 Hz above and below the path of the curve fit removed.

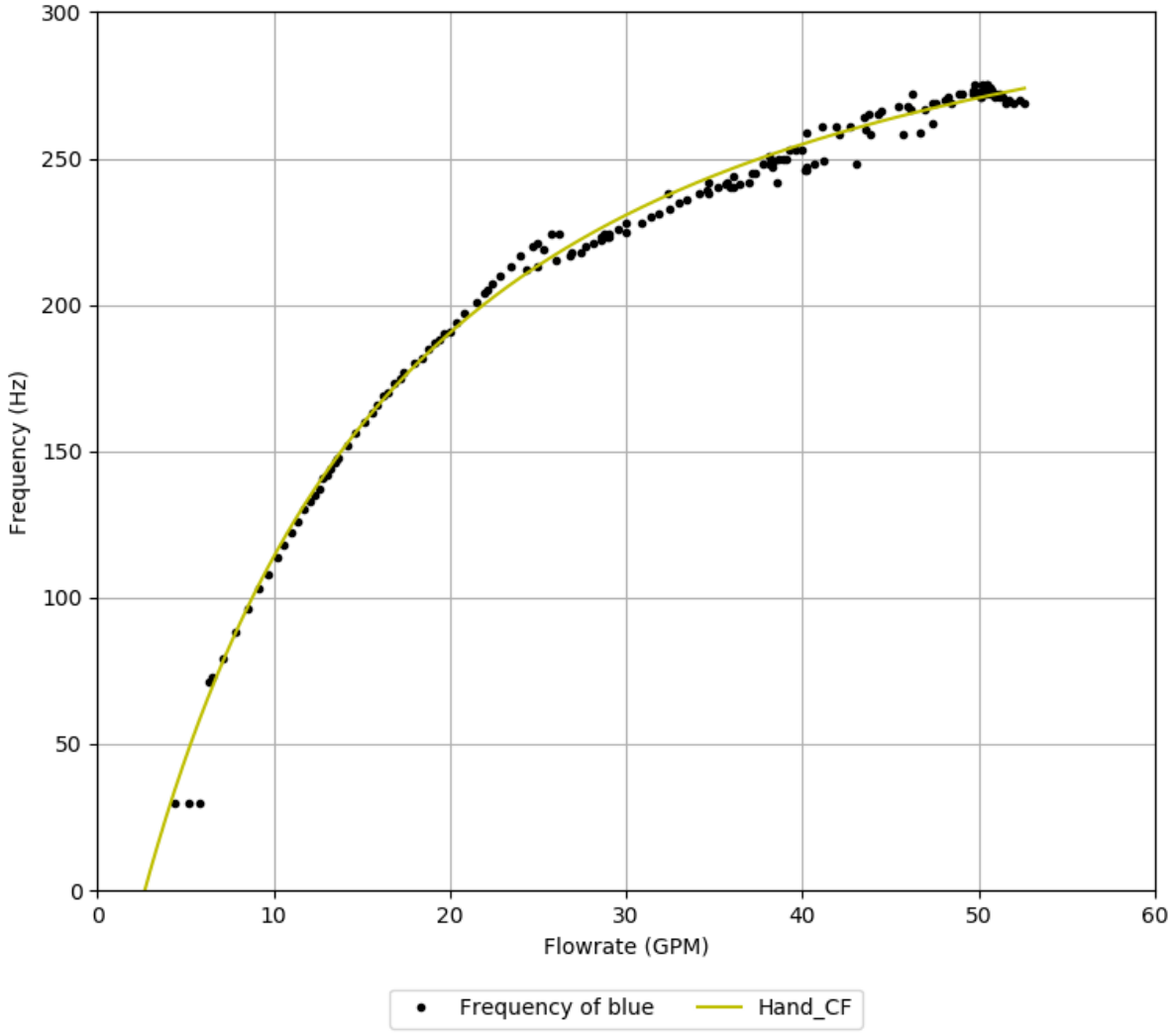

Figure 4.11: Stage one plotted against flow rate.

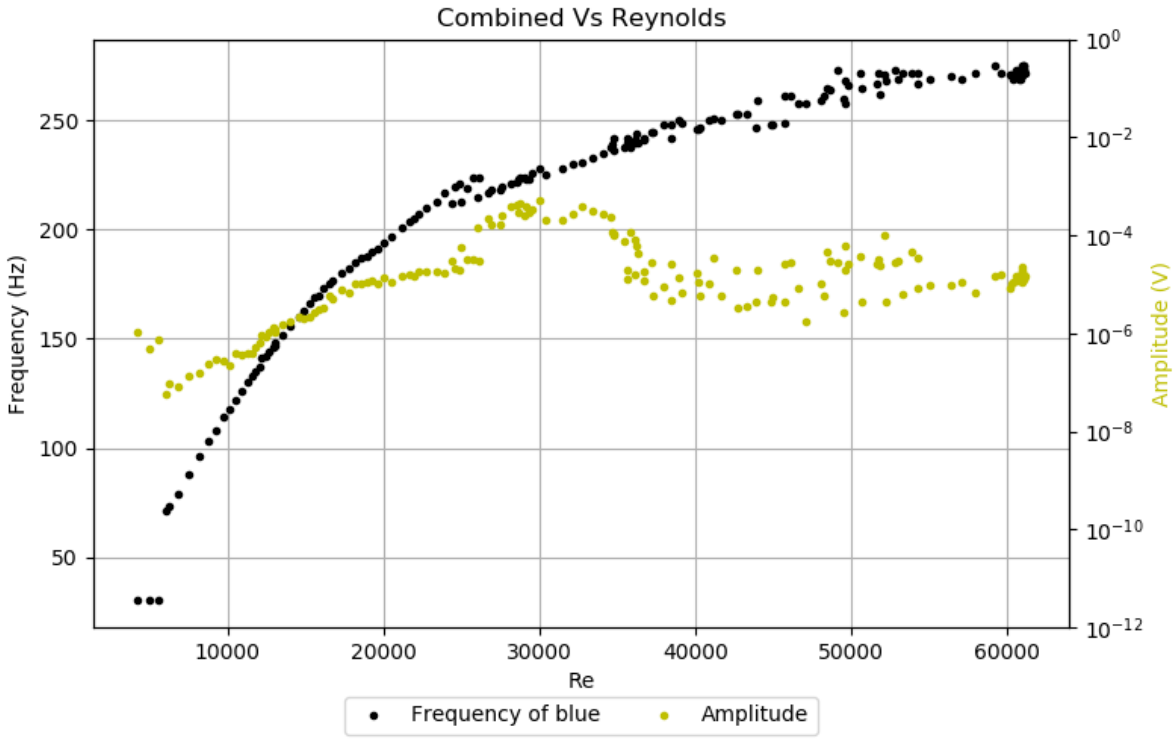

Figure 4.12: Stage one plotted against flow rate with amplitude data superimposed.

to tick up after steadily declining up to that point. This uptick is due to the method used to moderate flow in the loop. At 13 GPM the bypass valve was fully open and the valve after the prototype was used to further reduce flow. By closing that valve, the overall system pressure increased. The differential pressure drop was expectedly unaffected by this.

The energy required to produce the vibrations must come from the fluid pressure. Signals of greater amplitude have more energy and therefore must extract more energy from the potential of the fluid. Figure 4.14 shows that the amount of energy used to produce the vibrations at the current amplitudes are negligible. The current design of the prototype is clearly not optimized for pressure drop reduction. There are big areas, namely, in the corners where recirculation is certain to occur. In later iterations, these zones could likely be reduced to decrease the pressure drop without affecting the amplitude of vibrations produced.

The temperature of the fluid affects its viscosity and density. The average temperature measured across the prototype can be seen in figure 4.15 along with other relevant data. At higher flow rates there were some temperature fluctuations measured, the effects of

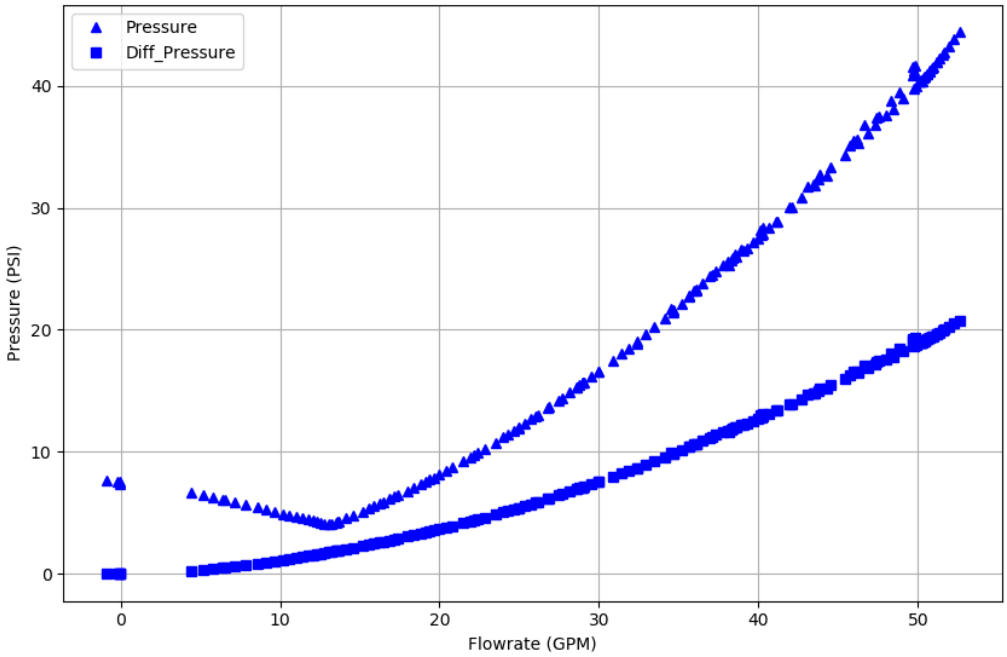

Figure 4.13: Pressures plotted at each tested flow rate.

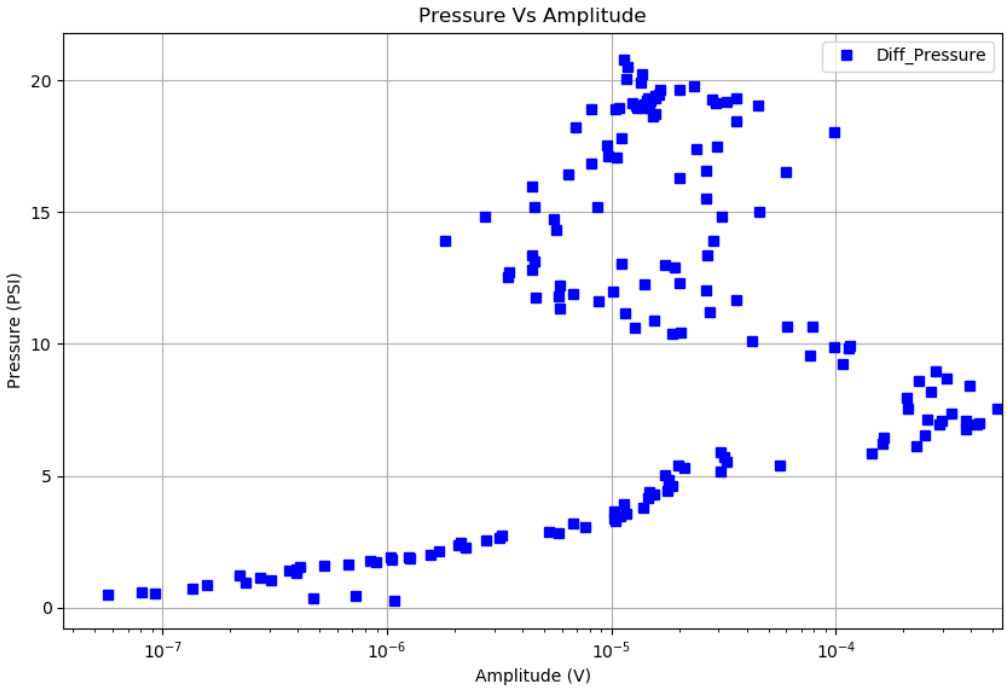

Figure 4.14: Pressure vs amplitude of stage one to see if there is a strong correlation between amplitude and pressure drop.

which are minor. At about the 50 GPM mark the frequency dips down at the same time there was a temperature drop. Other than at that location, the effects of temperature are relatively minor. Plotting frequency as a function of the Reynolds number rather than flow rate corrects temperature effects such as the data plotted in figure 4.13.

In liquid flows involving sound generation, there are two dimensionless numbers that are commonly of high interest, the Strouhal number and the Mach number. The Strouhal relates the fluid velocity to the shedding of vortices and the Mach number is the ratio of fluid speed to the speed of sound in the fluid. The Strouhal and Mach numbers can be seen in figure 4.16 as well as the Palmer number which will be discussed in the following paragraphs.

Because of the nature of edge tones and that of the systems where such a flow meter would be installed, the acoustic flow meter would need to be built and tuned to each unique application. The acoustic flow meter would need to be designed to produce a tone in the desired flow range. It would need to avoid producing natural frequencies of the system, as well as avoid producing frequencies that are currently present in the system. It would be incredibly time consuming and costly to perform a full range of tests required to find an edge tone configuration that would meet those parameters, especially since the edge tone phenomena is not well understood.

For these reasons, a non-experimental method is needed to determine the edge tone dimensions for a specific edge tone flow meter. This can be achieved via dimensional analysis and the Buckingham Pi Theorem. A dimensionless number can be used to relate the dimensions of an edge tone flow meter to the frequency produced in the n'th stage. The dimensionless numbers generated from the Buckingham Pi Theorem for the edge tone acoustic flow meter are shown below, Its derivation can be found in Appendix A.

$$\frac{\rho v^2}{\mu f} = F(Re_d, Re_h, Re_w) \tag{4.1}$$

Where ρ is the fluid density, v is the mean velocity of the jet, μ is the fluid viscosity and Re_d, Re_h, Re_w are the Reynolds numbers where the characteristic lengths are the key parameters: orifice diameter, mouth height, and width respectively. The left side of the equation is the Palmer number which is a function of Reynolds numbers for each characteristic length.

The Palmer number is an attempt to characterize the DCET phenomena using the parameters that can be most easily measured. At this time there is no direct physical

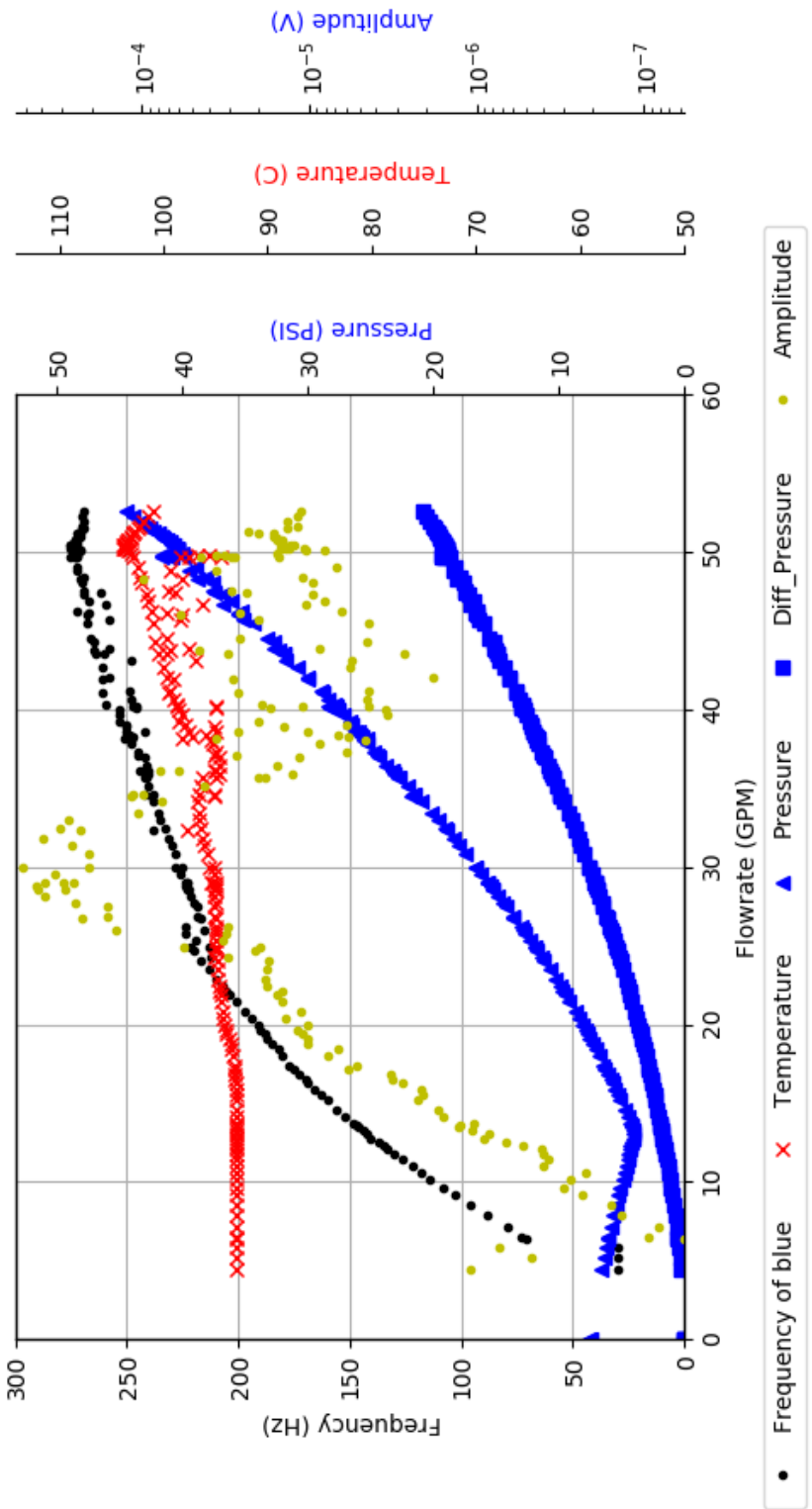

Figure 4.15: Plot of frequency, temperature, pressures, and amplitude vs flow rate of stage one.

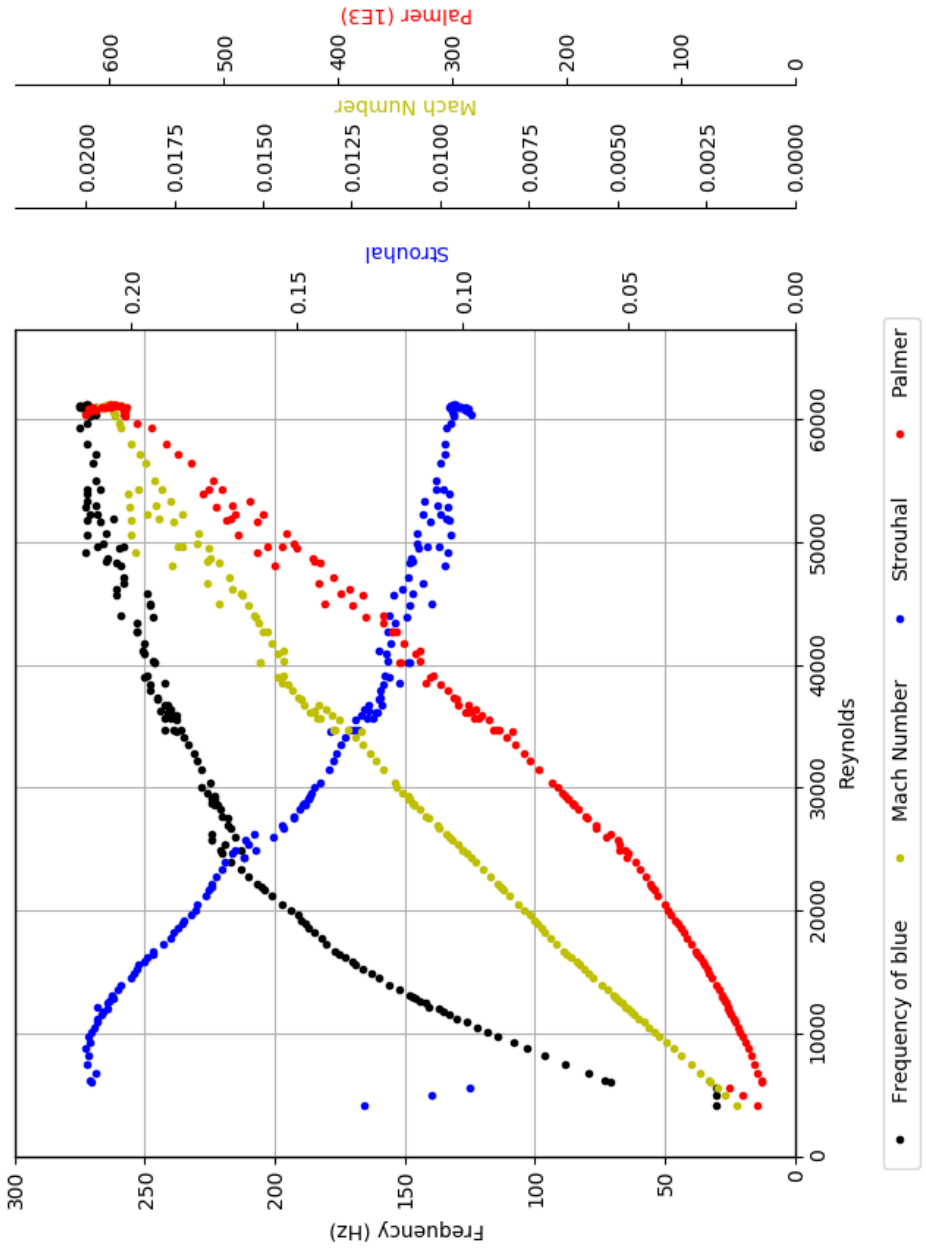

Figure 4.16: Plot of frequency, temperature, pressures, and amplitude vs flow rate of stage one.

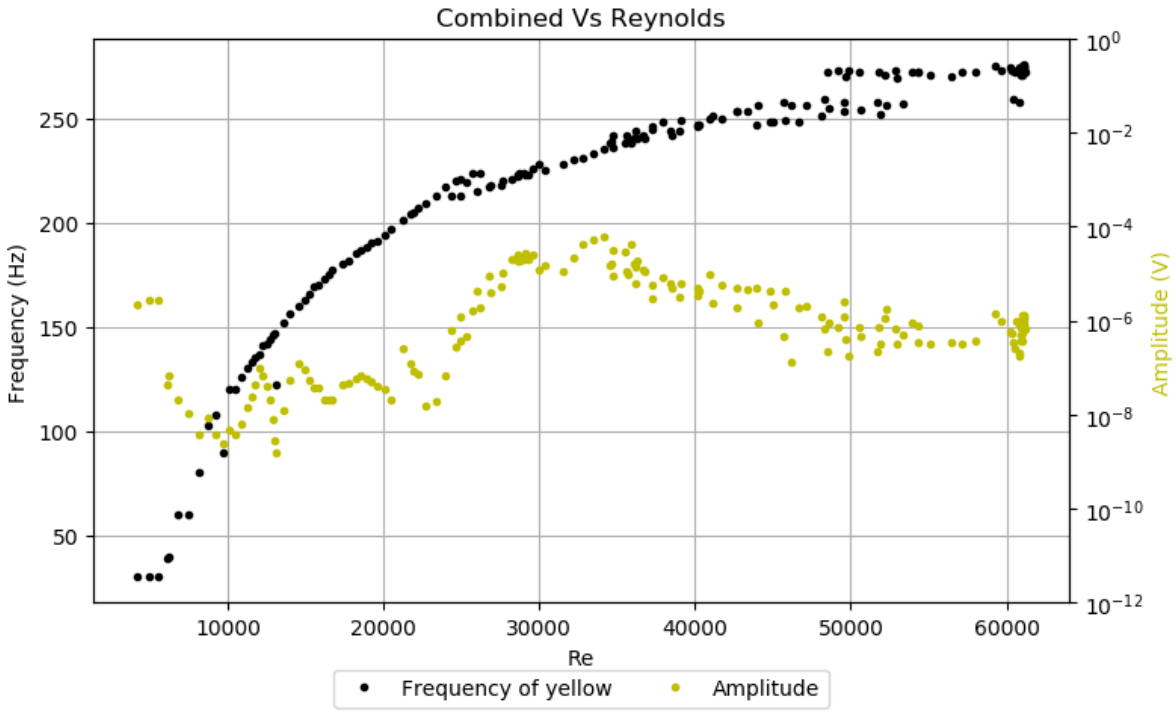

Figure 4.17: Stage one plotted against flow rate with amplitude data superimposed as measured by the yellow sensor.

interpretation of the Palmer number.

Using the Palmer number a series of configurations of the Aluminum prototype can be tested and then fit to a common curve. That curve fit provides the basis for new configurations and the resulting frequencies produced. The Palmer number can only be used to predict a single frequency. The stage of the frequency predicted depends on the stage that was used for the curve fit of the devices. For this reason, as well as for the previously mentioned qualities, the lowest stage is recommended to be used. This is also the main reason that only up to the bifurcation point of stage one, around 25 GPM, should be used as it appears that the stage splits around that point and the Palmer number correlation may no longer be valid.

The signal from the edge tone dampens the further from the ASGC the sensors are located. This can be exacerbated by many things such as acoustically poor piping and framework connections between the ASGC and the SPC, the distance between them, and the frequency of the signal. Low frequencies tend to lose energy slower than that of high frequency waves. The bottom stages of all three sensors can be seen in figures 4.13, 4.17 and 4.18.

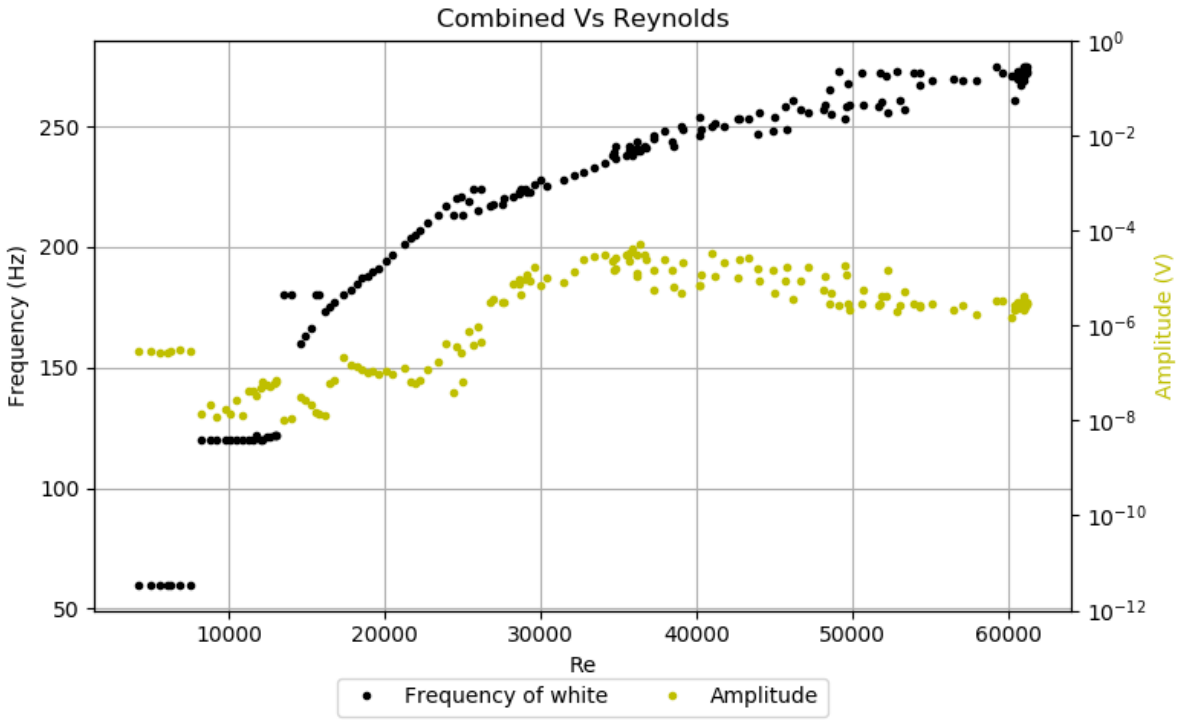

Figure 4.18: Stage one plotted against flow rate with amplitude data superimposed as measured by the white sensor.

It can be seen that the further the sensor was located from the ASGC the sooner the lowest amplitude signals damped out. The blue sensor started showing stage one at a Reynolds number of about 5000. The yellow sensor, which was located about 6 inches from the prototype, started to show stage one at a Reynolds number of about 10,000. The white sensor which was located abut 2 feet from the sensor started to show the signal at a Reynolds number of about 15,000. From this it is clear that the further the SPC is from the ASGC, the smaller the operational range of the acoustic flow meter could be. A louder, more efficient device, and/or more sensitive sensors will help to negate any loss in operational range.

Chapter 5: Summary and Conclusions

This project set out to begin the development of an acoustic flow meter, specifically for use in Molten Salt Reactors, where the acoustic signal produced could be measured some distance away from the signal generation device. This was done through a long exploratory process of designing and printing PLA prototypes and testing them on a simple test loop. It was found through this process that the edge tone phenomena could be used to generate the acoustic signals required for such a device. The edge tone acoustic flow meter was printed many times and tested to gain a working understanding of the phenomena. Then an aluminum prototype was machined and it received additional testing with a molten salt substitute, Therminol-66. The results from the Therminol-66 tests showed great promise for an acoustic flow meter that utilizes edge tones and paved the way for further testing. A dimensionless number was created to characterize and predict the signal output of future prototypes.

These tests show that an edge tone flow meter would need to determine the flow rate as a function of tone frequency. As the flow rate through the device changes the frequency also changes. An edge tone flow meter would measure the frequency of the tone and, using a curve fit of the Palmer number, determine the flow rate through it. Flow as a function of frequency poses problems such as the tones produced need to be in a range that excludes the natural frequencies of the system as well as other system noise where possible.

Data acquired and presented does not perfectly agree with data from other edge tone related literature. Reasons for the discrepancy may include that the edge tone tested, aptly named the DCET, is not exactly the same as others in literature such as a free and coupled edge tones. The tested DCET was also subjected to relatively high Reynolds numbers compared to previous research performed on free edge tones. Lastly, literature typically utilize gasses as the working fluid for edge tone research. The DCET tested used liquids which have vastly greater density and viscosity, and are virtually incompressible.

The edge tone acoustic flow meter developed during this project presents a potential solution to the harsh environments in nuclear reactors. The presented flow meter is essentially immune to radiation effects that plague current solutions, can be made from practically any material, and is solid state. However, the device is complicated, the edge tone phenomena is not yet very well understood, and the pressure drop is very large. The prototype presented is far from fully optimized but does provide a convincing proof of

concept for the idea. The Palmer number can be used for further development efforts.

Chapter 6: Future Work

There is lots of potential future work to be done on the edge tone acoustic flow meter, most importantly additional tests with a variety of DCET configurations. These tests will provide the data necessary to perform a curve fit using the Palmer number so that future prototypes can be manufactured with specific operational ranges.

The physics of the edge tone, more specifically the DCET, needs to be further explored. To the best of the author's knowledge, the data presented in this thesis is the only published data of such an edge tone. Better understanding of the physics will result in better prediction of prototype and later, actual flow meter operation.

The aluminum prototype tested only allowed for two key edge tone parameters to be adjusted, therefore any Palmer number curve would only be valid for flow meters that are dimensionally identical, short of those two parameters. The DCET likely has many more important internal dimensions than those presented. Additional experiments with a greater number of dimensional variations will provide a more robust Palmer number curve fit.

Acoustical differences resulting from the material the prototype is constructed from were not considered. It is well known in the musical world that the type of wood, metal, plastic, etc... an instrument is made from can greatly affect the timbre of the sound. How this would play into the acoustic flow meter's acoustics is unknown.

References

[1] Paul Marotta. Ceo of micronuclear llc.

[2] Istvan Vaik, Roxana Varga, and Gyorgy Paal. Frequency and phase characteristics of the edge tone part i. Sept 2013.

[3] SCIA ENGINEER. Karman vibration. *https://help.scia.net/17.0/nl/tb/dynamics/karman_vibratio*

[4] Chang H. Oh, Eung S. Kim, Hee C. No, and Nam Z. Cho. Final report on experimental validation of stratified flow phenomena, graphite oxidation, and mitigation strategies of air ingress accidents. Jan 2011.

[5] Man Hoi Wong, Akinori Takeyama, Takahiro Makino, Takeshi Ohshima, Kohei Sasaki, Akito Kuramata, Shigenobu Yamakoshi, and Masataka Higashiwaki. Radiation hardness of β-ga2o3 metal-oxide-semiconductor field-effect transistors against gamma-ray irradiation. Jan 2018.

[6] Intel. 10nm, creative improvements expand intel manufacturing capacity. *https://www.intel.com/content/www/us/en/newsroom/news/expand-intel-manufacturing-capacity.html?wapkw=10nm#gs.zdpbqc*, Dec 2020.

[7] lawrence S. Criscione. Analysis of the october 21, 2003 unintentional passive reactor shutdown at callaway plant with regard to aspects of reactivity management, corporate and regulatory oversight, nuclear safety culture, and operating experience. 2013.

[8] Dr. G. Burniston Brown. Organ pipes and edge tones. January 1938.

[9] Yuta Kawai, Yoshiyuki Tsuji, and Yutaka Kukita. Vortical structures in high-reynolds-number jet indicating edgetone oscillation. 2007.

[10] Peter Tamas Nagy, Andras Szabo, and Gyorgy Paal. A feedback model of the edge tone, using theadjoint orrâsommerfeld equation. Jan 2021.

[11] N. Curle. The mechanics of edge-tones. Feb 1953.

[12] Yunus A. Cengel and John M. Cimbala. *Fluid Mechanics Fundamentals and Applications*. McGraw-Hill, United States, third edition, 2014.

[13] New Jersey Department of Health and Senior Services. Hazardous substance fact sheet. Oct. 1986.

[14] Melecita M. Archuleta. Toxicity of materials used in the manufacture of lithium batteries.

[15] OSHA. Toxic metals. *https://www.osha.gov/toxic-metals*.

[16] D. E. Holcomb, G. F. Flanagan, B. W. Patton, J. C. Gehin, R. L. Howard, and T. J. Harrison. Fast spectrum molten salt reactor options. July 2011.

[17] Shenzhen eSun. Product manual, 3d printing material.

[18] G. BURNISTON BROWN. The vortex motion causing edge tones. April 1937.

[19] J. Bruce Brackenridge and Wesley L. Nyborg. Acoustical characteristics of oscillating jet-edge systems in water. Oct. 1956.

Appendix A: Palmer Number Derivation

A.1 Step 1

The parameters involved in the edge tone are as follows: fluid density, fluid viscosity, mean jet velocity, frequency, mouth height, orifice diameter, and width. It is important to note that there are very likely other characteristic lengths important to the proposed design, although those lengths are considered secondary and can very easily be added later if desired.

$$n = 7 \tag{A.1}$$

A.2 Step 2

The elementary dimensions of the parameters presented are length, mass, and time. Therefore:

$$j = 3 \tag{A.2}$$

A.3 Step 3

The number of Π groups is given by

$$k = n - j = 4 \tag{A.3}$$

A.4 Step 4

The chosen repeating parameters are density, viscosity, and mean jet velocity.

A.5 Step 5

Each parameter is listed in its elementary dimensions below in equation A.4.

$$\rho = \frac{m}{L^3}; \quad \mu = \frac{m}{tL}; \quad v = \frac{L}{t}; \quad h = L; \quad d = L; \quad w = L; \quad f = t^{-1} \tag{A.4}$$

Using combinations of these, dimensionless Π groups are created. Since frequency

is the dependant variable, it will be part of the first Π group, the other non repeating parameters will each form independent Π groups.

$$\Pi_1 = \frac{\rho v^2}{\mu f} = \frac{(\frac{m}{L^3})(\frac{L}{t})^2}{(\frac{m}{tL})(t^{-1})} = \frac{mL^3t^2}{mL^3t^2} \tag{A.5}$$

$$\Pi_2 = \frac{\rho v h}{\mu} = \frac{(\frac{m}{L^3})(\frac{L}{t})(L)}{(\frac{m}{tL})} = \frac{mL^3t}{mL^3t} \tag{A.6}$$

$$\Pi_3 = \frac{\rho v d}{\mu} = \frac{(\frac{m}{L^3})(\frac{L}{t})(L)}{(\frac{m}{tL})} = \frac{mL^3t}{mL^3t} \tag{A.7}$$

$$\Pi_4 = \frac{\rho v w}{\mu} = \frac{(\frac{m}{L^3})(\frac{L}{t})(L)}{(\frac{m}{tL})} = \frac{mL^3t}{mL^3t} \tag{A.8}$$

A.6 Step 6

Now the Π groups arranged as below and process complete.

$$\Pi_1 = F(\Pi_2, \Pi_3 ... \Pi_k) \tag{A.9}$$

$$\frac{\rho v^2}{\mu f} = F(Re_d, Re_h, Re_w) \tag{A.10}$$

Appendix B: Python Code

```
# -*- coding: utf-8 -*-
"""
Created on Tue Sep 24 10:03:11 2019

@author: Jason
"""

import numpy as np
import matplotlib.pyplot as plt
import os
import scipy.signal as sp
from collections import Counter

def ExpModelCF(xdata,ydata):

    Y=np.log(ydata)
    X=xdata
    alpha,beta,r2=LinCF(X,Y)
    a=np.exp(alpha)
    b=beta

    return a,b,r2

def LinCF(x,y):
    n=x.size

    Sx=np.sum(x)
    Sx2=np.sum(x**2)
    Sy=np.sum(y)
    Sy2=np.sum(y**2)
    Sxy=np.sum(x*y)
```

```
    A=np.array([[n,Sx],[Sx,Sx2]])
    b=np.array([Sy,Sxy])

    a,b=np.linalg.solve(A,b)

    R2=(a*Sy+b*Sxy-(1/n)*Sy**2)/(Sy2-(1/n)*Sy**2)

    return a,b,R2

def LogCF(xdata,ydata):
    x=np.log10(xdata)
    y=ydata
    alpha,beta,r2=LinCF(x,y)
    a=alpha
    b=beta

    return a,b,r2

def flatten(list_of_lists):
    """This is used to flatten a list of lists into a 1
       dimensional list"""
    if len(list_of_lists) == 0:
        return list_of_lists
    if isinstance(list_of_lists[0], list):
        return flatten(list_of_lists[0]) + flatten(list_of_lists
            [1:])
    return list_of_lists[:1] + flatten(list_of_lists[1:])

def Therminol_Viscosity(T):
    """This ouputs a Linear Curve fit of Therminol-66 viscosity
       data valid only between 90 and 110 degrees C"""
    A=-0.095
```

```
    B=13.1
    C=-0.068
    D=10.4
    V=[]
    for i in T:
        if i<100:
            V.append(A*i+B)
        else:
            V.append(C*i+D)
    V=np.array(V)
    return V/1000
def Therminol_Density(T):
    """This ouputs a Linear Curve fit of Therminol-66 density
       data valid only between 90 and 110 degrees C"""

    A=1207.59441
    B=-0.67874
    return A+B*(T+273.15)

def Therminol_SpeedOfSound(T):
    """This ouputs a Linear Curve fit of Therminol-66 Speed of
       Sound data valid only between 90 and 110 degrees C"""

    A=-2.9
    B=1536
    C=-2.8
    D=1526
    V=[]
    for i in T:
        if i<100:
            V.append(A*i+B)
        else:
            V.append(C*i+D)
```

```
    V=np.array(V)
    return V

def smooth(x,window_len=11,window='hanning'):
    """smooth the data using a window with requested size.

    This method is based on the convolution of a scaled window
        with the signal.
    The signal is prepared by introducing reflected copies of
        the signal
    (with the window size) in both ends so that transient parts
        are minimized
    in the begining and end part of the output signal.

    input:
        x: the input signal
        window_len: the dimension of the smoothing window;
            should be an odd integer
        window: the type of window from 'flat', 'hanning', '
            hamming', 'bartlett', 'blackman'
            flat window will produce a moving average smoothing.

    output:
        the smoothed signal

    example:

    t=linspace(-2,2,0.1)
    x=sin(t)+randn(len(t))*0.1
    y=smooth(x)

    see also:
```

```
    numpy.hanning, numpy.hamming, numpy.bartlett, numpy.blackman
        , numpy.convolve
    scipy.signal.lfilter

    TODO: the window parameter could be the window itself if an
        array instead of a string
    NOTE: length(output) != length(input), to correct this:
        return y[(window_len/2-1):-(window_len/2)] instead of
        just y.
    """

    if x.ndim != 1:
        raise ValueError("smooth only accepts 1 dimension arrays
            .")

    if x.size < window_len:
        raise ValueError("Input vector needs to be bigger than
            window size.")


    if window_len<3:
        return x


    if not window in ['flat', 'hanning', 'hamming', 'bartlett',
        'blackman']:
        raise ValueError("Window is on of 'flat', 'hanning', '
            hamming', 'bartlett', 'blackman'")


    s=np.r_[x[window_len-1:0:-1],x,x[-2:-window_len-1:-1]]

    if window == 'flat': #moving average
```

```
        w=np.ones(window_len,'d')
    else:
        w=eval('np.'+window+'(window_len)')

    y=np.convolve(w/w.sum(),s,mode='valid')
    return y



def FindMax(Color,DIR,FRange,Res,Distance,Prominence,Height,
    Width,Threshold,Range,SmoothingFactor,FilterInstances,
    CF_Function=False,Test_CF=False,nthPlot=0,Smoothed=False,
    Filter=False,FourierPlot=False,CombinedPlot=False,
    FrequencyVsFlow=False,TempVsFlow=False,PressureVsFlow=False,
    Normalize=False,AmplitudeVsFlow=False,FreqCFOnly=False,
    rel_height=0.5):
    nthPlot

    ListofPeaks2=[]
    ListofAmps=[]
    DIR2=DIR + "\\"

########################     SEARCHING FOR FILES
    ##########################

    onlyfiles = next(os.walk(DIR2))[2] #dir is your directory
        path as string

###############     SORTING DATA FROM FILES INTO LISTS
    ###################

    P1List=[]
```

```
PDList=[]
FRList=[]
T1List=[]
T1List=np.array(T1List)
T2List=[]
T2List=np.array(T2List)

Kill=[]

for k in range(len(onlyfiles)): # This unpacks each file
    into a list of values. Each file corresponds to an
    individual flowrate.
     F, R, Y, W, B = np.loadtxt((DIR2+onlyfiles[k]), usecols
        = (0,1,2,3,4), unpack=True)
     P1, PD, FR, T1, T2 = np.genfromtxt((DIR2+onlyfiles[k]),
         usecols = (5,6,7,8,9), skip_footer=(len(F)-1), unpack
        =False)


######### DELETEING DATA OUTSIDE SPECIFIED RANGE OF INTEREST
        ##########


     P1List.append(P1)
     PDList.append(PD)
     FRList.append(FR)
     T1List=np.append(T1List,T1)
     T2List=np.append(T2List,T2)

     if k == len(onlyfiles)-1:
         TAVEList=(T1List+T2List)/2
         for i in Kill:
             TAVEList[i]=None
```

```
if Color=='blue':
    Sensor=B
elif Color=='yellow':
    Sensor=Y
elif Color=='white':
    Sensor=W
elif Color=='red':
    Sensor=R
else:
    print("Color must be 'red' 'yellow' 'blue' 'white'")
    return

Sensor2=smooth(Sensor,SmoothingFactor,Window)

A=int(((SmoothingFactor+len(Sensor)-1)-len(Sensor))/2)

if CF_Function != False:

    PredictedPoint = CF_Function(FR)


    dl=np.arange(0,int((PredictedPoint-Range)))
    dh=np.arange(int((PredictedPoint+Range)),len(F))
    dhS=np.arange(int((PredictedPoint+Range+A)),len(
        Sensor2))
    dlS=np.arange(0,int(((PredictedPoint-Range)+A)))


    FFTShift=200

    if FR < 3:
        dl=[0]
```

```
            dh=np.arange(Range+1,len(F))
            P1=None
            PD=None
            Kill.append(k)
            FR=0

        elif CF_Function==False:
            dl=np.arange(0,int(FRange[0]))
            dh=np.arange(int(FRange[1]),len(F))
            dhS=np.arange(int((FRange[1]+A)),len(Sensor2))
            dlS=np.arange(0,int((FRange[0]+A)))
            FFTShift=0


        F=np.delete(F,dh)
        F=np.delete(F,dl)
        Sensor=np.delete(Sensor,dh)
        Sensor=np.delete(Sensor,dl)



        Sensor2=np.delete(Sensor2,dhS)
        Sensor2=np.delete(Sensor2,dlS)



#####################      FINDING PEAKS OF INTEREST
    ########################

        Peaks2,_= sp.find_peaks(Sensor2,distance=Distance,
            prominence=Prominence,height=Height,width=Width,
```

```
        threshold=Threshold, rel_height=Rel_height)      #
        PEAKS AFTER SMOOTHING

    Peaks, _= sp.find_peaks(Sensor, distance=Distance,
        prominence=Prominence, height=Height, width=Width,
        threshold=Threshold, rel_height=Rel_height)       #
        PEAKS BEFORE SMOOTHING

    if FR == 0:

        ListofPeaks2.append([None])
        ListofAmps.append([None])

    else:
        if Smoothed==True:
            ListofPeaks2.append(list(Peaks2+len(dl)))
            ListofAmps.append(list(Sensor2[Peaks2]))
        elif Smoothed==False:
            ListofPeaks2.append(list(Peaks+len(dl)))
            ListofAmps.append(list(Sensor[Peaks]))
        else:
            print('Smoothed must be either True or False')



############      FILTERING PEAKS BY NUMBER OF INSTANCES
    ################

    if Filter==True:
        FilteredPeaks=[]
```

```
#               FilterInstances    # ANY PEAK THAT HAS MORE
    INSTANCES THAN THIS NUMBER WILL HAVE ALL INSTANCES REMOVED

            c = Counter(i for a in (ListofPeaks2) for i in a)
            for i in np.arange(len(ListofPeaks2)):
                FilteredPeaks.append([i for i in ListofPeaks2[i]
                    if c[i] <= FilterInstances])


#########     PLOTS ONE FOURIER TRANSFORM WITH PEAKS FOR
    REFERANCE     ##########


        if nthPlot==k+1:
            if FourierPlot==True:



                plt.figure(figsize=(7,5))
                plt.plot(F, Sensor,'r',label=Color+' Raw Data')
                plt.plot(Peaks+len(dl), Sensor[Peaks], 'bx',
                    label='PEAKS')

#                A=(abs(len(Sensor)-len(Sensor2)))/2

                plt.plot(np.arange(len(Sensor2))+FFTShift,
                    Sensor2,'k',label="Smoothed Data")
                plt.plot(Peaks2+FFTShift, Sensor2[Peaks2], 'yX',
                    label='Smoothed PEAKS')
                plt.xlabel('Frequency (Hz)')
                plt.ylabel('Amplitude (V)')

                if NoiseCF != False:
                    a,b,R2 = ExpModelCF(F,Sensor)
```

```
                plt.plot(F,a*np.e**(b*F),'c',label='Noise␣CF
                    ␣\n'+'{:.4e}'.format(a)+'e^(x*'+'{:.4e}'.
                    format(b)+')')

            plt.yscale('log')
            plt.legend()
            plt.show()

            nthPlot=None

            print('flow␣rate␣of␣FFT␣',FR)

######################    PLOTS    PLOTS    PLOTS
    ######################

    PredictNextPointX=np.linspace(0,max(FRList),1000)

    FlowNow=[]

    for l in range(len(ListofPeaks2[:])):
        FlowNow.append([FRList[l]]*len(ListofPeaks2[l]))

    FlowNowFlat=flatten(FlowNow)
    FlowNowFlat=[x if x>0 else 0 for x in FlowNowFlat]


    ListofAmpsFlat=flatten(list(ListofAmps))
    ListofAmpsFlat0=[x if x != None else 0 for x in
        ListofAmpsFlat]
    ListofAmpsFlatNorm0=np.array(ListofAmpsFlat0)/max(
        ListofAmpsFlat0)
    ListofAmpsFlatNorm=[x if x != 0 else None for x in
        ListofAmpsFlatNorm0]
```

```
ListofPeaks2Flat=flatten(list(ListofPeaks2))
ListofPeaks2Flat0=[x if x != None else 0 for x in
    ListofPeaks2Flat]
ListofPeaks2Flat0Norm=np.array(ListofPeaks2Flat0)/max(
    ListofPeaks2Flat0)
ListofPeaks2FlatNorm=[x if x != 0 else None for x in
    ListofPeaks2Flat0Norm]


TAVEList0=[x if x != None else 0 for x in TAVEList]
TAVEListNorm0=np.array(TAVEList0)/max(TAVEList0)
TAVEListNorm=[x if x != 0 else None for x in TAVEListNorm0]


P1List0=[x if x != None else 0 for x in P1List]
P1ListNorm0=np.array(P1List0)/max(P1List0)
P1ListNorm=[x if x != 0 else None for x in P1ListNorm0]


PDList0=[x if x != None else 0 for x in PDList]
PDListNorm0=np.array(PDList0)/max(PDList0)
PDListNorm=[x if x != 0 else None for x in PDListNorm0]

Density=Therminol_Density(np.array(TAVEList0))
Viscosity=Therminol_Viscosity(np.array(TAVEList0))
SpeedOfSound=Therminol_SpeedOfSound(np.array(TAVEList0))


VelocityBig=np.array(FlowNowFlat)*0.0000630901964/(FW*FH)

VelocitySmall=np.array(FRList)*0.0000630901964/(FW*FH)
```

```
VelocitySmall=[x if x >0 else 0 for x in VelocitySmall]

Re=Density*VelocitySmall*MH/Viscosity
St0=np.array(ListofPeaks2Flat0)*MH/VelocityBig
MachNumber=VelocitySmall/SpeedOfSound


ReBig=[]

for l in range(len(ListofPeaks2[:])):
    ReBig.append([Re[l]]*len(ListofPeaks2[l]))

ReBigFlat=flatten(list(ReBig))

Palmer=np.array(ReBigFlat)/St0
St0=[x if x != np.inf else 0 for x in St0]
St=[x if x != 0 else None for x in St0]

if ReynoldsVsFlowrate != False:
    plt.figure(figsize=(8,5))
    plt.plot(FRList,Re,'k.', label='Reynolds')
    plt.grid()
    plt.legend()
    plt.title('Reynolds Vs FlowRate')
    plt.xlabel('Flowrate (GPM)')
    plt.ylabel('Re')
    plt.show()

if StrouhalVsFlowrate != False:
    plt.figure(figsize=(8,5))
    plt.plot(FlowNowFlat,St,'k.', label='Strouhal')
    plt.grid()
    plt.legend()
```

```
    plt.title('Strouhal Vs Flowrate')
    plt.xlabel('Flowrate (GPM)')
    plt.ylabel('St')
    plt.show()

if ViscosityVsFlowrate != False:
    plt.figure(figsize=(8,5))
    plt.plot(FRList,Viscosity,'k.', label='Viscosity')
    plt.grid()
    plt.legend()
    plt.title('Viscosity Vs Flowrate')
    plt.xlabel('Flowrate (GPM)')
    plt.ylabel('Viscosity (P)')
    plt.show()

if DensityVsFlowrate != False:
    plt.figure(figsize=(8,5))
    plt.plot(FRList,Density,'k.', label='Density')
    plt.grid()
    plt.legend()
    plt.title('Density Vs Flowrate')
    plt.xlabel('Flowrate (GPM)')
    plt.ylabel('Density (KG/M^3)')
    plt.show()

if PalmerVsFlowrate != False:
    plt.figure(figsize=(8,5))
    plt.plot(FlowNowFlat, Palmer, 'k.', label='Palmer')
    plt.grid()
    plt.legend()
    plt.title('Palmer Vs Flowrate')
    plt.xlabel('Flowrate (GPM)')
    plt.ylabel('Palmer')
```

```
#           plt.yscale('log')
            plt.show()

#
    if PalmerVsReynolds != False:
        plt.figure(figsize=(8,5))
        plt.plot(ReBigFlat, Palmer, 'k.', label='Palmer')
        plt.grid()
        plt.legend()
        plt.title('Palmer Vs Reynolds')
        plt.xlabel('Reynolds')
        plt.ylabel('Palmer')
#           plt.yscale('log')
        plt.show()

    if StrouhalVsReynolds != False:
        plt.figure(figsize=(8,5))
        plt.plot(ReBigFlat,St,'k.', label='Strouhal')
        plt.grid()
        plt.legend()
        plt.title('Strouhal Vs Reynolds')
        plt.xlabel('Re')
        plt.ylabel('St')
        plt.show()

    if FrequencyVsReynolds!=False:
        plt.figure(figsize=(8,5))
        plt.plot(ReBigFlat,ListofPeaks2Flat,'k.', label='
            Frequency of ' + Color)
        plt.grid()
        plt.legend()
        plt.title('Frequency Vs Reynolds')
        plt.xlabel('Re')
```

```
    plt.ylabel('Frequency (Hz)')
    plt.show()

if MachNumberVsReynolds != False:
    plt.figure(figsize=(8,5))
    plt.plot(Re,MachNumber,'k.', label='Frequency of ' +
        Color)
    plt.grid()
    plt.legend()
    plt.title('MachNumber Vs Reynolds')
    plt.xlabel('Re')
    plt.ylabel('MachNumber')
    plt.show()

if St_Re_Frequency != False:

    fig, host = plt.subplots(figsize=(8,5))
    host.grid()

    par1 = host.twinx()
    par2 = host.twinx()
    par3 = host.twinx()

    host.set_xlim(0, max(Re)*1.1)
    host.set_ylim(0, FRange[1])
    par1.set_ylim(0, max(St0)*1.1)
    par2.set_ylim(0, max(MachNumber)*1.1)
    par3.set_ylim(0, max(Palmer)*1.1/1000)

    host.set_xlabel("Reynolds")
    host.set_ylabel("Frequency (Hz)")
    par1.set_ylabel("Strouhal")
    par2.set_ylabel("Mach Number")
```

```
par3.set_ylabel("Palmer (1E3)")

p1, = host.plot(ReBigFlat, ListofPeaks2Flat,'k.', label=
    'Frequency of' + Color)
p2, = par2.plot(ReBigFlat, MachNumber,'y.', label='Mach
    Number')
p3, = par1.plot(ReBigFlat, St0, 'b.', label='Strouhal')
p4, = par3.plot(ReBigFlat, Palmer/1000, 'r.', label='
    Palmer')


#        lns = [p1, p2, p3, p4]
lns=[p1,p2,p3,p4]

host.yaxis.label.set_color(p1.get_color())
par2.yaxis.label.set_color(p2.get_color())
par1.yaxis.label.set_color(p3.get_color())
par3.yaxis.label.set_color(p4.get_color())


host.legend(handles=lns, loc='upper center',
    bbox_to_anchor=(0.5, -0.1), ncol=5)

par2.spines['right'].set_position(('outward', 60))
par3.spines['right'].set_position(('outward', 120))
#        par3.spines['right'].set_position(('outward', 135))



fig.tight_layout()

plt.title('Dimensionless Combined')
plt.draw()
```

```
    plt.show()

if Temp_Freq_Press_Amp != False:

    fig, host = plt.subplots(figsize=(8,5))
    host.grid()

    par1 = host.twinx()
    par2 = host.twinx()
    par3 = host.twinx()

    host.set_xlim(0, 60)
    host.set_ylim(0, FRange[1])
    par1.set_ylim(0, max(P1List)*1.2)
    par2.set_ylim(0, max(TAVEList)*1.1)
    par3.set_ylim(0, max(ListofAmpsFlat0)*1.1)

    host.set_xlabel("Flowrate (GPM)")
    host.set_ylabel("Frequency (Hz)")
    par1.set_ylabel("Pressure (PSI)")
    par2.set_ylabel("Temperature (C)")
    par3.set_ylabel("Amplitude (V)")

    p1, = host.plot(FlowNowFlat, ListofPeaks2Flat,'k.',
       label='Frequency of ' + Color)
    p2, = par2.plot(FRList, TAVEList,'rx', label='
       Temperature')
    p3, = par1.plot(FRList, P1List, 'b^', label='Pressure')
    p4, = par1.plot(FRList, PDList, 'bs', label='
       Diff_Pressure')
    p5, = par3.plot(FRList, ListofAmpsFlat, 'y.',  label='
       Amplitude')
```

```
        lns = [p1, p2, p3, p4, p5]


        host.yaxis.label.set_color(p1.get_color())
        par2.yaxis.label.set_color(p2.get_color())
        par1.yaxis.label.set_color(p3.get_color())
        par3.yaxis.label.set_color(p4.get_color())


        host.legend(handles=lns, loc='upper center',
            bbox_to_anchor=(0.5, -0.1), ncol=5)

        par2.spines['right'].set_position(('outward', 60))
        par3.spines['right'].set_position(('outward', 120))
#         par3.spines['right'].set_position(('outward', 135))



        fig.tight_layout()

        plt.title('Combined')
        plt.draw()
        plt.show()

    if Normalize != False:

        if CombinedPlot != False:


            fig, host = plt.subplots(figsize=(8,5))
            host.grid()
```

```
            par1 = host.twinx()
#           par2 = host.twinx()


            host.set_xlim(0, 60)
            host.set_ylim(0, 1.1)

#           par2.set_ylim(0, 1)


            host.set_xlabel("Flowrate (GPM)")
            host.set_ylabel("Frequency (Hz) \nPressure (PSI) \
                nTemperature (C) ")
#           par1.set_ylabel("Amplitude (V)")
#           par2.set_ylabel("TEMPERATURE (C)")


            p1, = host.plot(FlowNowFlat, ListofPeaks2FlatNorm,'k
                .', label='Frequency of ' + Color)

            if AmplitudeVsFlow != False:

                par1.set_ylabel("Amplitude (V)")
                par1.set_ylim(1E-6, 2)
                par1.set_yscale("log")
                p2, = par1.plot(FlowNowFlat, ListofAmpsFlatNorm,
                    'y.', label='Amplitude')
                par1.yaxis.label.set_color(p2.get_color())


            p3, = host.plot(FRList, P1ListNorm, 'b^', label='
                Pressure')
```

```
        p4, = host.plot(FRList, PDListNorm, 'bs',  label='
            Diff_Pressure')
        p5, = host.plot(FRList, TAVEListNorm, 'rx', label='
            Average_Temperature')

        if AmplitudeVsFlow != False:
            lns = [p1, p2, p3, p4, p5]

        else:
            lns = [p1, p3, p4, p5]




        host.legend(handles=lns, loc='upper_center',
            bbox_to_anchor=(0.5, -0.1), ncol=5)


        host.yaxis.label.set_color(p1.get_color())


        fig.tight_layout()

        plt.title('Combined_(Normalized)')
        plt.draw()
        plt.show()


    if FreqAndAmpVsReynolds != False:
        fig, host = plt.subplots(figsize=(8,5))
        host.grid()
```

```
par1 = host.twinx()



host.set_xlabel("Re")
host.set_ylabel("Frequency (Hz)")



p1, = host.plot(ReBigFlat, ListofPeaks2Flat,'k.',
    label='Frequency of ' + Color)


par1.set_ylabel("Amplitude (V)")
par1.set_ylim(1E-12, 1)
par1.set_yscale("log")
p2, = par1.plot(ReBigFlat, ListofAmpsFlat,'y.',
    label='Amplitude')
par1.yaxis.label.set_color(p2.get_color())



lns = [p1, p2]



host.legend(handles=lns, loc='upper center',
    bbox_to_anchor=(0.5, -0.1), ncol=5)
```

```
        host.yaxis.label.set_color(p1.get_color())



        fig.tight_layout()

        plt.title('Combined Vs Reynolds')
        plt.draw()
        plt.show()

if FrequencyVsFlow != False:
    plt.figure(figsize=(8,5))
    plt.plot(FlowNowFlat, ListofPeaks2Flat,'k.', label='
        Frequency of ' + Color)



    plt.grid()
    plt.legend()
    plt.title('Frequency Vs Flowrate')
    plt.xlabel('Flowrate (GPM)')
    plt.ylabel('Frequency (Hz)')
    plt.show()

if FrequencyVsMachNumber != False:
    plt.figure(figsize=(8,5))
    plt.plot(MachNumber, ListofPeaks2,'k.', label='Frequency
        of ' + Color)
    plt.grid()
    plt.legend()
    plt.title('Frequency Vs MachNumber')
    plt.xlabel('Mach Number')
```

```
    plt.ylabel('Frequency (Hz)')
    plt.show()

if TempVsFlow != False:
    plt.figure(figsize=(8,5))
    plt.plot(FRList, TAVEList, 'rx', label='T_AVE')
    plt.grid()
    plt.legend()
    plt.title('Average Temperature Vs Flowrate')
    plt.xlabel('Flowrate (GPM)')
    plt.ylabel('Temperature (C)')
    plt.show()

if PressureVsFlow != False:
    plt.figure(figsize=(8,5))
    plt.plot(FRList, P1List, 'b^', label='Pressure')
    plt.plot(FRList, PDList, 'bs', label='Diff_Pressure')
    plt.grid()
    plt.legend()
    plt.title('Pressure Vs FlowRate')
    plt.xlabel('Flowrate (GPM)')
    plt.ylabel('Pressure (PSI)')
    plt.show()

if PressureVsReynolds != False:
    plt.figure(figsize=(8,5))
    plt.plot(Re, P1List, 'b^', label='Pressure')
    plt.plot(Re, PDList, 'bs', label='Diff_Pressure')
    plt.grid()
    plt.legend()
    plt.title('Pressure Vs Reynolds')
    plt.xlabel('Re')
    plt.ylabel('Pressure (PSI)')
```

```
        plt.show()

    if PressureVsAmplitude != False:
        plt.figure(figsize=(8,5))
#         plt.plot(ListofAmps, P1List, 'b^', label='Pressure')
        plt.plot(ListofAmps, PDList, 'bs', label='Diff Pressure
            ')
        plt.grid()
        plt.legend()
        plt.title('Pressure Vs Amplitude')
        plt.xlabel('Amplitude (V)')
        plt.ylabel('Pressure (PSI)')
        plt.show()


    if CombinedPlot != False:

        fig, host = plt.subplots(figsize=(8,5))
        host.grid()




        host.set_xlim(0, 60)
        host.set_ylim(FRange[0], FRange[1])



        host.set_xlabel("Flowrate (GPM)")
        host.set_ylabel("Frequency (Hz)")
```

```
p1, = host.plot(FlowNowFlat, ListofPeaks2Flat,'k.',
   label='Frequency of '+ Color)
if CF_Function != False:
    p2, = host.plot(PredictNextPointX, CF_Function(
       PredictNextPointX),'y', label='Hand_CF')
elif Test_CF != False:
    p2, = host.plot(PredictNextPointX, Test_CF(
       PredictNextPointX),'y', label='Hand_CF')

if FreqCFOnly == False:
    par1 = host.twinx()
    par2 = host.twinx()

    p3, = par1.plot(FRList, P1List, 'b^', label='
       Pressure')
    p4, = par1.plot(FRList, PDList, 'bs',  label='
       Diff_Pressure')
    p5, = par2.plot(FRList, TAVEList, 'rx', label='T_AVE
       ')
    par2.spines['right'].set_position(('outward', 60))



lns=[p1]

if (CF_Function != False or Test_CF != False):
    lns.append(p2)

if FreqCFOnly == False:
    lns.append(p3)
    lns.append(p4)
    lns.append(p5)
    host.yaxis.label.set_color(p1.get_color())
```

```
        par1.yaxis.label.set_color(p3.get_color())
        par2.yaxis.label.set_color(p5.get_color())
        par1.set_ylim(0, 50)
        par2.set_ylim(70, 130)
        par1.set_ylabel("Pressure (PSI)")
        par2.set_ylabel("Temperature (C)")



    host.legend(handles=lns, loc='upper center',
        bbox_to_anchor=(0.5, -0.10), ncol=5)




    fig.tight_layout()

    plt.title('Combined')
    plt.draw()
    plt.show()



return


#    THERMINOL 3
DIR=r"Path"


def F(X):
```

```
        return -36918.4*(X+20)**-1.50977+331.211
#       return -3393.76*(X+10)**-0.862935+370.032

#       return -2185.81*(X+6.5)**-0.764789+379.519-5
#       return 5.1831*X+41.9437+10



NumSamp=20000  # The number of samples that the labview program
    aquired.
SampRate=20000 # The sample rate that the Labview Program
    aquired data.
Res=SampRate/NumSamp  # The size of the bins from the FFT. This
    must be 1 to function as the code is now.



############################        Old with Curve fit
#FRange=[0,350]
#Distance=4
#prominence=(1E-11,None)
#height=1E-11
#Threshold=None
#
#CF_Function=F
#Test_CF=False
#Smoothed=False
#Filter=False
#
#Normalize=True
#FouriexPlot=True
#CombinedPlot=True
#FrequencyVsFlow=False
```

```
#TempVsFlow=False
#PressureVsFlow=False
#AmplitudeVsFlow=False
#
#Range=5
#SmoothingFactor=5
##SmoothingFactor=50
#FilterInstances=5
#nthPlot=50

############################        For full 10k hz

#FRange=[1,10000]
#
#FH=3/1000
#MH=9/1000
#FW=44.45/1000
#
#Distance=50
#prominence=(5E-12,None)
#height=1E-12
#width=None
#Threshold=None
#Rel_height=0.5
#
#CF_Function=False
#Test_CF=False
#Smoothed=True
#Filter=True
#
#Normalize=False
#FourierPlot=True
#NoiseCF=False
```

```
#CombinedPlot=False
#FreqCFOnly=False
#FrequencyVsFlow=True
#TempVsFlow=False
#PressureVsFlow=False
#AmplitudeVsFlow=False
#PressureVsAmplitude = False
#FreqAndAmpVsReynolds = False
#PressureVsReynolds = False
#
#StrouhalVsFlowrate = False
#StrouhalVsReynolds = False
#ReynoldsVsFlowrate = False
#FrequencyVsReynolds = True
#FrequencyVsMachNumber = False
#St_Re_Frequency = False
#PalmerVsFlowrate = False
#PalmerVsReynolds = False
#MachNumberVsReynolds = False
#
#ViscosityVsFlowrate=False
#DensityVsFlowrate=False
#
#Range=1001
#SmoothingFactor=201
##SmoothingFactor=50
#Window='hanning'                #'flat', 'hanning', 'hamming', '
    bartlett', 'blackman'
#FilterInstances=1
#nthPlot=5
#NoiseStep=500

##########################      For 1000 hz
```

```
#FRange=[0,1150]
#
#FH=3/1000
#MH=9/1000
#FW=44.45/1000
#
#Distance=25
#prominence=(9E-9,None)
#height=5E-10
#width=None
#Threshold=None
#Rel_height=0.5
#
#CF_Function=False          #set equal to function name if not
    false
#Test_CF=F                  #set equal to function name if not
    false
#Smoothed=True
#Filter=True
#
#Normalize = False
#FourierPlot = True
#NoiseCF = False
#CombinedPlot = True
#FreqCFOnly = True
#FrequencyVsFlow = True
#TempVsFlow = False
#PressureVsFlow = False
#AmplitudeVsFlow = True
#PressureVsAmplitude = False
#FreqAndAmpVsReynolds = False
#
#StrouhalVsFlowrate = False
```

```
#StrouhalVsReynolds = False
#ReynoldsVsFlowrate = False
#FrequencyVsReynolds = True
#FrequencyVsMachNumber = False
#St_Re_Frequency = False
#PalmerVsFlowrate = False
#PalmerVsReynolds = False
#MachNumberVsReynolds = False
#
#ViscosityVsFlowrate = False
#DensityVsFlowrate = False
#PressureVsReynolds = False
#
#Range=1001
#SmoothingFactor=10
##SmoothingFactor=50
#Window='hanning'                #'flat', 'hanning', 'hamming', '
    bartlett', 'blackman'
#FilterInstances=1
#nthPlot=26
#NoiseStep=500

################################ This is the lowest and loudest
    stage
FRange=[0,300]

FH=3/1000    #Flue height in millimeters
MH=9/1000    #Mouth height in millimeters
FW=44.45/1000    #Width of the device in millimeters

Distance=60    #Distance for the peak detection function. No two
    peaks can exist within this many points from each other.
```

```
prominence=(1E-9,None)      #The minimum required prominence of
    the peak
height=1E-12      #The minimum required amlitude of an accepted
    peak
width=None      #The minimum required width of the peak
Threshold=None
Rel_height=0.5      #The Relative height of the peak compared to
    its width

CF_Function = F       #If false the curve fit filtering does not
     take place. If anything else the input must be the curve fit
     function
Test_CF = False      # This is to plot the curve fit without
    filtering along it.
Smoothed = False      #this causes all plots to use smoothed data
     rather than raw.
Filter = False       #This causes any peak that repeats
    FilterInstances number of times to be deleted

############################ These are all to turn on or off
    different plots ##############################

Normalize = True
FourierPlot = True
NoiseCF = False
CombinedPlot = True
FreqCFOnly = True
FrequencyVsFlow = True
TempVsFlow = False
PressureVsFlow = False
AmplitudeVsFlow = True
PressureVsAmplitude = False
FreqAndAmpVsReynolds = True
```

```
StrouhalVsFlowrate = True
StrouhalVsReynolds = True
ReynoldsVsFlowrate = True
FrequencyVsReynolds = True
FrequencyVsMachNumber = True
St_Re_Frequency = True
PalmerVsFlowrate = True
PalmerVsReynolds = True
MachNumberVsReynolds = True

Temp_Freq_Press_Amp=True

ViscosityVsFlowrate = True
DensityVsFlowrate = True
PressureVsReynolds = True

########################## These are inputs for the smoothing and
    filter functions ####################

Range=30    # how many Hz above and below the Curve fit are
    allowed to be searched for peaks
SmoothingFactor=15    #The level of smoothing applied to the data
#SmoothingFactor=50
Window='hanning'     # The type of smooting window used such as '
    flat', 'hanning', 'hamming', 'bartlett', 'blackman'
FilterInstances=1    # The number of allowable instances of a
    peak frequency
nthPlot=64        #the nth file to plot the FFT of.
NoiseStep=50

Color='blue'      # The color of the sensor to be analyzed
```

```
ListOfMax=[0,0,0,0]

ListOfMax[0]=FindMax(Color,DIR,FRange,Res,Distance,prominence,
    height,width,Threshold,Range,SmoothingFactor,FilterInstances,
     CF_Function,Test_CF,nthPlot,Smoothed,Filter,FourierPlot,
    CombinedPlot,FrequencyVsFlow,TempVsFlow,PressureVsFlow,
    Normalize,AmplitudeVsFlow,FreqCFOnly,Rel_height)
#AllFolders(DIR,FRange,NumSamp,SampRate)



# Note to self Next Step will be making the sensor chosen an
    input and only that colum will be extracted from files. then
    the function can easily be looped to look at all sensors.
```

Appendix C: LabView Code

Therminol runs.vi
C:\Users\User\Desktop\Therminol runs.vi
Last modified on 3/19/2021 at 7:12 PM
Printed on 4/30/2021 at 11:10 PM

Block Diagram

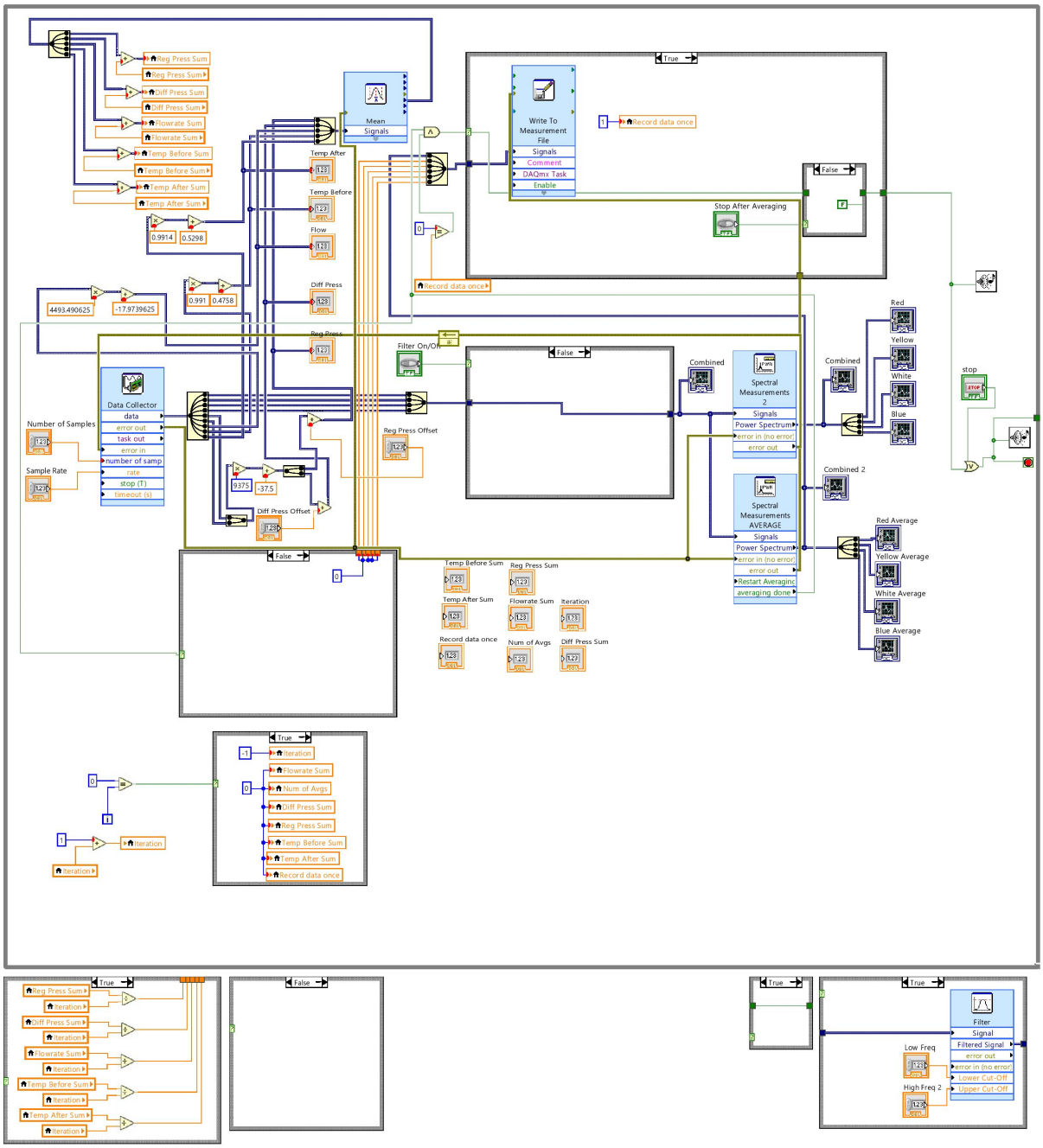

Figure C.1: LabVIEW Block Diagram

Therminol runs.vi
C:\Users\User\Desktop\Therminol runs.vi
Last modified on 3/19/2021 at 7:12 PM
Printed on 4/30/2021 at 11:10 PM

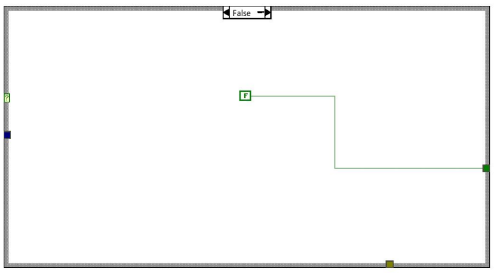

Figure C.2: LabVIEW Block Diagram